

**University of Alberta**

Inheritance of Peroxisomes in the Yeast *Yarrowia lipolytica*

by

Jinlan (Jenny) Chang

A thesis submitted to the Faculty of Graduate Studies and Research  
in partial fulfillment of the requirements for the degree of

Doctor of Philosophy

Department of Cell Biology

©Jinlan (Jenny) Chang  
Fall 2010  
Edmonton, Alberta

Permission is hereby granted to the University of Alberta Libraries to reproduce single copies of this thesis and to lend or sell such copies for private, scholarly or scientific research purposes only. Where the thesis is converted to, or otherwise made available in digital form, the University of Alberta will advise potential users of the thesis of these terms.

The author reserves all other publication and other rights in association with the copyright in the thesis and, except as herein before provided, neither the thesis nor any substantial portion thereof may be printed or otherwise reproduced in any material form whatsoever without the author's prior written permission.

## **Examining Committee**

Richard Rachubinski, Cell Biology

Gary Eitzen, Cell Biology

Zhixiang Wang, Cell Biology

Joseph Casey, Physiology

Robert Mullen, University of Guelph

## ABSTRACT

Peroxisomes are indispensable organelles that perform many essential metabolic activities. Thus, eukaryotic cells have evolved molecular mechanisms to ensure the inheritance of peroxisomes from mother cell to daughter cell at cell division. In the budding yeast *Saccharomyces cerevisiae*, the class V myosin motor, Myo2p, interacts with its peroxisomal receptor, Inp2p, to move peroxisomes along actin from mother cell to bud, while the peroxisomal membrane protein Inp1p functions to tether peroxisomes to the cell cortex.

In this thesis, I report the results of investigations of peroxisome inheritance using the dimorphic yeast *Yarrowia lipolytica* as a model system.

We showed that peroxisome mobility and inheritance are dependent on actin in *Y. lipolytica*. Interrogation of the *Y. lipolytica* genome revealed one class V myosin. This myosin V is involved in transporting peroxisomes from mother cell to bud. We characterized *YInp1p*, the orthologue of *S. cerevisiae* Inp1p, as the first peroxisomal protein required for peroxisome inheritance in *Y. lipolytica*. We demonstrated that *YInp1p* functions to anchor peroxisomes in both mother cell and bud. *YInp1p* has an additional role in the dimorphic transition from the yeast form to the hyphal form in *Y. lipolytica*.

We identified Pex3Bp, a paralogue of Pex3p, as the peroxisome-specific receptor for myosin V in *Y. lipolytica*. Pex3Bp interacts directly with the globular tail of myosin V. Pex3Bp also interacts with itself and with Pex3p. In cells lacking Pex3Bp, peroxisomes are preferentially retained in the mother cell, while the majority of peroxisomes gather and are transferred to the bud in cells overproducing Pex3Bp. Overexpression of *PEX3* can partially complement the phenotype of *pex3BΔ* cells, while overexpression of *PEX3B*

cannot complement the phenotype of *pex3Δ* cells. Interestingly, Pex3p, which has been shown previously to function in the de novo formation of peroxisomes from the ER, also interacts directly with the globular tail of myosin V. Therefore, Pex3p is involved in peroxisome inheritance. In addition, cells lacking Pex3Bp contain hyperelongated, tubuloreticular peroxisomes, indicating that Pex3Bp has a role in peroxisome morphology. Our findings suggest that both Pex3Bp and Pex3p are multifunctional proteins that are involved in different steps of the peroxisome biogenic cascade.

## ACKNOWLEDGEMENTS

I deeply thank Dr. Richard Rachubinski for his encouragement and enthusiasm throughout my graduate studies. He has set a good example for me. He makes every effort to be available to answer questions and provide guidance when needed. His invaluable advice in conducting research, assistance in writing research papers, and timely recognition for ideas and quality work all have contributed to my success so far in research.

I would like to recognize all my colleagues in the lab, both past and present, for their help and friendship, especially Andrei Fagarasanu, Fred Mast, Dorian Rachubinski, Barbara Knoblach, David Lancaster, Robert Tower, Richard Poirier, Hanna Kroliczak, Elena Savidov, Dwayne Weber, Erin Brown, Ryan Perry, Monica Fagarasanu, Melissa Dobson, and Chris Tam.

I would like to express my appreciation to the members of my supervisory committee, Dr. Zhixiang Wang and Dr. Gary Eitzen, for their support and guidance.

I would also like to thank the Department of Cell Biology, the Faculty of Medicine and Dentistry, the Faculty of Graduate Studies and Research, the Graduate Students' Association and the Canadian Institutes of Health Research for the financial support provided during my studies.

Finally, I am grateful to my cousins and friends in Edmonton who have shared both my happiness and sadness, and to my husband and daughter for their continuous support and tolerance.

## TABLE OF CONTENTS

<b>CHAPTER 1: INTRODUCTION</b>	<b>1</b>
1.1 Organelle inheritance	2
1.2 Peroxisome structure and functions	2
1.3 Peroxisomal disorders	5
1.4 Peroxisome multiplication	6
1.4.1 Peroxisome multiplication by de novo synthesis from the ER	7
1.4.2 Peroxisome multiplication by growth and division	10
1.4.2.1 Peroxisome elongation by the Pex11 protein family	11
1.4.2.2 Peroxisome fission by dynamin-related proteins and Fis proteins	13
1.4.2.3 Peroxisome constriction	14
1.5 Peroxisome inheritance	16
1.5.1 Peroxisome dynamics in <i>S. cerevisiae</i>	17
1.5.2 Actin cables and class V myosins	17
1.5.3 Peroxisome movement by Inp2p	19
1.5.4 Peroxisome retention by Inp1p	20
1.5.5 The relationship between Inp1p and Inp2p	21
1.6 The yeast <i>Y. lipolytica</i> as a model system	22
1.7 Focus of this thesis	24
<b>CHAPTER 2: MATERIALS AND METHODS</b>	<b>26</b>
2.1 Materials	27
2.1.1 Chemicals and reagents used in this study	27
2.1.2 Enzymes	29
2.1.3 Molecular size standards	29
2.1.4 Multicomponent systems	30
2.1.5 Plasmids	30
2.1.6 Antibodies	30
2.1.7 Oligonucleotides	32
2.1.8 Standard buffers and solutions	36
2.2 Microorganisms and culture conditions	37

2.2.1 Bacterial strains and culture conditions	37
2.2.2 Yeast strains and culture conditions	38
2.3 Introduction of DNA into microorganisms	40
2.3.1 Chemical transformation of <i>E. coli</i>	40
2.3.2 Electroporation of <i>E. coli</i>	40
2.3.3 Chemical transformation of <i>Y. lipolytica</i>	41
2.3.4 Electroporation of <i>Y. lipolytica</i>	42
2.4 Isolation of DNA from microorganisms	42
2.4.1 Isolation of plasmid DNA from bacteria	42
2.4.2 Isolation of chromosomal DNA from yeast	43
2.5 DNA manipulation and analysis	44
2.5.1 Amplification of DNA by the polymerase chain reaction (PCR)	44
2.5.2 Digestion of DNA by restriction endonucleases	44
2.5.3 Dephosphorylation of 5'-ends	45
2.5.4 Separation of DNA fragments by agarose gel electrophoresis	45
2.5.5 Purification of DNA fragments from agarose gel	45
2.5.6 Purification of DNA from solution	46
2.5.7 Ligation of DNA fragments	46
2.5.8 DNA sequencing	46
2.6 Protein manipulation and analysis	47
2.6.1 Preparation of yeast whole cell lysates	47
2.6.2 Precipitation of proteins	48
2.6.3 Determination of protein concentration	49
2.6.4 Separation of proteins by electrophoresis	49
2.6.5 Detection of proteins by gel staining	50
2.6.6 Detection of proteins by immunoblotting	50
2.7 Subcellular fractionation of <i>Y. lipolytica</i> cells	51
2.7.1 Peroxisome isolation from <i>Y. lipolytica</i>	51
2.7.2 Extraction and subfractionation of proxisomes	52
2.8 Microscopy	52
2.8.1 Immunofluorescence microscopy	52
2.8.2 Electron microscopy	53
2.8.3 Confocal 4D video microscopy	54

2.8.4 Quantification of rates of peroxisome inheritance	57
2.9 Construction of plasmids for gene expression	58
2.9.1 pTC3-YIINP1	58
2.9.2 pINA445-mRFP-SKL and pINA445-POT1-GFP	59
2.9.3 pTC3-PEX3B, pTC3-PEX3 and pTC3-MyoVtail	59
2.9.4 pTC3-PEX3B-mRFP and pTC3-YALI0E03124g-mRFP	60
2.9.5 pUB4-PEX3B, pUB4-PEX3, pUB4-MyoVtail and pUB4-PEX3B-mRFP	61
2.10 Integrative disruption of <i>Y. lipolytica</i> genes	61
2.10.1 Integrative disruption of <i>YIINP1</i>	61
2.10.2 Integrative disruption of <i>PEX3B</i>	62
2.10.3 Construction of the <i>PEX3Δ/PEX3BΔ</i> double deletion strain	62
2.11 Genomic tagging of <i>Y. lipolytica</i> genes with the ORF for GFP	63
2.11.1 <i>YIPOT1</i>	63
2.11.2 <i>YIINP1</i>	64
2.12 Split-ubiquitin membrane yeast two-hybrid analysis	64
2.12.1 Construction of chimeric genes	65
2.12.2 Assay for two-hybrid interaction	65
2.13 Assay for direct protein interaction	66
2.14 Staining cell structures	68
2.14.1 Staining actin	68
2.14.2 Staining vacuoles with FM 4-64	68
2.14.3 Staining mitochondria with MitoTracker Red	69
2.15 Cytoskeleton disruption	69
2.15.1 Actin depolymerization	69
2.15.2 Microtubule depolymerization	69
2.16 Antibody production	70
2.16.1 Production of antibodies to <i>YInp1p</i>	71
2.16.2 Production of antibodies to <i>Pex3Bp</i>	72
2.17 Computer-assisted DNA and protein sequence analysis	72

**CHAPTER 3: YLINP1P IS A PEROXISOMAL MEMBRANE PROTEIN  
REQUIRED FOR PEROXISOME RETENTION IN YARROWIA LIPOLYTICA 73**

3.1 Overview	74
3.2 Peroxisome dynamics in wild-type <i>Y. lipolytica</i> cells	74
3.3 Peroxisome movement in <i>Y. lipolytica</i> is dramatically reduced by depolymerization of actin but not of microtubules	75
3.4 <i>Ylinp1p</i> is a peripheral membrane protein of peroxisomes	80
3.5 Peroxisome inheritance is impaired in cells lacking or overexpressing <i>YLINP1</i>	85
3.6 The structure of actin and inheritance of other organelles are unaffected in <i>Ylinp1Δ</i> cells	88
3.7 <i>Ylinp1Δ</i> cells readily undergo the dimorphic transition from yeast to hyphal form	88
3.8 Discussion	90
3.8.1 Peroxisome inheritance in the yeast <i>S. cerevisiae</i>	90
3.8.2 Peroxisome movement in <i>Y. lipolytica</i> is actin-dependent	92
3.8.3 A role for <i>Ylinp1p</i> in peroxisome retention	93
3.8.4 <i>Ylinp1p</i> is involved in the dimorphic transition in <i>Y. lipolytica</i>	95

**CHAPTER 4: A ROLE FOR THE PEX3 PROTEIN FAMILY IN PEROXISOME  
MOTILITY IN YARROWIA LIPOLYTICA 97**

4.1 Overview	98
4.2 The <i>Y. lipolytica</i> genome encodes a paralogue of Pex3p designated Pex3Bp	99
4.3 Pex3Bp is an integral membrane protein of peroxisomes	99
4.4 Deletion of the <i>PEX3B</i> gene affects peroxisome morphology	104
4.5 Deletion of the <i>PEX3B</i> gene affects specifically peroxisome inheritance	106
4.6 Peroxisome dynamics in <i>pex3BΔ</i> cells	109
4.7 Peroxisome inheritance by buds depends on a class V myosin motor in <i>Y. lipolytica</i>	112

4.8 A candidate <i>Y. lipolytica</i> Inp2p orthologue, YALI0E03124p, is not the peroxisome-specific receptor for myosin V	113
4.9 Pex3Bp and Pex3p interact directly with the globular tail of the <i>Y. lipolytica</i> class V myosin	116
4.10 Peroxisome dynamics in <i>pex3BΔ</i> cells overexpressing <i>PEX3B</i> or <i>PEX3</i>	118
4.11 Overexpression of <i>PEX3B</i> or <i>PEX3</i> restores peroxisome inheritance to buds in <i>pex3BΔ</i> cells	121
4.12 Discussion	124
4.12.1 The putative Inp2p orthologue, YALI0E03124p, is not the peroxisome-specific myosin V receptor of <i>Y. lipolytica</i>	124
4.12.2 Pex3p and its paralogue, Pex3Bp, function as peroxisome-specific receptors for the class V myosin of <i>Y. lipolytica</i>	126
4.12.3 How <i>Y. lipolytica</i> and <i>S. cerevisiae</i> differ in peroxisome inheritance	127
4.12.4 Members of the Pex3p family may be multifunctional	128
4.12.5 Pex3Bp's action in peroxisome division	130
<b>CHAPTER 5: PERSPECTIVES</b>	<b>132</b>
5.1 Synopsis	133
5.2 Future research on <i>Y</i> Inp1p	133
5.3 Future research on Pex3Bp	135
5.4 Future research on Pex3p	137
<b>CHAPTER 6: REFERENCES</b>	<b>140</b>

## LIST OF TABLES

Table 1-1. Myosins in yeasts	19
Table 2-1. Primary antibodies	31
Table 2-2. Secondary antibodies	31
Table 2-3. Oligonucleotides	32
Table 2-4. Common solutions	36
Table 2-5. <i>E. coli</i> strains	37
Table 2-6. Bacterial culture media	37
Table 2-7. <i>Y. lipolytica</i> and <i>S. cerevisiae</i> strains	38
Table 2-8. Yeast culture media	39
Table 2-9. Construction of plasmids for two-hybrid analysis	65
Table 2-10. Construction of plasmids for direct protein interaction	67

## LIST OF FIGURES

Figure 1-1. Multiplication and inheritance of peroxisomes	23
Figure 3-1. Peroxisome dynamics in <i>Y. lipolytica</i>	76
Figure 3-2. Actin is involved in peroxisome dynamics	78
Figure 3-3. Quantification of peroxisome mobility	81
Figure 3-4. Sequence alignment of <i>S. cerevisiae</i> Inp1p (ScInp1p) with the hypothetical <i>Y</i> Inp1p encoded by the ORF <i>YALIOF31229g</i> of the <i>Y. lipolytica</i> genome	82
Figure 3-5. <i>Y</i> Inp1p is a peripheral membrane protein of peroxisomes	84
Figure 3-6. Deletion of the <i>YIINP1</i> gene affects specifically peroxisome inheritance	86
Figure 3-7. <i>YIINP1</i> overexpression leads to peroxisome retention in mother cells	87
Figure 3-8. Deletion or overexpression of the <i>YIINP1</i> gene affects peroxisome mobility	89
Figure 3-9. Deletion of the <i>YIINP1</i> gene affects the dimorphic transition	91
Figure 4-1. Sequence alignment of Pex3p with the hypothetical protein Pex3Bp encoded by the <i>Y. lipolytica</i> genome	100
Figure 4-2. Pex3Bp is a peroxisomal integral membrane protein	102
Figure 4-3. Pex3Bp cofractionates with peroxisomes	103
Figure 4-4. Deletion of the <i>PEX3B</i> gene affects peroxisome morphology	105
Figure 4-5. Deletion of the <i>PEX3B</i> gene affects specifically peroxisome inheritance	107
Figure 4-6. Peroxisome dynamics in wild-type and <i>pex3BΔ</i> cells	110
Figure 4-7. Peroxisome movement depends on class V myosin	114
Figure 4-8. A candidate <i>Y. lipolytica</i> Inp2p orthologue, YALIOE03124p, does not localize to peroxisomes	115
Figure 4-9. Pex3Bp and Pex3p interact directly with the cargo-binding tail of <i>Y. lipolytica</i> class V myosin	117

Figure 4-10. Peroxisome dynamics in <i>pex3BΔ</i> cells overexpressing <i>PEX3B</i> or <i>PEX3</i>	119
Figure 4-11. Overexpression of <i>PEX3</i> can substitute for Pex3Bp in peroxisome inheritance	122
Figure 5-1. Roles for Pex3 proteins in peroxisome multiplication and inheritance	138

## LIST OF SYMBOLS AND ABBREVIATIONS

20KgP	pellet obtained from centrifugation at $20,000 \times g$
20KgS	supernatant obtained from centrifugation at $20,000 \times g$
4D	three-dimensional time lapse
bp	base pair
dNTP	deoxyribonucleoside triphosphate
DRP	dynamain-related protein
ECL	enhanced chemiluminescence
ER	endoplasmic reticulum
<i>g</i>	gravitational force
GFP	green fluorescent protein
GST	glutathione-S-transferase
HRP	horseradish peroxidase
IPTG	isopropyl $\beta$ -D-thiogalactoside
PTS	peroxisome targeting signal
MBP	maltose binding protein
mRFP	monomeric red fluorescence protein
OD	optical density
ORF	open reading frame
PAGE	polyacrylamide gel electrophoresis
PBD	peroxisome biogenesis disorder
PCR	polymerase chain reaction
<i>PEX#</i>	wild-type gene encoding <i>Pex#</i> p
<i>pex#</i>	mutant <i>PEX#</i> gene
PMP	peroxisomal membrane protein
PNS	postnuclear supernatant
SDS	sodium dodecyl sulfate
TCA	trichloroacetic acid
X-gal	5-bromo-4-chloro-3-indolyl- $\beta$ -D-galactopyranoside
YFP	yellow fluorescent protein

## **CHAPTER 1**

### **INTRODUCTION**

## **1.1 Organelle inheritance**

Organelles are specialized membrane-bound compartments that perform different cellular functions in eukaryotic cells and include the nucleus, mitochondria, chloroplasts, endoplasmic reticulum (ER), Golgi apparatus, lysosomes/vacuoles and peroxisomes. To maintain the benefits of having organelles, cells must regulate their number, volume and position. Thus, eukaryotic cells have evolved highly regulated and coordinated molecular mechanisms to ensure the accurate partitioning of their organelle populations between mother and daughter cells at cell division. These inheritance mechanisms involve molecular motors that transport organelles between mother and daughter cells along cytoskeletal elements, specific organellar receptors that recognize the molecular motors, and proteins that retain organelles within both mother cell and daughter to ensure an equitable division of organelles between them (Fagarasanu and Rachubinski, 2007). This thesis focuses on some of the proteins involved in peroxisome inheritance in the budding yeast *Yarrowia lipolytica*. This chapter will introduce briefly peroxisome structure and functions and the peroxisomal disorders, as well as summarize our current understanding of peroxisome multiplication and inheritance.

## **1.2 Peroxisome structure and functions**

Peroxisomes are ubiquitous organelles found in diverse eukaryotic organisms and cell types. They are generally spherical with a diameter of 0.1 to 1  $\mu\text{m}$ , delimited by a single membrane and containing a fine granular matrix and more than 50 different enzymes. Unlike mitochondria and chloroplasts, peroxisomes do not contain DNA or an

independent protein synthesis machinery, and thus all peroxisomal proteins are encoded in the nucleus and synthesized on cytoplasmic polysomes.

Peroxisomes are involved in a myriad of biochemical processes. The oxidative metabolism of fatty acids and the decomposition of hydrogen peroxide are the most important conserved functions of peroxisomes (de Duve and Baudhuin, 1966; Lazarow and Fujiki, 1985; van den Bosch et al., 1992; Poirier et al., 2006). Peroxisomal functions differ according to the organism, cell type or environmental condition. For example, in yeast, peroxisomes are involved in biosynthesis of lysine and the degradation of methanol and amino acids. In filamentous fungi, peroxisomes are involved in the biosynthesis of penicillin. *Neurospora crassa*, a filamentous fungus, contains a specialized peroxisome-derived organelle named the Woronin body that functions as a plug for septal pores to avoid cytoplasmic bleeding caused by mechanical damage (Jedd and Chua, 2000). In plants, peroxisomes participate in the glyoxylate cycle and photorespiration. In mammals, peroxisomes play roles in the biosynthesis of cholesterol, bile acids, dolichol and ether glycerolipids (plasmalogens); the  $\beta$ -oxidation of prostaglandins and leukotrienes; and the  $\alpha$ -oxidation of branched chain fatty acids (Jansen and Wanders, 2006; Wierzbicki, 2007).

The functional diversity of peroxisomes relates to their extraordinary adaptability to environmental conditions. In yeast, peroxisomes are dramatically induced when cells are shifted from a culture medium containing a carbon source whose metabolism does not require peroxisomes (e.g. glucose) to a culture medium containing a carbon source whose metabolism requires peroxisomes (e.g. oleic acid or methanol) (Veenhuis et al., 1987; van der Klei and Veenhuis, 1997). On the other hand, peroxisomes are delivered to the vacuole for degradation when yeast cells are transferred from oleic acid- or methanol-

containing medium to glucose-containing medium (Gunkel et al., 1999; Farre and Subramani, 2004). The extensive proliferation of peroxisomes in the livers of rats can be observed when the rats are treated with peroxisome proliferators, such as hypolipidemic drugs or fatty acid analogs (Reddy and Mannaerts, 1994). Peroxisome proliferators bind to peroxisome proliferator-activated receptors, a group of nuclear transcription factors that enhance the transcription of responsive genes, such as those encoding peroxisomal  $\beta$ -oxidation enzymes (Issemann and Green, 1990).

Peroxisomes interact with other organelles to carry their functions. In mammals, peroxisomes and mitochondria cooperate in the  $\beta$ -oxidation of fatty acids and the metabolism of reactive oxygen species (Wanders, 2004; Poirier et al., 2006). Recently, a novel vesicular transport pathway from mitochondria to peroxisomes has been reported (Neuspiel et al., 2008). In plants, peroxisomes, mitochondria and chloroplasts collaborate in photorespiration (Reumann and Weber, 2006).

Peroxisome biogenesis relies on a group of proteins called peroxins that are encoded by the *PEX* genes (Schrader and Fahimi, 2006; Thoms et al., 2009a). Pex3p, Pex16p and Pex19p are essential for peroxisomal membrane biogenesis in mammalian cells (Fujiki et al., 2006; Schrader and Fahimi, 2008). In yeasts, Pex3p and Pex19p play similar roles as in mammalian cells (Hetteema et al., 2000), while Pex16p is absent in yeasts except for *Y. lipolytica*, in which Pex16p functions differently, serving as a negative regulator for peroxisome division (see Section 1.4.2.3). Other peroxins take part in the import of peroxisomal matrix proteins (Platta and Erdmann, 2007; Smith and Aitchison, 2009).

### 1.3 Peroxisomal disorders

Considering the diverse functions of peroxisomes, it is not unexpected that peroxisomes are essential for normal human development and physiology (Wanders and Waterham, 2006; Schrader and Fahimi, 2008). The essential requirement for peroxisomes is underscored by the existence of more than two dozen genetic metabolic disorders, collectively called the peroxisomal disorders, in which peroxisomes are either absent or dysfunctional (van den Bosch et al., 1992; Steinberg et al., 2006; Wanders and Waterham, 2006; Schrader and Fahimi, 2008). These peroxisomal disorders are divided into two groups: the peroxisome biogenesis disorders (PBDs) and single peroxisomal protein disorders.

The PBDs traditionally consist of Zellweger syndrome, neonatal adrenoleukodystrophy, infantile Refsum disease and rhizomelic chondrodysplasia punctata type 1. At least 13 *PEX* genes (*PEX1*, 2, 3, 5, 6, 7, 10, 12, 13, 14, 16, 19, 26) are responsible for the PBDs. Zellweger syndrome is the most common PBD to cause fatality in early infancy. Its incidence has been estimated to be 1 in 50,000-100,000. The symptoms include distinct dysmorphic features and severe muscular hypotonia from birth, failure to thrive, developmental delay, and especially brain and liver dysfunction. Cells from Zellweger syndrome patients contain no peroxisomes but do contain peroxisomal membrane ghosts that lack matrix proteins. Lack of peroxisomes in Zellweger syndrome patients lead to an accumulation of very-long chain fatty acids and a decrease in plasmalogen synthesis.

The second group of peroxisomal disorders is the single peroxisomal protein disorders in which a peroxisomal enzyme or transporter is deficient. X-linked

adrenoleukodystrophy is the largest subset of this group. Affected boys exhibit severe brain demyelination. Its incidence is approximately 1 in 20,000. X-linked adrenoleukodystrophy is identified by a dysfunction in the ATP-binding cassette, subfamily D, member 1 (ABCD1) gene. This gene encodes the ALD protein, an adenosine triphosphate-binding cassette transporter that resides in the peroxisome membrane that transports very-long chain fatty acids into peroxisomes. Mutation in the ABCD1 gene results in the accumulation of very-long chain fatty acids inside cells.

There are metabolic and physical interactions between peroxisomes and mitochondria. As a result, changes in the morphology of mitochondria have frequently been observed in PBD patients (Kelley, 1983). It has been speculated that mislocalization of peroxisomal proteins to mitochondria might lead to changes in mitochondrial function that contribute to the pathology of the PBDs (Thoms et al., 2009a). In addition, both peroxisomes and mitochondria are in close association with the ER. Recent studies showed activation of the ER stress pathway in a mouse PBD model (Kovacs et al., 2009).

Allogeneic hematopoietic cell transplantation (HCT) and hematopoietic stem cell (HSC) gene therapy (Shapiro et al., 2000; Cartier et al., 2009) have been used to clinically treat X-linked adrenoleukodystrophy; however, there is no relevant therapy for PBDs.

#### **1.4 Peroxisome multiplication**

Peroxisomes are indispensable for human life. Given the importance of peroxisomes for normal cell physiology and the catastrophic health consequences of loss of peroxisomal function, molecular mechanisms have evolved to ensure the continuity of

the peroxisome population during multiple rounds of cell division. When cells divide, they duplicate the number of their peroxisomes (peroxisome replication) and distribute them equitably between the two resulting cells (peroxisome inheritance). Peroxisomes can also increase in number and size during induction (peroxisome proliferation) (see Section 1.2). Peroxisome replication and proliferation can be achieved by two distinct pathways: de novo synthesis from the ER, and growth and division of preexisting peroxisomes (Fagarasanu et al., 2007).

#### **1.4.1 Peroxisome multiplication by de novo synthesis from the ER**

Pex3p, Pex16p and Pex19p are peroxisomal membrane proteins (PMPs). As mentioned above, they are required to maintain the peroxisomal membrane in mammalian cells. Cells lacking Pex3p, Pex16p or Pex19p are devoid not only of mature peroxisomes, but also of any peroxisomal remnants. However, when the corresponding wild-type gene is restored in these mutant cells, mature peroxisomes reform (Matsuzono et al., 1999; South et al., 2000; Kim et al., 2006). Yeast cells deficient in Pex3p or Pex19p can also regenerate peroxisomes after genetic complementation (Hoepfner et al., 2005; Tam et al., 2005). The ability of peroxisomes to form de novo suggested that another organelle must provide peroxisomal membrane components. Morphological and biochemical evidence suggested that the ER is the donor compartment.

Previous morphological studies showed that peroxisomes were closely associated with the ER (Novikoff and Novikoff, 1972; Yamamoto and Fahimi, 1987; Grabenbauer et al., 2000). Three-dimensional (3D) image reconstruction using electron tomography displayed membrane continuities among the specialized regions of the ER, called

lamellar structures, and mature peroxisomes (Tabak et al., 2003). In mouse dendritic cells, the integral PMP, Pex13p, was found in specific protrusions of the ER (Tabak et al., 2003). In the plant *Arabidopsis thaliana*, the peroxisomal enzyme, ascorbate peroxidase, was also shown to be localized to a specific ER region (Lisenbee et al., 2003). Evidence of ER involvement in de novo peroxisome biogenesis came from studies of temperature-sensitive Pex3p mutants of *Y. lipolytica* (Bascom et al., 2003). In addition, biochemical studies in pulse-labeled wild-type *Y. lipolytica* cells showed modification of the peroxisomal proteins Pex2p and Pex16p by posttranslational core *N*-linked glycosylation, which only occurs in the ER, indicating that these proteins trafficked through the ER (Titorenko and Rachubinski, 1998). Also studies in *Y. lipolytica* indicated a multistep assembly and maturation pathway for peroxisomes involving a series of fusions of preperoxisomal vesicles (Titorenko et al., 2000). Moreover, the large-scale phylogenetic analysis of the yeast and rat peroxisomal proteomes demonstrated that most conserved peroxisomal proteins involved in peroxisome biogenesis or maintenance are evolutionarily related to the ER (Gabaldon et al., 2006)

However, an ER origin for peroxisomes remained controversial until studies in *S. cerevisiae* provided incontrovertible evidence that the ER is indeed the site of de novo peroxisome biogenesis. These studies took advantage of advances in three-dimensional time lapse (4D) live cell imaging (Hoepfner et al., 2005; Tam et al., 2005). In 4D live cell imaging, fluorescent protein tags, including GFP, YFP and mRFP, are attached to proteins of interest as a reporter. A series of stacks of fluorescent images of a sample are taken at different time points. By combining the stacks chronologically, a video can be made that shows the dynamics of the reporter (Hammond and Glick, 2000).

Compelling evidence for involvement of the ER in peroxisome biogenesis came from Hoepfner and coworkers who made use of the properties of the integral PMP, Pex3p (Hoepfner et al., 2005). *pex3* mutant cells lacking peroxisomal membrane structures regain functional peroxisomes upon reintroduction of the *PEX3* gene. The authors visualized the dynamic movement of newly made YFP-tagged Pex3p in *pex3* mutant cells and found that Pex3p-YFP associates initially with the ER, then targets to discrete ER-localized punctae, forming a dynamic ER subcompartment en route to the peroxisomes.

Additional evidence for the role of Pex3p in peroxisome biogenesis from the ER came from work by Tam and colleagues (Tam et al., 2005). They showed that truncated Pex3p consisting of only its first 46 N-terminal amino acids cannot restore peroxisome biogenesis. When the truncated Pex3p tagged with GFP is expressed, it accumulates in the ER. Upon expression of full-length Pex3p, the truncated Pex3p-GFP was observed to traffic from the ER to functional peroxisomes, indicating the necessity of Pex3p for trafficking from the ER to peroxisomes.

Pex3p has been shown to act in the early events of peroxisome biogenesis and to play an essential role in peroxisomal membrane biogenesis in cells from a variety of organisms (Fujiki et al., 2006). Pex3p acts to dock Pex19p, a peroxin that functions as a receptor and/or chaperone for PMPs (Fang et al., 2004). The exit of Pex3p from the ER during de novo peroxisome formation also requires Pex19p, while ER insertion of Pex3p is independent of Pex19p. A recent study suggested a role for Sec61p in Pex3p incorporation into the ER (Thoms et al., 2009b), while the ER-resident proteins Sec20p, Sec39p, and Dsl1p apparently function in the exit of Pex3p-containing structures from the ER or in the delivery of peroxisomal membrane components (Perry et al., 2009).

However, the exact mechanism by which Pex3p is targeted to and inserted into the ER is still a mystery. Additionally, the constant levels of Pex3p in the membranes of mature peroxisomes raise the question of whether Pex3p has functions other than those demonstrated for de novo biogenesis at the ER and as a Pex19p docking factor for PMP import. Recently, Pex3p has been shown to act also in peroxisome inheritance (Chang et al., 2009; Munck et al., 2009; see also Chapter 4).

#### **1.4.2 Peroxisome multiplication by growth and division**

Peroxisomes multiply not only by de novo formation from the ER but also by growth and division of preexisting peroxisomes. Which process predominates seems to depend on the cell type. In dividing mammalian cells, newly synthesized peroxisomes from the ER are the main source for the increased numbers of peroxisomes, with only a small number of peroxisomes being produced by the fission of preexisting peroxisomes (Kim et al., 2006). However, it has been shown that peroxisome number is maintained in wild-type *S. cerevisiae* cells by growth and division of preexisting peroxisomes rather than by de novo synthesis of peroxisomes from the ER (Motley and Hettema, 2007). Only *S. cerevisiae* cells that have lost peroxisomes because of a partitioning defect were observed to produce new peroxisomes from the ER. Therefore, at least in *S. cerevisiae*, the function of the ER-to-peroxisome pathway must normally be to supply existing peroxisomes with membrane components to allow them to sustain multiple rounds of growth and division.

Peroxisome division is a process that is conserved in organisms from yeasts to mammal. It happens through three sequential steps: peroxisome elongation, peroxisome

constriction and peroxisome fission. The peroxisomal Pex11 protein family members are mainly involved in the initial elongation of peroxisomes, while the molecular components implicated in constriction of peroxisomes are still speculative. For the final fission step, dynamin-related proteins (DRPs) and Fis1p are the most important components. Interestingly, some of the fission components are shared between peroxisomes and mitochondria.

#### 1.4.2.1 Peroxisome elongation by the Pex11 protein family

Pex11p of *S. cerevisiae* was the first protein shown to be involved in controlling peroxisome size and number. Peroxisomes in yeast cells lacking Pex11p were fewer but considerably larger than those of wild-type cells. In contrast, cells in which Pex11p was overexpressed contained increased numbers of peroxisomes (Erdmann and Blobel, 1995; Marshall et al., 1995). Immuno electron microscopy also showed that Pex11p overproduction led to the appearance of elongated peroxisomal structures at early times of proliferation, suggesting that these elongated structures are necessary for efficient peroxisomal fission (Marshall et al., 1995). Subsequently, additional members of this family, namely Pex25p and Pex27p, were identified in *S. cerevisiae* (Rottensteiner et al., 2003; Tam et al., 2003). The function of Pex25p and Pex27p overlap somewhat with those of Pex11p.

All members of the Pex11 protein family in *S. cerevisiae* are peripheral PMPs and interact with themselves or sometimes with each other to form homo- and heterooligomers (Marshall et al., 1996; Rottensteiner et al., 2003; Tam et al., 2003), which might be crucial to their function. For example, Pex11p homodimerization causes

loss of function, while the "monomeric" form correlates with an increase in peroxisome number (Marshall et al., 1996). In addition, Pex11p-dependent control of peroxisome population is accomplished by the combined effect of transcriptional regulation and posttranslational phosphorylation of Pex11p (Knoblach and Rachubinski, 2010). Pex11 proteins possibly have other functions. Previous studies showed that Pex11p is required for medium-chain fatty acid transport into peroxisomes (van Roermund et al., 2000), while triple deletion of all three genes of the Pex11 protein family in *S. cerevisiae* leads to a severe defect in peroxisomal matrix protein import (Rottensteiner et al., 2003). The exact molecular mechanisms underlying these functions of Pex11p remain to be established.

Mammals possess three Pex11 isoforms, PEX11 $\alpha$ , PEX11 $\beta$  and PEX11 $\gamma$ . They are all integral PMPs with their N- and C-termini exposed to the cytosol. Overproduction of PEX11 $\beta$  initially leads to peroxisome elongation, followed by the formation of numerous small peroxisomes (Schrader et al., 1998). More strikingly, overproduction of PEX11 $\beta$  in the absence of a functional DRP, DLP1/Drp1, causes long-term hypertubulation of peroxisomes (Koch et al., 2003; 2004). *dnm1* cells of the yeast *Hansenula polymorpha* deleted for the DRP, Dnm1p, exhibit a similar phenotype in that they contain a single peroxisome that forms long extensions. *pex11/dnm1* double deletion cells lack these peroxisomal extensions (Nagotu et al., 2008). This suggests that Pex11 proteins function upstream of DRPs and act in peroxisome enlargement and elongation, the first steps of peroxisomal division.

Pex11 proteins in plants also control early events of peroxisome division. There are five Pex11 isoforms in cells of *A. thaliana*, named PEX11a-e, which are all integral

PMPs. PEX11a has only its N-terminus facing the cytosol, whereas the other members have both their N- and C-termini facing the cytosol (Lingard et al., 2006; Orth et al., 2007). As in *S. cerevisiae*, Pex11 proteins in mammals and plants can interact with themselves (Li and Gould, 2003; Lingard et al., 2008), but the role of Pex11 protein oligomerization in mammals and plants is not clear. *Y. lipolytica* has three Pex11 protein family members called Pex11p, Pex11/25p and Pex11Cp (Kiel et al., 2006) whose roles in peroxisome biogenesis have not been experimentally determined.

#### 1.4.2.2 Peroxisome fission by dynamin-related proteins and Fis1 proteins

The dynamin superfamily is composed of conventional dynamins and DRPs. These proteins are large GTPases that function as membrane tubulation and fission molecules (Praefcke and McMahon, 2004). The *S. cerevisiae* DRP, Vps1p, was the first DRP found to be involved in peroxisome fission. Electron microscopy showed that peroxisomes exhibit a “beads-on-a-string” appearance in the absence of Vps1p (Hoepfner et al., 2001). Highly elongated peroxisomes that are already constricted, but cannot be divided, have also been observed in mammalian cells after knock down of the mammalian DRP, DLP1/Drp1 (Koch et al., 2004). These findings indicate that DRPs are not required for the constriction of peroxisomes but function at the last step of peroxisome division to pinch off small peroxisomes from constricted peroxisomal tubules (Yan et al., 2005). Vps1p is required for peroxisome fission during peroxisome replication and peroxisome proliferation. Another *S. cerevisiae* DRP, Dnm1p, is involved in peroxisome fission only during peroxisome proliferation (Kuravi et al., 2006; Motley and Hettema, 2007). Surprisingly, Dnm1p is also required for mitochondrial fission. The

C-terminal tail-anchored protein Fis1p, which is located both the peroxisomal membrane and the mitochondrial outer membrane, recruits Dnm1p to peroxisomes and mitochondria to promote their fission. However, recruitment of Vps1p to peroxisomes is independent of Fis1p but requires Pex19p (Vizeacoumar et al., 2006).

Like the Pex11 proteins, the main proteins required for fission of peroxisomes and mitochondria are also conserved from yeasts to mammals. In mammals, the Dnm1p homologue is DLP1/Drp1, and the Fis1p homologue is Fis1. In plants, the important DRPs for the fission of peroxisomes and mitochondria are DRP3A and DRP3B, while there are two Fis1p homologues, FIS1A and FIS1B. It is unclear how the cells manage to coordinate the fission of peroxisomes and mitochondria. Studies in mammalian cells showed that PEX11 $\beta$  expression causes increased recruitment of DLP1/Drp1 to the peroxisomal membrane (Koch et al., 2003; Li and Gould, 2003). In plants, all five PEX11 members interact with FIS1B. Furthermore, FIS1B cannot target to peroxisomes by itself, but is localized to peroxisomes when coexpressed with PEX11d or PEX11e (Lingard et al., 2008). Based on these observations, it is possible to speculate that Pex11 protein, which is controlled by transcriptional regulation and posttranslational phosphorylation, induces peroxisomal membrane elongation and recruits Fis protein to the peroxisomal membrane, where it recruits DRP to ensure peroxisome fission.

#### 1.4.2.3 Peroxisome constriction

As already discussed, Pex11 proteins control the early steps of peroxisome division, while DRPs and Fis proteins mediate the final peroxisome fission. However, the

molecular components mediating the constriction of the peroxisomal membrane are unclear.

Studies in *Y. lipolytica* have revealed a novel mechanism involving Pex16p that regulates peroxisome constriction from the peroxisome lumen. *Y. lipolytica* Pex16p is a PMP that resides on the matrix side of the peroxisomal membrane and is a negative regulator of peroxisome division (Eitzen et al., 1997; Guo et al., 2003). Pex16p acts to inhibit the formation of diacylglycerol, a cone-shaped lipid responsible for membrane curvature. The import of matrix proteins into the peroxisome promotes relocation of the peroxisomal enzyme acyl-CoA oxidase from the matrix to the membrane. The binding of acyl-CoA oxidase to Pex16p initiates the biosynthesis and transbilayer movement of diacylglycerol. The accumulation of diacylglycerol in the outer leaflet of the lipid bilayer leads to curvature and constriction of the peroxisome membrane. The fission machinery is then recruited to the peroxisome membrane to cause the final fission of peroxisomes (Guo et al., 2007).

There is no homologue of Pex16p in *S. cerevisiae*, while in mammalian cells, Pex16p is an integral PMP and functions at the ER at an early step in peroxisome biogenesis (Kim et al., 2006). Whether *S. cerevisiae* and mammalian cells use a constriction mechanism similar to the one found in *Y. lipolytica* is unknown. Intriguingly, studies have shown that some factors involved in peroxisome elongation or fission might also be involved in constriction of the peroxisome membrane. For example, Pex11 proteins exhibit domains that have the potential to bind phospholipid (Barnett et al., 2000). Phospholipid binding by Pex11p could possibly deform the peroxisomal membrane to induce peroxisome elongation and constriction. Moreover, oligomerization

of mammalian Fis protein might also mediate constriction of the tubular membrane (Serasinghe and Yoon 2008).

### **1.5 Peroxisome inheritance**

*S. cerevisiae* grows asymmetrically by budding. In order for *S. cerevisiae* cells to maintain their organelle population during the cell cycle, half of the organelles must be delivered to the growing bud before cytokinesis, while the remaining half must be retained in the mother cell. This makes *S. cerevisiae* an excellent model organism to study organelle inheritance. Some organelles, such as the ER and mitochondria, have to be inherited by the bud because they cannot be made de novo. Although *S. cerevisiae* peroxisomes can form de novo from the ER, studies have shown that the time needed for de novo peroxisome formation is longer than the length of the cell cycle (Motley and Hettema, 2007). Therefore, in order to maintain peroxisome population, the bud must efficiently inherit its peroxisomes from the mother cell upon cell division.

The successful inheritance of peroxisomes in *S. cerevisiae* has been shown to be accomplished by the transport of approximately half of the peroxisomes to the growing bud, concomitant with the active retention of the remaining peroxisomes in the mother cell (Hoepfner et al., 2001; Fagarasanu et al., 2005; Fagarasanu et al., 2006). Peroxisomes are propelled along actin cables by the class V myosin motor protein, Myo2p, which attaches to the peroxisomal membrane via the integral PMP, Inp2p (Fagarasanu et al., 2006). Meanwhile, the peripheral PMP, Inp1p, acts to retain peroxisomes in the mother cell by linking peroxisomes to an as of yet unidentified anchoring structure at the cell cortex (Fagarasanu et al., 2005).

### **1.5.1 Peroxisome dynamics in *S. cerevisiae***

During cell division in *S. cerevisiae*, peroxisomes display coordinated movements from mother cell to bud, and the average number of peroxisomes per cell is maintained. There are approximately 10 recognizable peroxisomes in each cell under fluorescence microscopy (Hoepfner et al., 2001). These peroxisomes are normally found at the cell cortex. Immediately upon bud emergence from the mother cell, a subset of peroxisomes moves into the nascent bud from the mother cell. This directional migration continues until about half of the peroxisomes are transferred to the bud. The peroxisomes retained in the mother cell maintain relatively fixed positions, while the peroxisomes transferred to the bud display complicated movements. Peroxisomes initially cluster at the growing bud tip, then spread over the entire bud cortex. Before cytokinesis, most peroxisomes are retained on the cell cortex, while a few peroxisomes in both the mother cell and bud move directionally to the bud neck region (Hoepfner et al., 2001; Fagarasanu et al., 2005; Fagarasanu et al., 2006).

### **1.5.2 Actin cables and class V myosins**

The directional movements of peroxisomes in *S. cerevisiae* are dependent on actin cables and driven by the myosin motor protein, Myo2p (Hoepfner et al., 2001).

In *S. cerevisiae*, actin filaments are primarily assembled into two structures, cortical patches and cables, both of which are concentrated toward areas of cell growth (Adams and Pringle, 1984; Kilmartin and Adams, 1984). Actin patches are nucleated by the Arp2/3 complex and mediate endocytosis, while actin cables are nucleated and

assembled by formins and serve as tracks for ATP-powered myosin V motor proteins that ferry cargoes.

Formins are a conserved class of proteins found in essentially all eukaryotic cells. They locate in the buds of *S. cerevisiae*, and from there actin polymerization occurs. Formins can bind two actin subunits and hold them so that their barbed, or plus, end is toward the formins. A new filament can grow at the plus end, while the formins remain attached to protect the plus end of the growing filament from termination by capping protein. As a result, bundles of actin filaments are dynamically formed and radiate under the cell cortex, with their plus ends anchored in the bud and their minus ends oriented toward the mother cell (Pruyne et al., 2004).

In yeasts, the myosin superfamily can be divided into 3 classes: class I myosins, class II myosins and class V myosins (Table 1-1). In *S. cerevisiae*, the class V myosin motor proteins, Myo2p and Myo4p, move diverse cargoes to distinct places at different times. For instance, Myo4p is nonessential and is responsible for the transportation of cortical ER (Estrada et al., 2003) and some mRNAs (Shepard et al., 2003) to the bud. Myo2p is essential and is involved in the inheritance of most organelles, including the trans-Golgi network (Rossanese et al., 2001), the vacuole (Tang et al., 2003), mitochondria (Altmann et al., 2008) and peroxisomes (Hoepfner et al., 2001; Fagarasanu et al., 2006). Myo2p also drives the plus ends of microtubule into the bud for orientation of the nucleus before mitosis (Yin et al., 2000) and delivers secretory vesicles to polarized sites at the cell surface (Schott et al., 1999).

**Table 1-1. Myosins in yeasts**

yeast	myosin I	myosin II	myosin V
<i>S. cerevisiae</i>	Myo3p, Myo5p	Myo1p	Myo2p, Myo4p
<i>S. pombe</i>	Myo1	Myo2, Myp2	Myo51, Myo52
<i>Y. lipolytica</i>	YALI0E02046p	YALI0F13343p	YALI0E00176p

Members of the class V myosin motor proteins possess two heavy chains and function as homodimers. Their two heads move down toward the plus ends of actin cables by ATP hydrolysis. The step size for the motor is 36 nm, consistent with the length between the helical repeats in actin filaments (Lodish et al., 2008). The long neck of class V myosins combines six light chains. The tail regions dimerize and terminate with two globular domains, which bind different cargoes through their specific receptors (Fagarasanu and Rachubinski, 2007).

### 1.5.3 Peroxisome movement by Inp2p

Inp2p has been identified as the peroxisome-specific receptor for Myo2p in *S. cerevisiae* by virtue of the following observations: First, Inp2p is an integral PMP that interacts directly with the globular tail of Myo2p. Second, in cells lacking Inp2p, peroxisome inheritance is abolished or seriously compromised, while in cells overexpressing Inp2p, the whole peroxisome population is driven from mother cell to bud. Third, Inp2p affects specifically peroxisome inheritance. In cells lacking or overexpressing Inp2p, the segregation of other organelles is normal (Fagarasanu et al., 2006).

Inp2p and its corresponding mRNA levels oscillate during the cell cycle (Spellman et al., 1998; Fagarasanu et al., 2006). Fluorescent images combined with biochemical studies showed that Inp2p becomes visible early in the cell cycle when buds emerge. Its level increases to a maximum at a time when most peroxisome transfer to the buds occurs. Then, the level of Inp2p gradually decreases until the end of the cell cycle (Fagarasanu et al., 2006). Interestingly, Inp2p is also posttranslationally regulated during the cell cycle. Phosphorylated Inp2p is more pronounced early and late in the cell cycle, when overall Inp2p levels are lower (Fagarasanu et al., 2009). Furthermore, Inp2p is not evenly distributed on all peroxisomes but preferentially accumulates on a subset of peroxisomes that eventually are transferred to buds (Fagarasanu et al., 2006).

There are two subdomains in the globular tail region of Myo2p. The vacuole-binding site of Myo2p is within subdomain I, while the binding site of Myo2p for secretory vesicles resides in subdomain II. By screening cells containing single point mutations in the tail region of Myo2p, the surface region of Myo2p that binds Inp2p has recently been identified. This Inp2p binding region in the Myo2p tail overlaps partially with the secretory vesicle binding region (Fagarasanu et al., 2009).

#### **1.5.4 Peroxisome retention by Inp1p**

During cell division, buds inherit about half of the peroxisomes from mother cells, while mother cells must actively retain half of the peroxisomes. Inp1p is a peripheral PMP of *S. cerevisiae* that is responsible for retaining peroxisomes at the mother cell cortex. In cells lacking Inp1p, peroxisomes are more mobile and are transferred completely to buds. Overexpression of Inp1p retains all peroxisomes at the mother cortex

(Fagarasanu et al., 2005). Recent studies showed Inp1p is recruited to peroxisomes by the integral PMP, Pex3p, which provides the anchor for Inp1p at the peroxisome membrane (Munck et al., 2009). Besides its function in peroxisome retention, Inp1p also has a role in peroxisome division. Cells lacking Inp1p have fewer and larger peroxisomes compared to wild-type cells. Consistent with a role in peroxisome division, Inp1p was found to interact with Vps1p and the Pex11 family member, Pex25p (Fagarasanu et al., 2005).

### **1.5.5 The relationship between Inp1p and Inp2p**

During the cell cycle, transport of half of the peroxisomes to the bud must coordinate with retention of half of the peroxisomes in the mother cell. Accordingly, there should be a temporal and spatial interplay between Inp1p and Inp2p. A tug-of-war for peroxisomes between Inp1p and Inp2p has been suggested (Fagarasanu et al., 2007). In this scenario, a certain amount of Inp1p is expressed throughout the cell cycle, implying a continuous need for Inp1p both in the mother cell and bud (Fagarasanu et al., 2005). During bud growth, increased accumulation of Inp2p on a subset of peroxisomes brings Inp2p-Myo2p complexes to actin cables, which pulls peroxisomes off the cell cortex and allows for their transport to buds. Moreover, it has been shown that cytoskeletal tracks together with motor proteins can exert tension on the membranes of organelles and aid in their division (Schrader and Fahimi, 2006). Thus, this tug-of-war for peroxisomes between Inp1p and Inp2p might also contribute to the division of peroxisomes, as has been shown in *vps1Δ/dnm1Δ* mutant cells. *vps1Δ/dnm1Δ* mutant cells normally contain one large peroxisome per cell. This giant peroxisome elongates in the bud neck region, then divides and correctly segregates between mother cell and bud

(Kuravi et al., 2006). The pulling force exerted by Inp2p-Myo2p in the bud and retention by Inp1p in the mother cell might split this big peroxisome in two (Fagarasanu et al., 2007).

Another scenario for the interplay between Inp1p and Inp2p is that their functions could be spatially and temporally regulated by the same proteins. It has been shown that Inp1p interacts with Pex3p in *S. cerevisiae* (Munck et al., 2009), while Pex3Bp, the peroxisomal receptor of myosin V of *Y. lipolytica*, also directly interacts with Pex3p (Chang et al., 2009; see also Chapter 4). Therefore, Pex3p might function as a link between peroxisome retention in mother cells and peroxisome transportation to buds. The exact mechanism by which Pex3p functions in peroxisome inheritance is unknown.

A simplified working model for peroxisome multiplication and inheritance is presented in Figure 1-1.

## **1.6 The yeast *Y. lipolytica* as a model system**

There are several advantages to using yeasts to investigate peroxisome function and biogenesis. First, the mechanisms of peroxisome assembly have been strongly conserved during evolution. Second, peroxisomes are the sole site of fatty acid  $\beta$ -oxidation in yeast, making functional peroxisomes a requirement for growth of yeast on fatty acids such as oleic acid but not on a fermentable carbon source like glucose (van der Klei and Veenhuis, 2006; Platta and Erdmann, 2007; Schrader and Fahimi, 2008). *S. cerevisiae* has been used extensively and successfully to study peroxisome assembly and inheritance; however, other yeasts divergent from *S. cerevisiae* can provide

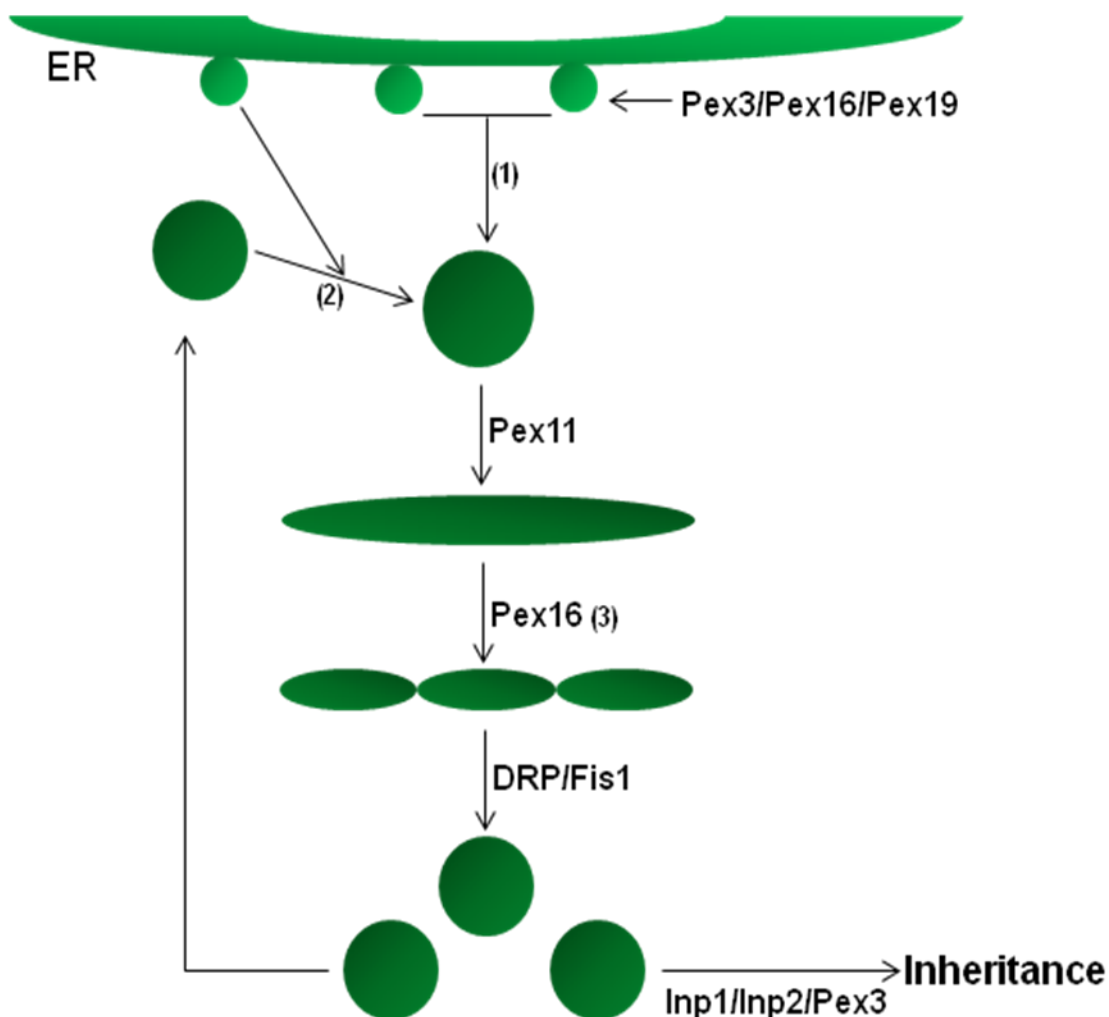


**Figure 1-1. Multiplication and inheritance of peroxisomes.** Pex3p, Pex16p and Pex19p are involved in the de novo synthesis of peroxisomes from the ER. Preperoxisomal vesicles from a specialized region of the ER fuse, which is followed by the import of other PMPs and matrix proteins (not shown here) to form mature peroxisomes (1). Preperoxisomal vesicles might also fuse with peroxisomes to supply essential membrane components (2). Peroxisome division is accomplished in three steps. Elongation of peroxisomes is initiated by the Pex11 protein family. Components involved in peroxisome constriction are largely unknown but include Pex16p in *Y. lipolytica* (3). The final fission step is catalyzed by DRPs and Fis1 proteins. In *S. cerevisiae*, inheritance of peroxisomes is mediated by Inp1p, Inp2p and Pex3p.

complementary and independent information with regards to peroxisome function, biogenesis and inheritance. Such a yeast is *Y. lipolytica*.

*Y. lipolytica* is routinely isolated from lipid-rich food, such as cheese and sausage. It is a dimorphic fungus, having the ability to change its growth pattern between yeast-like and filamentous (pseudohyphae and septate hyphae) forms in response to different environments (Barth and Gaillardin, 1996).

Compared to *S. cerevisiae*, *Y. lipolytica* grows very well on oleic acid with an accompanying massive proliferation of peroxisomes, and has proven to be an excellent model system with which to identify and characterize the processes and molecules of the peroxisome biogenic program, particularly in regards to the mechanisms of recognition and import of proteins destined for the peroxisome and of de novo synthesis of peroxisomes from the ER (van der Klei and Veenhuis, 2006). The complete sequencing of the genome of *Y. lipolytica* showed that *Y. lipolytica* is very distantly related to *S. cerevisiae* but shares a number of properties with filamentous fungi (Dujon et al., 2004). Peroxisome function and biogenesis in *Y. lipolytica* and filamentous fungi resemble more these processes in mammalian cells than in *S. cerevisiae*. Accordingly, Pex16p and isoforms of Pex11p have been identified in *Y. lipolytica* and all filamentous fungi but not in *S. cerevisiae* (Kiel et al., 2006; van der Klei and Veenhuis, 2006). For these reasons, I chose *Y. lipolytica* as my model system to study peroxisome dynamics and inheritance.

## **1.7 Focus of this thesis**

The focus of this thesis is the study of peroxisome dynamics and inheritance using the yeast *Y. lipolytica* as a model system. Herein, I report the identification and

characterization of two peroxisomal proteins, *YInp1p* and *Pex3Bp*, involved in peroxisome retention and motility, respectively, and a novel role for *Pex3p* in peroxisome inheritance.

## **CHAPTER 2**

### **MATERIALS AND METHODS**

## 2.1 Materials

### 2.1.1 Chemicals and reagents used in this study

2-mercaptoethanol	BioShop
2-( <i>N</i> -morpholino)ethanesulfonic acid (MES)	Sigma-Aldrich
2,4,6-tri-(dimethylaminomethyl)phenol (DMP30)	Marivac
3-( <i>N</i> -morpholino)propanesulfonic acid (MOPS)	EM Science
4-(2-hydroxyethyl)-1-piperazineethanesulfonic acid (HEPES)	Roche
5-bromo-4-chloro-3-indolyl- $\beta$ -D-galactoside (X-gal)	Rose Scientific
acetic acid	Sigma-Aldrich
acetone	Fisher
acrylamide	Roche
agar	Difco
agarose, UltraPure	Invitrogen
albumin, bovine serum (BSA)	Roche
ammonium bicarbonate ( $\text{NH}_4\text{HCO}_3$ )	Sigma-Aldrich
ammonium chloride ( $\text{NH}_4\text{Cl}$ )	EM Science
ammonium persulfate ( $(\text{NH}_4)_2\text{S}_2\text{O}_8$ )	BDH
ammonium sulfate ( $(\text{NH}_4)_2\text{SO}_4$ )	BDH
ampicillin	Sigma-Aldrich
anhydrous ethyl alcohol (ethanol)	Commercial Alcohols
antipain	Roche
aprotinin	Roche
benzamidine hydrochloride	Sigma-Aldrich
boric acid	EM Science
Brij 35	EM Science
bromophenol blue	BDH
chloroform	Fisher
Complete Protease Inhibitor Cocktail Tablets	Roche
complete supplement mixture (CSM)	BIO 101
concanavalin A	BIOMEDA
Coomassie Brilliant Blue R-250	ICN
<i>D</i> -(+)-glucose	EM Science
dodecenylsuccinic anhydride (DDSA)	Marivac
dithiothreitol (DTT)	Fisher
ethidium bromide	Sigma-Aldrich
ethylenediaminetetraacetic acid (EDTA)	EM Science
formaldehyde, 37% (v/v)	Biochemicals
Freund's adjuvant	Sigma-Aldrich
glass beads	Sigma-Aldrich
glutaraldehyde, 25% EM grade	EM Science
glycerol	EM Science
glycine	Roche
hygromycin B	Sigma-Aldrich

isoamyl alcohol	Fisher
isopropanol (2-propanol)	Fisher
isopropyl $\beta$ -D-thiogalactopyranoside (IPTG)	Roche
latrunculin A	Molecular Probes
leupeptin	Roche
lithium acetate	Sigma-Aldrich
<i>L</i> -leucine	Sigma-Aldrich
<i>L</i> -lysine	Sigma-Aldrich
magnesium sulfate (MgSO <sub>4</sub> )	Sigma-Aldrich
magnesium chloride (MgCl <sub>2</sub> )	Sigma-Aldrich
maltose	Sigma-Aldrich
methanol	Fisher
methyl nadic anhydride (MNA)	Marivac
MitoTracker Red CMXRos	Molecular Probes
<i>N</i> -(3-triethylammoniumpropyl)- (6(4(diethylamino)phenyl)hexatrienyl)pyridium dibromide (FM 4-64)	Molecular Probes
<i>N, N, N', N'</i> -tetramethylethylenediamine (TEMED)	EM Science
<i>N, N'</i> -dimethyl formamide (DMF)	BDH
<i>N</i> -propyl gallate	Sigma-Aldrich
nocodazole	Sigma-Aldrich
oleic acid	Fisher
Pefabloc SC	Roche
pepstatin A	Sigma-Aldrich
peptone	Difco
phenanthroline	Roche
phenol, buffer-saturated	Invitrogen
phenylmethylsulfonylfluoride (PMSF)	Roche
poly- <i>L</i> -lysine	Sigma-Aldrich
polyethylene glycol, M.W. 3350 (PEG)	Sigma-Aldrich
Ponceau S	Sigma-Aldrich
potassium acetate	BDH
potassium chloride (KCl)	BDH
potassium permanganate (KMnO <sub>4</sub> )	BDH
potassium phosphate, dibasic (K <sub>2</sub> HPO <sub>4</sub> )	EM Science
potassium phosphate, monobasic (KH <sub>2</sub> PO <sub>4</sub> )	EM Science
propylene oxide	Marivac
rhodamine-phalloidin	Molecular Probes
salmon sperm DNA, sonicated	Sigma-Aldrich
skim milk	Carnation
sodium acetate	EM Science
sodium cacodylate	Fisher
sodium carbonate (Na <sub>2</sub> CO <sub>3</sub> )	BDH
sodium chloride (NaCl)	EM Science
sodium dodecylsulfate (SDS)	Bio-Rad

sodium fluoride (NaF)	Sigma-Aldrich
sodium hydroxide (NaOH)	Sigma-Aldrich
sodium periodate (NaIO <sub>4</sub> )	Marivac
sodium phosphate, dibasic (Na <sub>2</sub> HPO <sub>4</sub> )	BDH
sodium sulfite (Na <sub>2</sub> SO <sub>3</sub> )	Sigma-Aldrich
sorbitol	EM Science
sucrose	EM Science
TAAB 812 resin	Marivac
trichloroacetic acid (TCA)	EM Science
tris(hydroxymethyl)aminomethane (Tris)	Roche
Triton X-100	VWR
tryptone	Difco
Tween 20	Sigma-Aldrich
Tween 40	Sigma-Aldrich
uracil	Sigma-Aldrich
xylene cyanol FF	Sigma-Aldrich
yeast extract	Difco
yeast nitrogen base without amino acids (YNB)	Difco

### 2.1.2 Enzymes

CIP (calf intestinal alkaline phosphatase)	NEB
Easy-A high-fidelity DNA polymerase	Stratagene
Phusion high-fidelity DNA polymerase	Biolabs
Platinum <i>Pfx</i> DNA polymerase	Invitrogen
restriction endonucleases	NEB
Quick T4 DNA ligase	NEB
RNase A (ribonuclease A), bovine pancreas	Sigma-Aldrich
T4 DNA ligase	NEB
Zymolyase 100T	ICN

### 2.1.3 Molecular size standards

1 kb DNA ladder (500-10,000 bp)	NEB
prestained protein marker, broad range (6-175 kDa)	NEB

### 2.1.4 Multicomponent systems

BigDye Terminator Cycle Sequencing Ready Reaction Kit	Applied Biosystems
DUALmembrane Kit (K20303-1)	Dualsystems Biotech AG
ECL Western Blotting Detection Kit	Amersham Biosciences
pGEM-T Vector System	Promega
pGEX Protein Fusion and Purification System	GE Healthcare
QIAprep Spin Miniprep Kit	Qiagen
QIAquick Gel Extraction Kit	Qiagen
QIAquick PCR Purification Kit	Qiagen
Ready-To-Go PCR Beads	Amersham Biosciences
Re-Blot Plus (2504)	Millipore

### 2.1.5 Plasmids

pADL-xN	Dualsystems Biotech AG
pGEM-T	Promega
pGEX-4T-1	Amersham Biosciences
pINA445	Dr. Claude Gaillardin
pMAL-c2	NEB
pTC3	Smith, 2000
pTMBV4	Dualsystems Biotech AG
pUB4	Dr. Stefan Kerscher

### 2.1.6 Antibodies

The antibodies used in this study are described in Tables 2-1 and 2-2.

**Table 2-1. Primary antibodies**

Specificity	Type	Name	Dilution <sup>a</sup>	Reference
<i>Y. lipolytica</i> Inp1p	guinea pig	T20-final	1:1,000	This study
<i>Y. lipolytica</i> Pex3Bp	guinea pig	V12-final	1:1,000	This study
<i>Y. lipolytica</i> thiolase	guinea pig	N-3 <sup>o</sup>	1:10,000	Eitzen et al., 1996
<i>Y. lipolytica</i> Pex2p	guinea pig	Pay5-NN	1:2,000	Eitzen et al., 1996
DsRed	rabbit	DsRed	1:1,000	Clontech
MBP <sup>b</sup>	rabbit	E8030S	1:10,000	NEB
GST	mouse	GST-2	1:10,000	Sigma-Aldrich
<i>S. cerevisiae</i> Sdh2p <sup>c</sup>	rabbit	Sdh2	1:5,000	Dibrov et al., 1998
tubulin <sup>d</sup>	rat	Tubulin	1:1,000	Serotec

<sup>a</sup>Dilutions are for use in immunoblotting. Dilutions used in microscopy were ten-times less.

<sup>b</sup>A gift from Dr. Gary Eitzen (University of Alberta, Edmonton, Canada).

<sup>c</sup>A gift from Dr. Bernard Lemire (University of Alberta, Edmonton, Canada).

<sup>d</sup>A gift from Dr. Neil Adames (University of Alberta, Edmonton, Canada).

**Table 2-2. Secondary antibodies**

Specificity	Type	Dilution	Source
horseradish peroxidase (HRP)-conjugated anti-rabbit IgG	donkey	1:30,000	Amersham Biosciences
HRP-conjugated anti-guinea pig IgG	goat	1:30,000	Sigma-Aldrich
rhodamine-conjugated anti-guinea pig IgG	donkey	1:250	Jackson ImmunoResearch Laboratories
AlexaFluor 680-conjugated anti-mouse IgG	goat	1:10,000	Invitrogen
AlexaFluor 750-conjugated anti-rabbit IgG	goat	1:10,000	Invitrogen
rhodamine-conjugated anti-rat IgG	guinea pig	1:1,000	Jackson ImmunoResearch Laboratories

### 2.1.7 Oligonucleotides

The oligonucleotides used in this study were synthesized by Sigma-Genosys (Oakville, Ontario) and are listed in Table 2-3.

**Table 2-3. Oligonucleotides**

Name	Sequence <sup>a,b,c</sup>	Application
0847-JC-pr7	ACGTCTCTGACTACGAGAACT	Check gene deletion
0848-JC-pr8	AGTTCTCGTAGTCAGAGACGT	Check gene deletion
1224-JC-PrP-THI	ATT <u>ATCGATA</u> AACCTACCGGTTGTTGCTCTC	pTC3 THI promoter and terminator
1225-JC-PrT-THI	ATT <u>ATCGATAT</u> CTACGACCTGGGAAACATG	pTC3 THI promoter and terminator
1262-JC-yl-inp1-Pr1	TGTTGTCGAAGAAACCGTCCC	<i>YIINP1</i> deletion
1263-JC-yl-inp1-Pr2	atactcgtcgacAAATGCTGGACGCGTAGGTAC	<i>YIINP1</i> deletion
1264-JC-yl-inp1-Pr3	gcctttgctcgacAGCTCATGAGCTCTCCCTTAC	<i>YIINP1</i> deletion
1265-JC-yl-inp1-Pr4	GGAACGTCCGAGTCGTCAATA	<i>YIINP1</i> deletion
1266-JC-yl-inp1-Pr5	cgtccagcatttGTCGACGAGTATCTGTCTGAC	<i>YIINP1</i> deletion
1267-JC-yl-inp1-Pr6	agctcatgagctGTCGACAAAGGCCTGTTTCTC	<i>YIINP1</i> deletion
1268-JC-yl-inp1-Pr7	GATATGCACTTGGCGTTTCTC	<i>YIINP1</i> deletion
1269-JC-yl-inp1-Pr8	GTAGTAGTATCAGGCTACAGC	<i>YIINP1</i> deletion
1295-JC-Pr-P1-THI	<b>GTCGACATTGGCAAGATGGTCTGCCAGGAG AGAGATATGACTAAATGGTCTGTCTGGTGGT CGTCGCCTGAGTCATCATT</b>	Integrate <i>POT1-GFP</i>
1296-JC-Pr-end-THI	GCTTGACACTTGATTTCTTCC	Check <i>POT1-GFP</i> integration
1297-JC-Pr-in GFP	AGACAACCATTACCTGTGCGAC	Check <i>POT1-GFP</i> integration
1671-JC-Inp1Pr 4	ATT <u>GAAATTCT</u> TACTTGTACAGCTCGTCCATG	mRFP tagging
1708-JC-Pr P-TC3	CCGAAAGTTGCAACTACC	Sequencing in pTC3
1709-JC-Pr T-TC3	ACTCGTACACTCGTACTC	Sequencing in pTC3

1738-JC-Pr1	ATT <u>GAATTC</u> ATGTTGTCGAAGAAACCGTCC	<i>YIINP1</i> -GFP construction
1739-JC-Pr2	tttgctagccatGGGGGTTGGAACGTCCGA	<i>YIINP1</i> -GFP construction
1741-JC-Pr3	gttccaacccccATGGCTAGCAAAGGAGAAGAA	<i>YIINP1</i> -GFP construction
1743-JC-Pr4	ATT <u>GAATTC</u> TTATTTGTAGAGCTCATCCATG	<i>YIINP1</i> -GFP construction
1784-JC-Pr-tail1	<u>GAATTC</u> ATGAACGCCAAGCGACGAAAC	Express MyoV tail in pTC3
1785-JC-Pr-tail2	<u>GAATTC</u> TTATTGGCTTGCCACTTCTTGG	Express MyoV tail in pTC3
1786-JC-Pr-pex3-1	<u>GAATTC</u> ATGGATTTCTTCAGACGGCAC	<i>YIPEX3</i> expression
1787-JC-Pr-pex3-2	<u>GAATTC</u> CCTAGAGAGCCCAATCAAAAGAT	<i>YIPEX3</i> expression
1851-JC-Pr3'-2	<a href="#">ACCATACCATAACATAATAGATCATACTCT</a> <a href="#">ACTGTACAAGTACAAGTACTGTACAAGTTCT</a> <a href="#">TGTACCTTTATCGTGAGGGTTCGTCGCCTGAG</a> TCATCATT	Integrate <i>YIINP1</i> -GFP
1852-JC-Pr1	ATT <u>GCATGC</u> ATGTTGTCGAAGAAACCGTCC	<i>YIINP1</i> -GFP construction
1853-JC-Pr4	ATT <u>GCATGC</u> TTATTTGTAGAGCTCATCCATG	<i>YIINP1</i> -GFP construction
1862-JC-Inp1start	GCC <u>GAATTC</u> ATGTTGTCGAAGAAACCGTCCC	<i>GST-YIINP1</i>
1863-JC-Inp1stop	GCC <u>GTCGAC</u> CTAGGGGGTTGGAACGTCCG	<i>GST-YIINP1</i>
1864-JC-Inp1-orf-5' for integration	<a href="#">TGCCACAACCGTCTCAAGATACAACCCAAAG</a> <a href="#">GATACGACCGACTGTGACACTCCCCATGCA</a> <a href="#">ATAATGTTGTCGAAGAAACCGTCC</a>	Integrate <i>YIINP1</i> -GFP
1971-JC-Inp1Pr4-2	ATT <u>GAATTC</u> CCTAGGGGGTTGGAACGTCCGA	pTC3- <i>YIINP1</i>
1972-PrA	ACGTTACTGGCGTGTAGAAC	Sequencing <i>YIINP1</i>
1973-PrB	TGGAAGATGATAATAACACC	Sequencing <i>YIINP1</i>
1974-PrC	TCCGAAGAACACGACTTGGA	Sequencing <i>YIINP1</i>
1975-PrD	ATGCTGACCAGAATGACGAC	Sequencing <i>YIINP1</i>
2061-JC- Pr-myotail 3	CGG <u>GAATTC</u> ATGAACGCCAAGCGACGAAAC	<i>GST-YIMyoV</i>
2062-JC-Pr-myotail 4	ATT <u>GCGGCCG</u> CTTATTGGCTTGCCACTTCTTG G	<i>GST-YIMyoV</i>
2073-JC-MBP-pex3- 5'	CGG <u>GAATTC</u> ATGGATTTCTTCAGACGGCAC	<i>MBP-PEX3</i>
2074-JC-MBP-pex3- 3'	CGG <u>AAGCTT</u> CTAGAGAGCCCAATCAAAAGA T	<i>MBP-PEX3</i>

2558-JC-Pr1	GGAACATTGGTTGATAGGCAAC	<i>PEX3B</i> deletion
2559-JC-Pr2	atactcgtcgacACGACAGTCGTCTGTGATTTCT	<i>PEX3B</i> deletion
2560-JC-Pr3	gcctttgctgacGTGTGTAGAGTGCCAGAGATTT	<i>PEX3B</i> deletion
2561-JC-Pr4	TCGTTGAGAGTGGAGTGTTTGT	<i>PEX3B</i> deletion
2562-JC-Pr5	gacgactgctgtGTCGACGAGTATCTGTCTGAC	<i>PEX3B</i> deletion
2563-JC-Pr6	cactctacacacGTCGACAAAGGCCTGTTTCTC	<i>PEX3B</i> deletion
2564-JC-Pr7	CTCTTGAGGGCGTTGTTTGAT	<i>PEX3B</i> deletion
2565-JC-Pr8	GACATGACAAAGCCCAATCGA	<i>PEX3B</i> deletion
2717-JC-Pr1	ATTGAATTCATGCTTCAGTCGCTCAACCGA	<i>PEX3B-mRFP</i>
2718-JC-Pr2	agttgttgagtCTCTCCTTAGCACGCTCCTC	<i>PEX3B-mRFP</i>
2719-JC-Pr3	tgctaaggagagACTCAAACAACGTTTGCACAG	<i>PEX3B-mRFP</i>
2720-JC-Pr4	tatatctcttcTTGTTCAAAGCTGCTGTAAATC	<i>PEX3B-mRFP</i>
2721-JC-Pr5	agctttgaacaaGAAGGAGATATACATGGCGG	<i>PEX3B-mRFP</i>
2732-JC-Pr2	tcaggcgacgacACGACAGTCGTCTGTGATTTCT	<i>PEX3B</i> deletion (Leu <sup>+</sup> )
2733-JC-Pr3	tttgttgacatGTGTGTAGAGTGCCAGAGATTT	<i>PEX3B</i> deletion (Leu <sup>+</sup> )
2734-JC-Pr5	gacgactgctgtGTCGTCGCCTGAGTCATCATT	<i>PEX3B</i> deletion (Leu <sup>+</sup> )
2735-JC-Pr6	cactctacacacATGTCACACAAACCGATCTTCG	<i>PEX3B</i> deletion (Leu <sup>+</sup> )
2736-JC-Pr7 in leu	AACGAGGCGTTCGGTCTGTA	<i>PEX3B</i> deletion (Leu <sup>+</sup> )
2738-JC-Pr8 in leu	GCAGACAGAATGGTGGCAAT	<i>PEX3B</i> deletion (Leu <sup>+</sup> )
2892-JC-Pr-Pex3B-1	CCGGAATTC AAGCGGCTCATCGAGAAGC	<i>GST-PEX3B</i>
2893-JC-Pr-Pex3B-2	CCGGTTCGACCTATTGTTCAAAGCTGCTGTAA	<i>GST-PEX3B</i>
2894-JC-Pr-P2-THI	ATCGTCGCTACTTTGCCAGT	Sequencing in pUB4
2895-JC-Pr-T2-THI	CATGAGACAGTCGGACAGAT	Sequencing in pUB4
2896-JC-Pr-3B-C'	CCGGAATTCCTATTGTTCAAAGCTGCTGTAA	<i>PEX3B</i> expression
2990-JC-TH1	CCGTCTAGAAAAATGCTTCAGTCGCTCAACCG	pTMBV4- <i>PEX3B</i>
2991-JC-TH2	CCGCCATGGAAATTGTTCAAAGCTGCTGTAAATC	pTMBV4- <i>PEX3B</i>

2992-JC-TH3	CCGGGATCCAAAAATGCTTCAGTCGCTCAAC CG	pADSL-xN-PEX3B
2993-JC-TH4	CCGGAATTCTTGTTCAAAGCTGCTGTAAATC	pADSL-xN-PEX3B
2994-JC-TH5	CCGTCTAGAAAAATGGATTTCTTCAGACGGC AC	pTMBV4-PEX3
2995-JC-TH6	CCGCCATGGAAGAGAGCCCAATCAAAGAT GAA	pTMBV4-PEX3
2996-JC-TH7	CCGGGATCCAAAAATGGATTTCTTCAGACGG CAC	pADSL-xN-PEX3
2997-JC-TH8	CCGGAATTCGAGAGCCCAATCAAAGATGA	pADSL-xN-PEX3
3000-JC-TH11	CCGGGATCCAAAAATGAACGCCAAGCGACG AAAC	pADSL-xN-YIMyoV
3001-JC-TH12	CCGGAATTCTTGGCTTGCCACTTCTTGGTAG	pADSL-xN-YIMyoV
3099-JC-MBP-3B	CGGGAATTCATGCTTCAGTCGCTCAACCGA	<i>MBP-PEX3B</i>
3100-JC-MBP-3B	CGGAAGCTTCTATTGTTCAAAGCTGCTGTAA	<i>MBP-PEX3B</i>
3327-JC-Ylinp2- mRFP Pr1	GCCGAATTCATGAACGTCATATTCGAAAACA C	<i>YAL10E03124g-mRFP</i>
3328-JC-Ylinp2- mRFP Pr2	TATATCTCCTTCACGGTTTTTCGAGGACCGTT	<i>YAL10E03124g-mRFP</i>
3329-JC-Ylinp2- mRFP Pr3	CTCGAAAACCGTGAAGGAGATATACATGGC GGA	<i>YAL10E03124g-mRFP</i>
3330-JC-Ylinp2Pr1	GCCGAATTCATGAACGTCATATTCGAAAACA C	pTC3-YAL10E03124g and <i>MBP-YAL10E03124g</i>
3331-JC-Ylinp2Pr2	ATTGAATTCTCAACGGTTTTTCGAGGACCG	pTC3-YAL10E03124g and <i>MBP-YAL10E03124g</i>
3495-Ylinp2-GFP-2	tttgtagccatACGGTTTTTCGAGGACCGTTT	<i>YAL10E03124g-GFP</i>
3496-Ylinp2-GFP-3	ctcgaaaaccgtATGGCTAGCAAAGGAGAAGAA	<i>YAL10E03124g-GFP</i>
4397-Ylinp2-GFP-4	CCGGAATTCTTATTTGTAGAGCTCATCCATG	<i>YAL10E03124g-GFP</i>

<sup>a</sup> Restriction endonuclease recognition sites are underlined.

<sup>b</sup> Overlapping parts for fusion PCR are in lowercase.

<sup>c</sup> Extra base pairs added to amplified DNA are colored blue.

### 2.1.8 Standard buffers and solutions

The compositions of routinely used buffered solutions are given in Table 2-4.

**Table 2-4. Common solutions**

Solution	Composition	Reference
1 × PBS	137 mM NaCl, 2.7 mM KCl, 8 mM Na <sub>2</sub> HPO <sub>4</sub> , 1.5 mM K <sub>2</sub> HPO <sub>4</sub> , pH 7.4	Pringle et al., 1991
1 × protease inhibitor (PIN) cocktail	1 µg/ml each of antipain, aprotinin, leupeptin, pepstatin, 0.5 mM benzamidine hydrochloride, 5 mM NaF, 1 mM PMSF or 0.5 mg Pefabloc SC/ml	Smith, 2000
1 × TBST	20 mM Tris-HCl, pH 7.5, 150 mM NaCl, 0.05% (w/v) Tween 20	Huynh et al., 1988
1 × Transfer buffer	20 mM Tris, 150 mM glycine, 20% (v/v) methanol	Towbin et al., 1979; Burnette, 1981
5 × SDS-PAGE running buffer	0.25 M Tris-HCl, pH 8.8, 2 M glycine, 0.5% SDS	Ausubel et al., 1989
10 × TBE	0.89 M Tris-borate, 0.89 M boric acid, 0.02 M EDTA	Maniatis et al., 1982
2× sample buffer	20% (v/v) glycerol, 167 mM Tris-HCl, pH 6.8, 2% SDS, 0.005% bromophenol blue	Ausubel et al., 1989
6 × DNA loading dye	0.25% bromophenol blue, 0.25% xylene cyanol, 30% (v/v) glycerol	Maniatis et al., 1982
Breakage buffer	2% (v/v) Triton X-100, 1% SDS, 100 mM NaCl, 10 mM Tris-HCl, pH 8.0, 1 mM EDTA, pH 8.0	Ausubel et al., 1989
Disruption buffer	20 mM Tris-HCl, pH 7.5, 0.1 mM EDTA, pH 7.5, 100 mM KCl, 10% (w/v) glycerol	Eitzen, 1997
Ponceau stain	0.1% Ponceau S, 1% TCA	Szilard, 2000
Solution B	100 mM KH <sub>2</sub> PO <sub>4</sub> , 100 mM K <sub>2</sub> HPO <sub>4</sub> , 1.2 M sorbitol	Pringle et al., 1991
TE	10 mM Tris-HCl, pH 7.0-8.0 (as needed), 1 mM EDTA	Maniatis et al., 1982

## 2.2 Microorganisms and culture conditions

### 2.2.1 Bacterial strains and culture conditions

The *Escherichia coli* strains and culture media used in this study are described in Tables 2-5 and 2-6, respectively. Bacteria were grown at 37°C. Cultures of 5 ml or less were grown in culture tubes in a rotary shaker at 200 rpm. Cultures greater than 5 ml were grown in flasks in a rotary shaker at 250 rpm. Culture volumes were approximately 20% of flask volumes.

**Table 2-5. *E. coli* strains**

Strain	Genotype	Source
<i>DH5α</i>	F <sup>+</sup> , Φ80 <i>dlacZ</i> ΔM15, Δ( <i>lacZYA-argF</i> ), U169, <i>recA1</i> , <i>endA1</i> , <i>hsdR17</i> (r <sub>k</sub> <sup>-</sup> , m <sub>k</sub> <sup>+</sup> ), <i>phoA</i> , <i>supE44</i> , λ <sup>-</sup> , <i>thi-1</i> , <i>gyrA96</i> , <i>relA1</i>	Invitrogen
<i>BL21(DE3)</i>	F <sup>+</sup> , <i>ompT</i> , <i>hsdSB</i> (r <sub>B</sub> <sup>-</sup> m <sub>B</sub> <sup>-</sup> ) <i>gal</i> , <i>dcm</i> (DE3)	Novagen

**Table 2-6. Bacterial culture media**

Medium	Composition	Reference
LB <sup>a,b</sup>	1% tryptone, 0.5% yeast extract, 1% NaCl	Maniatis et al., 1982
SOB	2% tryptone, 0.5% yeast extract, 10 mM NaCl, 2.5 mM KCl	Maniatis et al., 1982
TYP <sup>a</sup>	1.6% tryptone, 1.6% yeast extract, 0.5% NaCl, 0.25% K <sub>2</sub> HPO <sub>4</sub>	Promega Protocols and Applications Guide, 1989/1990

<sup>a</sup>Ampicillin was added to 100 μg/ml for plasmid selection when necessary.

<sup>b</sup>For solid media, agar was added to 1.5%.

## 2.2.2 Yeast strains and culture conditions

The *Y. lipolytica* and *S. cerevisiae* strains used in this study are listed in Table 2-7. Yeast culture media are described in Table 2-8. Yeasts were grown at 30°C unless otherwise indicated. Cultures of 10 ml or less were grown in 16 × 150-mm glass tubes in a rotating wheel. Cultures greater than 10 ml were grown in flasks in a rotary shaker at 250 rpm. Culture volumes were approximately 20% of flask volumes.

**Table 2-7. *Y. lipolytica* and *S. cerevisiae* strains**

Strain	Genotype	Reference
<i>Y. lipolytica</i> <i>E122<sup>a</sup></i>	<i>MATA, ura3-302, leu2-270, lys8-11</i>	Claude Gaillardin, Thiverval-Grignon,
<i>Ylinp1Δ</i>	<i>MATA, ura3-302, leu2-270, lys8-11, Ylinp1::URA3</i>	This study
<i>E122/POT1-GFP</i>	<i>MATA, ura3-302, leu2-270, lys8-11, pot1::POT1-GFP(LEU2)</i>	This study
<i>Ylinp1Δ/POT1-GFP</i>	<i>MATA, ura3-302, leu2-270, lys8-11, Ylinp1::URA3, pot1::POT1-GFP(LEU2)</i>	This study
<i>YIINP1-GFP</i>	<i>MATA, ura3-302, leu2-270, lys8-11, Ylinp1::YIINP1-GFP(LEU2)</i>	This study
<i>pex3BΔ</i>	<i>MATA, ura3-302, leu2-270, lys8-11, pex3B::URA3</i>	This study
<i>pex3Δ</i>	<i>MATA, ura3-302, leu2-270, lys8-11, pex3::URA3</i>	Bascom et al., 2003
<i>pex3BΔ/POT1-GFP</i>	<i>MATA, ura3-302, leu2-270, lys8-11, pex3B::URA3, pot1::POT1-GFP(LEU2)</i>	This study
<i>pex3Δ/POT1-GFP</i>	<i>MATA, ura3-302, leu2-270, lys8-11, pex3::URA3, pot1::POT1-GFP(LEU2)</i>	This study
<i>pUB4-PEX3B-mRFP</i>	<i>MATA, ura3-302, leu2-270, lys8-11, pUB4(HygB<sup>R</sup>)PEX3B-mRFP</i>	This study
<i>pUB4-PEX3B-mRFP/POT1-GFP</i>	<i>MATA, ura3-302, leu2-270, lys8-11, pUB4(HygB<sup>R</sup>)PEX3B-mRFP, pot1::POT1-GFP(LEU2)</i>	This study
<i>pUB4-MyoVtail/POT1-GFP</i>	<i>MATA, ura3-302, leu2-270, lys8-11, pUB4(HygB<sup>R</sup>)MyoVtail, pot1::POT1-GFP(LEU2)</i>	This study

<i>pTC3-YAL10E3124g-mRFP/POT1-GFP</i>	<i>MATA, ura3-302, leu2-270, lys8-11, pTC3(URA3) YAL10E3124g-mRFP, pot1::POT1-GFP(LEU2)</i>	This study
<i>pex3BΔ/pUB4-PEX3B/POT1-GFP</i>	<i>MATA, ura3-302, leu2-270, lys8-11, pex3B::URA3, pUB4(HygB<sup>R</sup>)PEX3B, pot1::POT1-GFP(LEU2)</i>	This study
<i>pex3BΔ/pUB4-PEX3/POT1-GFP</i>	<i>MATA, ura3-302, leu2-270, lys8-11, pex3B::URA3, pUB4(HygB<sup>R</sup>)PEX3, pot1::POT1-GFP(LEU2)</i>	This study
<i>pex3Δ/pUB4-PEX3B/POT1-GFP</i>	<i>MATA, ura3-302, leu2-270, lys8-11, pex3::URA3, pUB4(HygB<sup>R</sup>)PEX3B, pot1::POT1-GFP(LEU2)</i>	This study
<i>pex3Δ/pUB4-PEX3/POT1-GFP</i>	<i>MATA, ura3-302, leu2-270, lys8-11, pex3::URA3, pUB4(HygB<sup>R</sup>)PEX3, pot1::POT1-GFP(LEU2)</i>	This study
<i>S. cerevisiae DSY-1</i>	<i>MATa, his3Δ200, trp1-901, leu2-3, 112 ade2, LYS2::(lexAop)4-HIS3, URA3::(lexAop)8-LacZ) GAL4</i>	Dualsystems Biotech AG

**Table 2-8. Yeast culture media**

Medium	Composition <sup>a,b</sup>	Reference
Nonfluorescent medium	6.61 mM KH <sub>2</sub> PO <sub>4</sub> , 1.32 mM K <sub>2</sub> HPO <sub>4</sub> , 4.06 mM MgSO <sub>4</sub> ·7H <sub>2</sub> O, 26.64 mM (NH <sub>4</sub> )SO <sub>4</sub> , 1 × CSM, 2% glucose, 1% agarose	Tam, 2005
SM	0.67% YNB, 2% glucose, 1× CSM without leucine, lysine or uracil, as required	Tam, 2005
YPA <sup>d</sup>	1% yeast extract, 2% peptone, 2% sodium acetate	Brade, 1992
YPD <sup>d</sup>	1% yeast extract, 2% peptone, 2% glucose	Rose et al., 1988
YNA <sup>c</sup>	0.67% YNB, 2% sodium acetate	Brade, 1992
YND <sup>c</sup>	0.67% YNB, 2% glucose	Rose et al., 1988
YNO <sup>c</sup>	0.67% YNB, 0.05% (w/v) Tween 40, 0.1% (v/v) oleic acid	Nuttley et al., 1993
YPBO <sup>d</sup>	0.3% yeast extract, 0.5% peptone, 0.5% K <sub>2</sub> HPO <sub>4</sub> , 0.5% KH <sub>2</sub> PO <sub>4</sub> , 0.2% (w/v) Tween 40 or 1% (v/v) Brij 35, 1% (v/v) oleic acid	Kamiryo et al., 1982

<sup>a</sup>For solid media, agar was added to 2%.

<sup>b</sup>Glucose and oleic acid were added after autoclaving.

<sup>c</sup>Supplemented with leucine, lysine or uracil, each at 50 μg/ml, as required.

<sup>d</sup>Supplemented with hygromycin B at 125 μg/ml, as required.

## **2.3 Introduction of DNA into microorganisms**

### **2.3.1 Chemical transformation of *E. coli***

Plasmid DNA was introduced into subcloning efficiency, chemically competent *E. coli* DH5 $\alpha$  cells, as recommended by the manufacturer (Invitrogen). Essentially, 1 to 2  $\mu$ l of ligation reaction (Section 2.5.7) or 0.5  $\mu$ l (0.25  $\mu$ g) of plasmid DNA was added to 25  $\mu$ l of cells. The mixture was incubated on ice for 30 min, subjected to a 45 sec heat shock at 37°C, and chilled on ice for 2 min. One ml of LB medium (Table 2-6) was added, and the cells were incubated in a rotary shaker for 45 to 60 min at 37°C. Cells were spread onto LB agar plates (Table 2-6) containing ampicillin and incubated overnight at 37°C. 100  $\mu$ l of 2% X-gal in DMF and 50  $\mu$ l of 100 mM IPTG were added to agar plates to allow for blue/white selection of colonies carrying recombinant plasmids, when necessary.

### **2.3.2 Electroporation of *E. coli***

For high-efficiency transformation of *E. coli* DH5 $\alpha$  or BL21(DE3) cells with plasmid DNA, cells were made electrocompetent as recommended by Invitrogen. Cells were grown overnight in 10 ml of SOB medium (Table 2-6). 0.5 ml of this overnight culture was transferred to and incubated in 500 ml of SOB medium until the culture reached an OD<sub>600</sub> (optical density at a wavelength of 600 nm) of 0.5. Cells were harvested by centrifugation at 2,600  $\times$  g for 15 min at 4°C, washed twice with 500 ml of ice-cold 10% (v/v) glycerol, and resuspended in a minimal amount of 10% (v/v) glycerol. Cells were either used immediately or frozen as 100  $\mu$ l aliquots by immersion in a dry

ice/ethanol bath and stored at  $-80^{\circ}\text{C}$ . For transformation,  $1\ \mu\text{l}$  of ligation reaction or  $0.5\ \mu\text{l}$  of plasmid DNA was added to  $20\ \mu\text{l}$  of cells. The mixture was placed between the bosses of an ice-cold disposable microelectroporation chamber (width  $\sim 0.15\ \text{cm}$ ) (Whatman Biometra) and submitted to an electrical pulse of  $395\ \text{V}$  (amplified to  $\sim 2.4\ \text{kV}$ ) at a capacitance of  $2\ \mu\text{F}$  and a resistance of  $4\ \text{k}\Omega$  using a Cell-Porator connected to a Voltage Booster (Whatman Biometra). Cells were then immediately transferred to  $1\ \text{ml}$  of LB, incubated in a rotary shaker at  $37^{\circ}\text{C}$  for 45 to 60 min, and spread on LB agar plates containing ampicillin.

### **2.3.3 Chemical transformation of *Y. lipolytica***

Plasmid DNA was introduced into *Y. lipolytica* according to the procedure of Gietz and Woods (2002). Essentially,  $25\ \mu\text{l}$  of cells were scraped with a sterile toothpick from a plate not more than one week old and resuspended in  $1\ \text{ml}$  of water. Cells were harvested by centrifugation, resuspended in  $1\ \text{ml}$  of  $100\ \text{mM}$  lithium acetate, and incubated at  $30^{\circ}\text{C}$  for 5 min. Cells were again harvested by centrifugation, and the following components were added in order on top of the cell pellet:  $240\ \mu\text{l}$  of 50% PEG,  $36\ \mu\text{l}$  of  $1\ \text{mM}$  lithium acetate,  $10\ \mu\text{l}$  of  $10\ \text{mg}$  sheared salmon sperm DNA/ml,  $3\ \mu\text{l}$  of plasmid DNA and  $63\ \mu\text{l}$  of water. The mixture was vortexed vigorously for 1 min and incubated at  $42^{\circ}\text{C}$  for 20 min. Cells were harvested by centrifugation, resuspended gently in  $200\ \mu\text{l}$  of water and plated onto SM agar plates (Table 2-8) or YPD plates supplemented with hygromycin B at  $125\ \mu\text{g/ml}$ . Plates were incubated at  $30^{\circ}\text{C}$  for 3 days for colony formation.

### **2.3.4 Electroporation of *Y. lipolytica***

Cells were made electrocompetent as recommended by Ausubel et al. (1989). Cells were grown overnight in 10 ml of YPA, and the culture was transferred to 40 ml of YPA and incubated for 4 to 5 h or until it reached an  $OD_{600}$  of  $\sim 1.0$ . Cells were then harvested by centrifugation at  $2,000 \times g$ , resuspended in 50 ml TE 7.5 (Table 2-4) containing 100 mM lithium acetate, and incubated for 30 min at room temperature or  $30^{\circ}\text{C}$  with gentle agitation. DTT was added to a final concentration of 20 mM, and the incubation was continued for another 15 min. Cells were harvested by centrifugation at  $2,000 \times g$ , washed once with 50 ml each of room-temperature water, ice-cold water, and ice-cold 1 M sorbitol. Cells were resuspended in a minimal volume of ice-cold 1 M sorbitol. 20  $\mu\text{l}$  of cells were mixed with 1  $\mu\text{l}$  of plasmid DNA or 500 to 750 ng of purified DNA fragment, placed between the bosses of an ice-cold microelectroporation chamber, submitted to an electrical pulse of 250 V (amplified to  $\sim 1.6$  kV) at a capacitance of 2  $\mu\text{F}$  and a resistance of 4  $\text{k}\Omega$  using a Cell-Porator connected to a Voltage Booster (Whatman Biometra). Cells were immediately resuspended in 100  $\mu\text{l}$  of ice-cold 1 M sorbitol and plated onto SM agar plates or YPD plates supplemented with hygromycin B at 125  $\mu\text{g}/\text{ml}$ . Plates were incubated at  $30^{\circ}\text{C}$  for 3 to 5 days for colony formation.

## **2.4 Isolation of DNA from microorganisms**

### **2.4.1 Isolation of plasmid DNA from bacteria**

Single bacterial colonies were inoculated into 2 ml of LB containing ampicillin and incubated overnight at  $37^{\circ}\text{C}$ . Cells were harvested by microcentrifugation, and plasmid DNA was isolated using a QIAprep Spin Miniprep Kit according to the

manufacturer's instructions (Qiagen). This method is based on the alkaline lysis of bacterial cells, followed by adsorption of DNA onto silica in the presence of high salt and elution of DNA in low salt buffer. Plasmid DNA was usually eluted in 30 to 50  $\mu$ l of the supplied elution buffer.

#### **2.4.2 Isolation of chromosomal DNA from yeast**

Yeast genomic DNA was prepared as recommended by Ausubel et al. (1989). Cells were grown overnight in 10 ml of YPD, harvested by centrifugation for 5 min at  $2,000 \times g$ , washed twice in 10 ml of water, and transferred to a 2.0-ml microcentrifuge tube. 200  $\mu$ l each of breakage buffer (Table 2-4), glass beads and phenol/chloroform/isoamyl alcohol (25:24:1) were added to the cells. The mixture was vortexed for 3 to 5 min at  $4^{\circ}\text{C}$  to break yeast cells and separate nucleic acids from proteins. 200  $\mu$ l of TE 8.0 (Table 2-4) were added, and the mixture was vortexed briefly. The organic and aqueous phases were separated by centrifugation at  $16,000 \times g$  for 5 min at room temperature. The aqueous phase was extracted once against an equal volume of phenol/chloroform/isoamyl alcohol (25:24:1). DNA was precipitated by the addition of 2.5 volumes of absolute ethanol and centrifugation at  $16,000 \times g$  for 5 min at room temperature. The pellet was washed once with 1 ml of 70% (v/v) ethanol, dried in a rotary vacuum desiccator and dissolved in 50  $\mu$ l of TE 8.0 containing 100  $\mu$ g RNase A/ml. DNA was incubated at  $37^{\circ}\text{C}$  for 1 to 2 h to allow for digestion of RNA.

## **2.5 DNA manipulation and analysis**

Unless otherwise indicated, reactions were carried out in 1.5-ml microcentrifuge tubes, followed by centrifugation at  $16,000 \times g$ .

### **2.5.1 Amplification of DNA by the polymerase chain reaction (PCR)**

PCR was used to amplify specific DNA sequences or to introduce modifications in the amplified DNA sequence. Primer design, reaction components and cycling conditions were performed following standard protocols (Innis and Gelfand, 1990; Saiki, 1990). A reaction usually contained 0.1 to 0.5  $\mu\text{g}$  of yeast genomic DNA or 0.1 to 0.2  $\mu\text{g}$  of plasmid DNA, 20 pmol of each primer, 0.25 mM of each dNTP, 1 mM  $\text{MgSO}_4$ , and 1.25 U of Easy-A high-fidelity polymerase or Platinum *Pfx* DNA polymerase in a final volume of 50  $\mu\text{l}$  in the supplied reaction buffer (Stratagene). Reactions were performed in 0.6-ml microcentrifuge tubes in a Robocycler 40 with a Hot Top attachment (Stratagene). Alternatively, Ready-to-Go PCR Beads were used as recommended by the manufacturer (Amersham Biosciences).

### **2.5.2 Digestion of DNA by restriction endonucleases**

In general, 1 to 2  $\mu\text{g}$  of plasmid DNA or purified DNA were digested by restriction endonucleases for 1 to 1.5 h according to the manufacturer's instructions. Digestion was immediately terminated by agarose gel electrophoresis of the DNA fragments, except for plasmid DNA, which first required dephosphorylation.

### **2.5.3 Dephosphorylation of 5'-ends**

Plasmid DNA linearized by one restriction endonuclease was subjected to dephosphorylation at its 5'-ends to prevent intramolecular ligation. After digestion of plasmids, reactions were mixed with 10 U of CIP and incubated at 37°C for 30 min. The dephosphorylation reaction was terminated by agarose gel electrophoresis of the DNA fragments.

### **2.5.4 Separation of DNA fragments by agarose gel electrophoresis**

DNA fragments in solution were mixed with 0.2 volume of 6 × DNA loading dye (Table 2-4) and separated by electrophoresis in 1% agarose gels in 1 × TBE (Table 2-4) containing 0.5 µg of ethidium bromide/ml. Gels were subjected to electrophoresis at 10 V/cm in 1 × TBE. DNA fragments were visualized on an ultraviolet transilluminator (Photodyne, Model 3-3006).

### **2.5.5 Purification of DNA fragments from agarose gel**

A DNA fragment of interest was excised from the agarose gel using a razor blade. DNA was extracted from the agarose slice using the QIAquick Gel Extraction Kit according to manufacturer's instructions (Qiagen). This method is based on the dissolution of agarose gel and adsorption of DNA to the silica membrane in the presence of a high concentration of chaotropic salts, followed by washing and elution of DNA in the presence of low salt. DNA was usually eluted in 30 to 50 µl of the supplied elution buffer.

### **2.5.6 Purification of DNA from solution**

Contaminants (oligonucleotides, salts, enzymes, etc.) were removed from a DNA solution using the QIAquick PCR Purification Kit as described by the manufacturer (Qiagen). The principle of this method is similar to that of the QIAquick Gel Extraction Kit (Section 2.5.5), except that no dissolution of agarose gel was involved. DNA was usually eluted in 30 to 50  $\mu$ l of the supplied elution buffer.

### **2.5.7 Ligation of DNA fragments**

DNA fragments treated with restriction endonucleases and purified as described in Section 2.5.5 were ligated using 1  $\mu$ l of T4 DNA ligase in the buffer supplied by the manufacturer (NEB). The reaction was typically done in a volume of 10  $\mu$ l, with the molar ratio of plasmid to insert being between 1:3 and 1:10, and incubated overnight at 16°C. Alternatively, 1  $\mu$ l of Quick T4 DNA ligase (NEB) in 1  $\times$  Quick Ligation Buffer was used in a reaction volume of 20  $\mu$ l. The reaction was incubated at room temperature for 10 min.

Occasionally, PCR products after purification by agarose gel electrophoresis were ligated to the vector pGEM-T using the pGEM-T Vector System according to the manufacturer's instructions (Promega).

### **2.5.8 DNA sequencing**

DNA sequencing was performed using the BigDye Terminator v1.1/3.1 Cycle Sequencing Ready Reaction Kit as described by the manufacturer (Applied Biosystems). This method is based on the method of Sanger et al. (1977) and involves the random

incorporation of fluorescent dideoxy terminators during the elongation of DNA sequences with a modified version of *Taq* DNA polymerase. Essentially, a reaction contained 1  $\mu$ l of plasmid DNA, 3.2 pmol of primer, 3  $\mu$ l of Terminator Ready Reaction Mix, and 2.5  $\mu$ l of the supplied 5  $\times$  buffer in a total volume of 20  $\mu$ l. The reaction was subjected to cycle sequencing using the Robocycler 40 with a Hot Top attachment and the following conditions: 1 cycle at 96°C for 2 min; 25 cycles at 96°C for 46 sec, 50°C for 51 sec and 60°C for 4 min 10 sec; 1 cycle at 6°C to hold until ready to purify DNA. Reaction products were precipitated by addition of 80  $\mu$ l of 75% (v/v) 2-propanol for 20 min at room temperature, subjected to microcentrifugation at 16,000  $\times$  g for 20 min, washed twice with 250  $\mu$ l of 75% 2-propanol, dried in a rotary vacuum desiccator, resuspended in 15  $\mu$ l of Template Suppression Reagent, heated at 95°C for 2 min, immediately cooled on ice, and separated by capillary electrophoresis. Fluorescence was detected and recorded by an ABI 310 Genetic Analyzer (Applied Biosystems).

## **2.6 Protein manipulation and analysis**

### **2.6.1 Preparation of yeast whole cell lysates**

Lysates were prepared from yeast cells by disruption with glass beads (adapted from Needleman and Tzagoloff, 1975). Cells were harvested by centrifugation at 2,000  $\times$  g for 5 min, washed twice with 10 ml of water, and resuspended in an equal volume of ice-cold disruption buffer (Table 2-4) containing 1  $\times$  PIN (Table 2-4) and 1 mM DTT. Ice-cold glass beads were added until they reached the meniscus of the cell suspension. The mixture was vortexed for 5 min at 4°C, and the glass beads were pelleted by

microcentrifugation for 20 sec at 4°C. The supernatant was recovered and clarified by microcentrifugation for 20 min at 4°C.

Alternatively, yeast lysates were prepared by denaturation of cells with alkaline and reducing agents. Cells were harvested by centrifugation at  $2,000 \times g$  for 5 min, transferred to a microcentrifuge tube, and resuspended in 240 to 500  $\mu\text{l}$  of 1.85 M NaOH and 7.4% 2-mercaptoethanol. The cell suspension was incubated on ice for 5 min and mixed with an equal volume of 50% TCA by vortexing. The mixture was further incubated on ice for 5 min and subjected to microcentrifugation at  $16,000 \times g$  for 10 min at 4°C. The pellet was washed once with water, resuspended first in 50 to 150  $\mu\text{l}$  of Magic A (1 M unbuffered Tris, 13% SDS) and then in an equal volume of Magic B (30% (v/v) glycerol, 200 mM DTT, 0.25% bromophenol blue). The mixture was boiled for 10 min and subjected to microcentrifugation at  $16,000 \times g$  for 1 min. The supernatant was collected for sodium dodecyl sulfate-polyacrylamide gel electrophoresis (SDS-PAGE) (Section 2.6.4).

### **2.6.2 Precipitation of proteins**

Proteins were precipitated from solution by addition of TCA to a final concentration of 10% and incubation on ice for 30 min to overnight. Precipitates were collected by microcentrifugation at  $16,000 \times g$  for 30 min at 4°C. The pellet was washed twice with 1 ml of ice-cold acetone, dried in a rotary vacuum dessicator and dissolved in  $2 \times$  sample buffer (Table 2-4).

### **2.6.3 Determination of protein concentration**

The protein concentration of a sample was determined by the method of Bradford (1976). A standard curve was prepared by adding 1 ml of Bio-Rad Protein Assay Dye to 100  $\mu$ l aliquots of water containing 0, 2, 4, 6, 8, 10, 12, 14, 16, 18 or 20  $\mu$ g of BSA. Samples were incubated for 5 min at room temperature, and absorbance was measured at 595 nm using a Beckman DU640 spectrophotometer. Absorbance values were plotted against the BSA concentrations to generate a standard curve. Absorbance of a protein sample was measured in the same way as for the BSA standards, and the protein concentration was estimated by comparing the absorbance value of the sample to the standard curve.

### **2.6.4 Separation of proteins by electrophoresis**

Proteins were separated by SDS-PAGE as described by Ausubel et al. (1989). Protein samples were mixed with an equal volume of 2  $\times$  sample buffer containing 10 mM DTT, denatured by boiling for 5 min, and separated by electrophoresis on discontinuous slab gels. Stacking gels contained 3% acrylamide, 60 mM Tris-HCl, pH 6.8, 0.1% SDS, 0.1% (v/v) TEMED, and 0.1% ammonium persulfate. Resolving gels contained 10% acrylamide, 370 mM Tris-HCl, pH 8.8, 0.1% SDS, 0.1% (v/v) TEMED, and 0.043% ammonium persulfate. Electrophoresis was done in 1  $\times$  SDS-PAGE running buffer (Table 2-4) at 50-200 V using a Bio-Rad Mini Protean II vertical gel system.

### **2.6.5 Detection of proteins by gel staining**

Proteins in polyacrylamide gels were visualized by staining with 0.1% Coomassie Brilliant Blue R-250, 10% (v/v) acetic acid, 35% (v/v) methanol for 1 h with gentle agitation. Unbound dye was removed by multiple washes in 10% (v/v) acetic acid, 35% (v/v) methanol. Gels were dried for 1 h at 80°C on a Bio-Rad Model 583 gel drier.

### **2.6.6 Detection of proteins by immunoblotting**

Proteins separated by SDS-PAGE were transferred to nitrocellulose membrane (Bio-Rad) in 1 × transfer buffer (Table 2-4) at 100 mA for 16 h at room temperature using a Trans-Blot tank transfer system with plate electrodes (Bio-Rad). Proteins transferred to nitrocellulose were visualized by staining in Ponceau stain (Table 2-4) for several min and destaining in water. The nitrocellulose was incubated in blocking solution (1% skim milk powder, 1 × TBST (Table 2-4)) with gentle agitation to prevent nonspecific binding of antibodies. Specific proteins on nitrocellulose were detected by incubation with primary antibody in blocking solution for 1 h at room temperature with gentle agitation. The nitrocellulose was then incubated with appropriate HRP-labeled secondary antibody in blocking solution for 1 h. After each antibody incubation, unbound antibodies were removed by washing the nitrocellulose three times with 1 × TBST for 10 min each. Antigen-antibody complexes were detected using an ECL Western Blotting Detection Kit according to the manufacturer's instructions (Amersham Biosciences) and exposing the nitrocellulose to X-Omat BT film (Kodak).

Used nitrocellulose could be reblotted using a Re-Blot Plus (2504) Kit according to the manufacturer's instructions (Millipore). The nitrocellulose was incubated with 1 ×

Antibody Stripping Solution at room temperature for 15 to 30 min with gentle agitation, rinsed with  $1 \times$  TBST, and blotted as described above.

## **2.7 Subcellular fractionation of *Y. lipolytica* cells**

### **2.7.1 Peroxisome isolation from *Y. lipolytica***

Peroxisomes were isolated from *Y. lipolytica* cells according to Aitchison (1992). Essentially, cells grown in oleic acid-containing medium were harvested by centrifugation at  $800 \times g$  in a Beckman JA10 rotor at room temperature and washed twice with water. Cells were then resuspended in spheroplasting solution (0.5 M KCl, 5 mM MOPS, pH 7.2, 10 mM sodium sulfite, 0.25 mg Zymolyase 100T/ml) at a concentration of 4 ml per g of wet cells and incubated at 30°C for 30 min with gentle agitation. Spheroplasts were harvested by centrifugation at  $2,200 \times g$  in a Beckman JS13.1 rotor for 8 min at 4°C and resuspended in homogenization buffer (5 mM MES, pH 5.5, 1 M sorbitol) containing  $1 \times$  PIN (Table 2-4) at a ratio of 3 ml per g of wet cells. Resuspended spheroplasts were transferred to a homogenization mortar and disrupted by 10 strokes of a Teflon pestle driven at 1,000 rpm by a stirrer motor (Model 4376-00, Cole-Parmer). Cell debris, unbroken cells and nuclei were separated from the postnuclear supernatant (PNS) by centrifugation at  $1,000 \times g$  in a Beckman JS13.1 rotor for 10 min at 4°C. The PNS was fractionated by centrifugation at  $20,000 \times g$  in a Beckman JS13.1 rotor for 30 min at 4°C into a pellet (20KgP) enriched for heavy organelles including peroxisomes and mitochondria and a supernatant (20KgS) enriched for cytosol.

The 20KgP was resuspended in homogenization buffer and loaded onto a discontinuous sucrose gradient (4.67 ml of 25%, 7 ml of 35%, 14 ml of 42% and 7 ml of

53% (w/w) sucrose in 5 mM MES, pH 5.5). Organelles were separated by centrifugation at  $100,000 \times g$  for 80 min at 4°C in a Beckman VTi50 rotor. 18 fractions of 2 ml each were collected from the bottom of the gradient.

### **2.7.2 Extraction and subfractionation of peroxisomes**

Extraction and subfractionation of peroxisomes were performed according to Smith (2000) with modifications. Essentially, organelles in the 20KgP fraction (containing ~50  $\mu$ g of protein) were lysed by incubation in 10 volumes of ice-cold Ti8 buffer (10 mM Tris-HCl, pH 8.0) containing 2  $\times$  complete protease inhibitor cocktail (Roche) on ice for 1 h with occasional vortexing and separated by ultracentrifugation at  $200,000 \times g$  for 1 h at 4°C in a Beckman TLA120.2 rotor into a membrane-enriched pellet fraction (Ti8P) and a matrix-enriched soluble fraction (Ti8S). The Ti8P fraction was resuspended in ice-cold Ti8 to a final protein concentration of 0.5 mg/ml and mixed with 10 volumes of ice-cold 0.1 M Na<sub>2</sub>CO<sub>3</sub>, pH 11.3. The mixture was incubated on ice for 45 min with occasional vortexing and subjected to ultracentrifugation at  $200,000 \times g$  for 1 h at 4°C in a TLA120.2 rotor to yield a fraction enriched for integral membrane proteins (CO<sub>3</sub>P) and a fraction enriched for peripheral membrane proteins (CO<sub>3</sub>S).

## **2.8 Microscopy**

### **2.8.1 Immunofluorescence microscopy**

Indirect immunofluorescence microscopy of yeast cells was performed according to Pringle et al. (1991) with modifications. Cells grown in oleic acid-containing medium were fixed in 3.7% (v/v) formaldehyde for 30 min at room temperature with occasional

agitation. Cells were then collected by centrifugation at  $2,000 \times g$  for 5 min, washed with 4 ml of solution B (Table 2-4), and resuspended in solution B at a concentration of 1 ml per 100  $\mu$ l of wet cells. The cell suspension was mixed with 40  $\mu$ g of Zymolyase 100T/ml and 38 mM 2-mercaptoethanol and incubated for 15 to 60 min at 30°C with gentle rotation. Spheroplasts were spotted onto slides precoated with poly-*L*-lysine and allowed to dry at room temperature. Spheroplasts were permeabilized by immersion of the slides in -20°C methanol for 6 min and -20°C acetone for 30 sec and allowed to dry. Slides were put in a dark humid box at room temperature for the following procedures. Spheroplasts were covered with 50  $\mu$ l of blocking solution (Section 2.6.6) for 1 h. They were incubated with primary antibody diluted in blocking solution for 1 h, washed 10 to 20 times with  $1 \times$  TBST, and then incubated with secondary antibody conjugated to rhodamine diluted in blocking solution for 1 h. Spheroplasts were washed again 10 to 20 times with  $1 \times$  TBST and covered with one drop of mounting medium (0.4% *N*-propyl gallate, 74.8% (w/v) glycerol in PBS, pH 7.4). Coverslips were placed on top of slides, and the edges were sealed with nail polish. Images were captured on a LSM510 META (Carl Zeiss) laser scanning microscope or on an Olympus 1X2 UCB microscope equipped with a digital fluorescence camera.

### **2.8.2 Electron microscopy**

Cells were processed for electron microscopy as described by Goodman et al. (1990). All microcentrifugations were performed at  $16,000 \times g$  for 1 min, and all incubations were done in 1.5-ml microcentrifuge tubes at room temperature with agitation, unless indicated otherwise.

Cells were harvested and washed twice with water. Approximately 100  $\mu$ l of cell pellet were fixed in 1 ml of 3%  $\text{KMnO}_4$  for 15 min, washed twice with water, and incubated in 1 ml of 1% sodium periodate for 10 min. Cells were pelleted, washed once with water, and incubated with 1 ml of 1%  $\text{NH}_4\text{Cl}$  for 10 min. Cells were again pelleted, washed once with water, and subjected to serial dehydration in 60%, 80%, 95%, and 100% ethanol and in propylene oxide. Each incubation was for 5 min. Incubation in propylene oxide was repeated four times. Cells were collected and incubated in 1 ml of a 1:1 mixture of propylene oxide and resin (a mixture of TAAB 812 resin, DDSA, MNA and DMP30 in proportions suggested by the manufacturer (Marivac)) for 1 h. Cells were then pelleted and resuspended in 1 ml of resin. Incubation in resin was for 1 h with agitation and for 3 h in a fume hood with open microcentrifuge tubes. Finally, cells were harvested by microcentrifugation for 8 min, and small amounts of cells were transferred to embedding capsules (EM Science) containing resin. Embedding capsules were placed in an oven at 60°C to allow the resin to polymerize. Ultra-thin sections were cut by Honey Chan using an Ultra-Cut E Microtome (Reichert-Jung) and examined on a Phillips 410 electron microscope. Images were captured with a digital camera (Soft Imaging System). Occasionally, cells were prefixed in 1 ml of 3% glutaraldehyde in 0.1 M cacodylate buffer, pH 7.2, for 20 min at 4°C with agitation. Cells could be stored at 4°C until needed for processing for electron microscopy, as described above.

### **2.8.3 Confocal 4D video microscopy**

Cells synthesizing a genomically encoded chimera between Pot1p and GFP (Pot1p-GFP) were grown in YPD medium and then incubated in YPBO medium as

described in legends to figures. 4-Dimensional (4D) in vivo video microscopy was performed on an Axiovert 200 microscope equipped with a LSM 510 META confocal scanner (Fagarasanu et al., 2006). For Figures 4-6 A and B and Movies 4-S1 and S2, cells were placed in a 35-mm petri dish with a 14-mm microwell No. 1.5 borosilicate coverglass (MatTek) coated with concanavalin A and incubated at a constant temperature of 28°C on a microscope stage in a cage dual incubator controlled by Read-Temperature software (Okolab, Italy). Images were captured with a LCI Plan-Neofluar 63×/1.3 numerical-aperture multi-immersion differential interference contrast objective with an adjustable correction collar (Carl Zeiss). For other figures and movies, cells were placed in a chambered #1.0 borosilicate coverglass (Lab-Tek) coated with concanavalin A and incubated at room temperature (23°C) for image capture with a Plan-Apochromat 63×/1.4 numerical-aperture oil differential interference contrast objective (Carl Zeiss). A piezoelectric actuator was used to drive continuous objective movement, allowing for the rapid collection of *z*-stacks (Hammond and Glick, 2000). The sides of each pixel represent 0.085 (for figures and movies in Chapter 3) or 0.09 μm (for figures and movies in Chapter 4) of the sample. In Chapter 3, stacks of 13 (Movie 3-S4), 14 (Movies 3-S5, 6 and 7), 15 (Movie 3-S2) or 16 (Movies 3-S1 and 3) optical sections spaced 0.45 μm apart were captured every 12 sec, except for Movie 3-S4 in which stacks were captured every 2 min. In Chapter 4, stacks of 30 optical sections spaced 0.3 μm apart were captured every 60 sec. GFP was excited using a 488-nm laser, and its emission was collected using a 505-nm long-pass filter.

In Chapter 3, images were filtered three times using a 3 × 3 hybrid median filter to reduce shot noise. Fluorescence images from each stack were projected using an

average intensity algorithm that involved multiplication of each pixel value by an appropriate enhancement factor for better contrast. Correction for exponential photobleaching of GFP was performed by exponentially increasing the enhancement factor with each projection. The transmitted light images from each stack were projected using a maximum intensity algorithm. The resulting projections were smoothed by means of a blurring algorithm. These operations were performed with NIH Image (<http://rsb.info.nih.gov/nih-image/>). Adobe Photoshop (Adobe Systems) was used to merge the fluorescent and transmitted light projections. Processed projections were assembled into videos using Apple QuickTime Pro 6.5.2 at a rate of 10 frames per second, except for Movie 3-4, which was at 6 frames per second. Postprocessing operations such as peroxisome tracking and 3D reconstruction were performed using Imaris 4.1 (Bitplane).

In Chapter 4, experimentally generated 3D and 4D data sets were deconvolved through an iterative classic maximum likelihood estimation algorithm and an experimentally derived point spread function using Huygens Professional software (Scientific Volume Imaging BV, The Netherlands) to remove blur. Imaris software (Bitplane) was subsequently used to prepare maximum intensity projections or “Blend-view” projections of the deconvolved 3D and 4D data sets. These projections were used to generate single images or videos. The collections of images were then assembled into figures using Adobe Photoshop CS3 and Adobe Indesign CS3 (Adobe Systems). The transmission images with labeled mitochondria or vacuoles in Figure 4 B were altered to display only the cell border, thereby allowing better visualization, but no alteration, of

data from the fluorescent channels. The “Circular Marquee” tool in Adobe Photoshop CS3 was used to select data from the transmission channel and delete them from images.

In Chapter 3, peroxisome velocity was measured as the frame-to-frame displacement of peroxisomes over the time interval between two consecutive frames using MetaMorph software (Universal Imaging). Movements in both mother cells and buds were measured. For each peroxisome, maximal velocity achieved is presented. Velocities may be underestimates, since movements perpendicular to the focal plane were not considered.

In Chapter 4, Figure 4-4 D, peroxisomes were outlined for better visualization using the “Pencil” tool in Adobe Photoshop CS3.

#### **2.8.4 Quantification of rates of peroxisome inheritance**

Rates of peroxisome inheritance were quantified as described (Fagarasanu et al., 2006). Essentially, cells expressing Pot1p-GFP were grown in YPD medium for 16 h and then transferred to and incubated in YPBO medium for different times as described in figure legends. Peroxisomes were visualized by direct fluorescence confocal microscopy. For each randomly chosen field, three optical sections of 5- $\mu\text{m}$  thickness each were collected at a z-axis spacing of 1.6  $\mu\text{m}$  using a high detector gain to ensure the capture of weak fluorescent signals. Optical sections were then projected onto a single image. All visibly budded cells were considered for analysis, and buds were assigned to four categories of bud volume, expressed as a percentage of mother cell volume (Category I, 0-12%; Category II, 13-24%; Category III, 25-36%; Category IV, 37-48%). Since cell volume is not directly accessible, bud area was first measured using Zeiss LSM510 Image Browser software and grouped into four “area” categories, which superimpose on

the aforementioned “volume” categories if a spherical geometry is assumed for all cells, according to bud cross-sectional area expressed as a percentage of mother cell cross-sectional area (Category I, 0-24%; Category II, 25-39%; Category III, 40-50%; Category IV, 50-61%). Bud tips were then scored using an all-or-none criterion for the presence or absence of peroxisomal fluorescence. To measure the efficiency of peroxisome inheritance in cells expressing the globular tail domain of the type V myosin of *Y. lipolytica*, budded cells were assigned to two size categories: “small budded cells” representing the merger of Categories I and II and “large budded cells” representing the merger of Categories III and IV.

## **2.9 Construction of plasmids for gene expression**

### **2.9.1 pTC3-YIINP1**

The *Y. lipolytica* expression plasmid pTC3 contains a unique EcoRI site between the promoter and terminator regions of the *POT1* gene encoding the peroxisomal matrix enzyme 3-ketoacyl-coenzyme A (CoA) thiolase (Pot1p) (Smith, 2000). The ORF of *YIINP1* was amplified by PCR using primers 1738 and 1971, which contain the recognition sequence for EcoRI. The PCR product was digested with EcoRI and ligated into the EcoRI site of pTC3 to produce the plasmid pTC3-YIINP1. Sequencing using primers 1708 and 1709 was used to confirm the insertion of *YIINP1* in the correct orientation into pTC3.

### 2.9.2 pINA445-mRFP-SKL and pINA445-POT1-GFP

To construct the *Y. lipolytica* expression plasmid pINA445-mRFP-SKL, DNA encoding mRFP-SKL and flanked by promoter and terminator sequences of the *POT1* gene was amplified by PCR from pTC3-mRFP-SKL (Tam, 2005) using primers 1224 and 1225 and Easy-A enzyme. The amplified DNA was ligated into pGEM-T and transformed into *E. coli*. Plasmid was isolated and cut with ClaI, and the insert was ligated into the ClaI site of pINA445 to produce pINA445-mRFP-SKL. pINA445-POT1-GFP was constructed in essentially the same manner as pINA445-mRFP-SKL except that *POT1-GFP* flanked by the promoter and terminator sequences of the *POT1* gene was amplified from pTC3-THI-GFP (Tam, 2005).

### 2.9.3 pTC3-PEX3B, pTC3-PEX3 and pTC3-MyoVtail

The *PEX3B* gene has a 203-bp intron. Fusion PCR was used to construct an expression plasmid, pTC3-PEX3B, lacking this intron. Primers 2717 and 2718 were used to amplify by PCR the portion of the *PEX3B* ORF 5' to the intron, while primers 2719 and 2896 were used to amplify the portion of the *PEX3B* ORF 3' to the intron. These two fragments were linked by PCR using primers 2717 and 2896, which contain the EcoRI recognition sequence. The product was cleaved with EcoRI and ligated into the EcoRI site of pTC3 to produce pTC3-PEX3B. Sequencing was used to confirm the correct orientation of *PEX3B*.

The ORF of *PEX3* was amplified by PCR using primers 1786 and 1787 containing the EcoRI recognition sequence, ligated into pGEM-T, and transformed into *E. coli*. Plasmid was isolated from transformants and cut with EcoRI, and the insert was

ligated into the EcoRI site of pTC3 to produce pTC3-PEX3. Sequencing was used to confirm the correct orientation of *PEX3*.

To construct pTC3-MyoVtail, a DNA fragment encoding the globular tail region (amino acids 1092-1594) of the class V myosin of *Y. lipolytica* was amplified by PCR using primers 1784 and 1785 containing the EcoRI recognition sequence, ligated into pGEM-T, and transformed into *E. coli*. Plasmid was isolated from transformants and cut with EcoRI, and the insert was ligated into the EcoRI site of pTC3 to produce pTC3-MyoVtail. Sequencing was used to confirm the correct orientation of *MyoVtail*.

#### **2.9.4 pTC3-PEX3B-mRFP and pTC3-YALI0E03124g-mRFP**

The *PEX3B* ORF was amplified by PCR from pTC3-PEX3B using primers 2717 and 2720 (Section 2.9.3). Primers 2721 and 1671 were used to amplify DNA encoding mRFP. The PEX3B-mRFP fusion was amplified by fusion PCR using primers 2717 and 1671 containing the EcoRI recognition sequence. The fusion product was cleaved with EcoRI and ligated into the EcoRI site of pTC3 to produce pTC3-PEX3B-mRFP. Sequencing was used to confirm the correct orientation of *PEX3B-mRFP*.

The ORFs of YALI0E03124g and for mRFP were amplified by PCR using primer pairs 3327 and 3328, and 3329 and 1671, respectively. The amplified ORFs were linked by PCR using primers 3327 and 1671 containing the EcoRI recognition sequence. The linked product was cleaved with EcoRI and ligated into the EcoRI site of pTC3 to produce pTC3-YALI0E03124g-mRFP. Sequencing was used to confirm the correct orientation of *YALI0E03124g-mRFP*.

### **2.9.5 pUB4-PEX3B, pUB4-PEX3, pUB4-MyoVtail and pUB4-PEX3B-mRFP**

*PEX3B* flanked by the promoter and terminator regions of the *POT1* gene encoding peroxisomal thiolase (Pot1p) was amplified by PCR from pTC3-PEX3B using primers 1224 and 1225 containing the *Cla*I recognition sequence. The PCR product was cleaved with *Cla*I and ligated into the *Cla*I site of pUB4 to make the plasmid pUB4-PEX3B. The genes *PEX3*, *MyoVtail* and the chimeric gene *PEX3B-mRFP* were amplified from pTC3-PEX3, pTC3-MyoVtail and pTC3-PEX3B-mRFP, respectively, together with the promoter and terminator regions of *POT1* by PCR using primers 1224 and 1225 containing the *Cla*I recognition site, cleaved with *Cla*I and ligated into *Cla*I-cleaved pUB4 to make the plasmids pUB4-PEX3, pUB4-MyoVtail and pUB4-PEX3B-mRFP.

## **2.10 Integrative disruption of *Y. lipolytica* genes**

### **2.10.1 Integrative disruption of *YIINP1***

The *URA3* gene of *Y. lipolytica* was used for targeted integrative disruption of the *YIINP1* gene. Targeted integrative disruption of the *YIINP1* gene was performed by overlapping PCR. An ~1.7-kilobase pair fragment containing the *Y. lipolytica URA3* gene, a 282 base pair fragment from the 5'-end of the *YIINP1* gene ORF, and a 268 base pair fragment from the 3'-end of the *YIINP1* gene ORF were amplified by PCR using primer pairs 1266 and 1267, 1262 and 1263, and 1264 and 1265, respectively. The three amplified products were used as templates for overlapping PCR using primers 1262 and 1265 to produce a fragment containing the *URA3* gene flanked at its 5'-end by 282 base pairs and at its 3'-end by 268 base pairs of the *YIINP1* ORF. This fragment was used to transform *Y. lipolytica* wild-type strain *E122* or the wild-type *E122/POT1-GFP* strain

(Section 2.11.1) to uracil prototrophy (Section 2.3.4). Ura<sup>+</sup> transformants were selected and screened by PCR using primer pairs 0847 and 1269, and 0848 and 1268 for determination of correct integration of the *URA3* gene into the *YIINP1* locus.

### **2.10.2 Integrative disruption of *PEX3B***

*PEX3B* was deleted by PCR-based integrative transformation of yeast, essentially as described for integrative disruption of the *YIINP1* gene. An ~1.7-kilobase pair fragment containing the *Y. lipolytica* *URA3* gene, a 507-base pair fragment from the 5'-end of the *PEX3B* gene ORF, and a 431-base pair fragment from the 3'-end of the *PEX3B* gene ORF were amplified by PCR using primer pairs 2562 and 2563, 2560 and 2561, and 2558 and 2559, respectively. The three amplified products were used as templates for overlapping PCR using primers 2558 and 2561 to produce a fragment containing the *URA3* gene flanked at its 5'-end by 501 base pairs and at its 3'-end by 431 base pairs of the *PEX3B* ORF. This fragment was used to transform *Y. lipolytica* wild-type strain *E122* or the wild-type *E122/POT1-GFP* strain to uracil prototrophy. Ura<sup>+</sup> transformants were selected and screened by PCR using primer pairs 0847 and 2564, and 0848 and 2565, for determination of correct integration of the *URA3* gene into the *PEX3B* locus.

### **2.10.3 Construction of the *PEX3A/PEX3BA* double deletion strain**

Targeted integrative disruption of the *PEX3* gene by the *URA3* gene of *Y. lipolytica* to make the strain *pex3Δ* was done by Roger Bascom as previously described (Bascom et al., 2003). An ~2.3-kilobase pair fragment containing the *Y. lipolytica* *LEU2* gene, a 507-base pair fragment at the 5'-end of the *PEX3B* gene ORF, and a 431-base pair

fragment at the 3'-end of the *PEX3B* gene ORF were amplified by PCR using primer pairs 2734 and 2735, 2733 and 2561, and 2558 and 2732, respectively. The three amplified products were used as templates for overlapping PCR using primers 2558 and 2561 to produce a fragment containing the *LEU2* gene flanked at its 5'-end by 501 base pairs and 3'-end by 431 base pairs of the *PEX3B* ORF. This fragment was used to transform the *Y. lipolytica pex3Δ* strain to leucine prototrophy (Section 2.3.4). Leu<sup>+</sup> transformants were selected and screened by PCR using primer pairs 2736 and 2564, and 2738 and 2565 for determination of correct integration of the *LEU2* gene into the *PEX3B* locus of the *pex3Δ* strain to make the *pex3Δ/pex3BΔ* double deletion strain.

## **2.11 Genomic tagging of *Y. lipolytica* genes with the ORF for GFP**

### **2.11.1 *YIPOT1***

Sequencing was used to confirm the correct orientation of *POT1-GFP* in pINA445-POT1-GFP. An ~6-kilobase pair fragment containing the *LEU2* gene and the *POT1-GFP* fusion flanked by the promoter and terminator regions of the *POT1* gene were amplified by PCR from the plasmid pINA445-POT1-GFP (Section 2.9.2) using Phusion polymerase and primers 1225 and 1295. The DNA fragment was used to transform *Y. lipolytica* wild-type strain *E122* and the *pex3Δ* mutant strain to leucine prototrophy. Leu<sup>+</sup> transformants were selected and screened by PCR using primers 1296 and 1297 for determination of correct integration of *POT1-GFP* into the *POT1* locus.

### 2.11.2 *YIINP1*

The ORF of the *YIINP1* gene was amplified by PCR using primers 1738 and 1739. The ORF for GFP was amplified by PCR using primers 1741 and 1743. These two fragments were linked together by fusion PCR using primers 1738 and 1743 containing the EcoRI recognition sequence. The linked product, *YIINP1-GFP*, was cleaved with EcoRI and ligated into the EcoRI site of pTC3 to produce pTC3-*YIINP1-GFP*. Primers 1852 and 1853 containing the SphI recognition sequence were used to amplify *YIINP1-GFP* from pTC3-*YIINP1-GFP* with Easy-A enzyme, and the product was ligated into pGEM-T. *YIINP1-GFP* was cleaved from pGEM-T by SphI and ligated into the SphI site of pINA445 to produce pINA445-*YIINP1-GFP*. Sequencing was used to confirm the correct orientation of *YIINP1-GFP*. An ~5.6-kilobase pair fragment containing the *LEU2* gene and the *YIINP1-GFP* fusion was amplified by PCR from pINA445-*YIINP1-GFP* using Phusion polymerase and primers 1864 and 1851. The DNA fragment was used to transform *Y. lipolytica* wild-type strain *E122* to leucine prototrophy. Leu<sup>+</sup> transformants were selected and screened by PCR to determine correct integration of *YIINP1-GFP* into the *YIINP1* locus.

### 2.12 Split-ubiquitin membrane yeast two-hybrid analysis

Split-ubiquitin membrane yeast two-hybrid analysis was performed using the DUALmembrane Kit (K20303-1) (Dualsystems Biotech AG).

### 2.12.1 Construction of chimeric genes

Physical interactions between Pex3Bp, Pex3p and the globular tail (amino acids 1092-1594) of the class V myosin of *Y. lipolytica* were detected using the split-ubiquitin membrane yeast two-hybrid system (Stagljar et al., 1998). Bait vectors were constructed by amplifying the sequences of target genes by PCR and ligating them into the plasmid vector pTMBV4 in-frame and upstream of DNA encoding the C-terminal half of ubiquitin (Cub) and the chimeric transcriptional reporter LexA-VP-16 to make the construct, gene-Cub-LexA-VP-16. Prey vectors were constructed by ligating target genes into the vector plasmid pADL-xN in-frame and upstream of DNA encoding the N-terminal half of ubiquitin (NubG) to make the construct, gene-NubG. The primers used to amplify the DNA fragments of interest for two-hybrid analysis are listed in Table 2-9.

**Table 2-9. Construction of plasmids for two-hybrid analysis**

DNA	Primers	Plasmid for insertion
<i>PEX3</i>	2994, 2995	pTMBV4
<i>PEX3B</i>	2990, 2991	pTMBV4
<i>PEX3</i>	2996, 2997	pADL-xN
<i>PEX3B</i>	2992, 2993	pADL-xN
<i>YIMyoV</i> (aa 1092-1594)	3000, 3001	pADL-xN

### 2.12.2 Assay for two-hybrid interaction

*S. cerevisiae* strain *DSY-1* was transformed with both bait and prey plasmids. Transformants were grown on SM agar lacking the amino acids leucine (auxotrophic

selection marker for the bait vector pTMBV4) and tryptophan (auxotrophic selection marker for the prey vector pADL-xN). Interaction between bait and prey was shown by expression of *HIS3* and growth on SM agar lacking histidine and by activation of the *LacZ* reporter gene and production of blue color from a chromogenic substrate in a  $\beta$ -galactosidase filter assay.

### 2.13 Assay for direct protein interaction

A glutathione-S-transferase (GST) fusion protein of the globular tail (amino acids 1092-1594) of the class V myosin of *Y. lipolytica* (GST-YIMyoV) was constructed using the GST fusion vector, pGEX-4T-1 (GE Healthcare). The recombinant plasmid encoding the fusion between GST and the tail of the class V myosin Myo2p of *S. cerevisiae* (GST-ScMyoV) (Fagarasanu et al., 2006) was a kind gift from Dr. Andrei Fagarasanu (Department of Cell Biology, University of Alberta). Recombinant expression and immobilization of GST, GST-YIMyoV and GST-ScMyoV were done according to the manufacturer's instructions. Maltose-binding protein (MBP) fusions to Pex3p, Pex3Bp, and YALIOE03124p were made using pMAL-c2 (NEB) and expressed in the *E. coli* strain *BL21* (Invitrogen). The recombinant plasmid encoding the fusion between MBP and *S. cerevisiae* Vam6p was kindly provided by Dr. Gary Eitzen (Department of Cell Biology, University of Alberta). MBP-ScInp2p has been reported (Fagarasanu et al., 2006). The primers used to amplify the DNA fragments of interest for direct protein interaction are listed in Table 2-10.

**Table 2-10. Construction of plasmids for direct protein interaction**

DNA	Primers	Plasmid for insertion
<i>YIMyoV</i> (aa 1092-1594)	2061, 2062	pGEX-4T-1
<i>PEX3</i>	2073, 2074	pMAL-c2
<i>PEX3B</i>	3099, 3100	pMAL-c2
<i>YALI0E03124g</i>	3330, 3331	pMAL-c2

250  $\mu$ g of purified GST, GST-ScMyoV or GST-YIMyoV protein immobilized on glutathione resin were incubated with 250  $\mu$ g of *E. coli* lysate containing an MBP fusion or MBP alone in H-buffer (20 mM HEPES, pH 7.4, 120 mM NaCl, 5 mM MgCl<sub>2</sub>, 0.5 mM DTT, 0.5% (v/v) Triton X-100, 1  $\times$  complete protease inhibitors (Roche)) for 3 h at 4°C on a rocking platform. The immobilized fractions were allowed to settle and were then washed five times with H-buffer and eluted in sample buffer (50 mM Tris-HCl, pH 6.8, 2% SDS, 5% (v/v) glycerol, 0.001% bromophenol blue, 5% (v/v) 2-mercaptoethanol). The eluted proteins were subjected to SDS-PAGE. Immunoblotting with rabbit antibodies to MBP (NEB) and mouse monoclonal antibodies to GST (Sigma-Aldrich), combined with AlexaFluor 680/750-conjugated goat anti-mouse/anti-rabbit antibodies (Invitrogen), was used to detect protein interactions in the assay for direct protein binding. Immunoblots were processed using an Odyssey digital imaging system (Li-Cor Biosciences) with resolution set at 84  $\mu$ m and at highest quality.

## **2.14 Staining cell structures**

### **2.14.1 Staining actin**

Yeast cells grown in 10 ml of YPD overnight at 30°C were subcultured in fresh YPD, grown to an OD<sub>600</sub> of ~0.2, and fixed by addition of formaldehyde to a final concentration of 4% for 5 min. The cells were then resuspended in PBS (Table 2-4), mixed with formaldehyde for a final concentration of 4%, and incubated for 30 min at room temperature on a rotating wheel. The fixed cells were washed twice with PBS and resuspended in 500 µl of PBS. 10 µl of rhodamine-conjugated phalloidin (Molecular Probes, Eugene, OR) dissolved in methanol were added to 100 µl of cells. The cells were incubated in the dark on a rotating wheel for 1 h at 4°C, washed five times with PBS, and visualized by epifluorescence or confocal microscopy.

### **2.14.2 Staining vacuoles with FM 4-64**

Vacuoles were labeled with the lipophilic styryl dye, *N*-(3-triethylammoniumpropyl)-4-(*p*-diethylaminophenyl-hexatrienyl) pyridinium dibromide (FM 4-64) (adapted from Vida and Emr, 1995). Cells were grown in 10 ml of YPD overnight at 30°C, subcultured into fresh YPD, and grown to an OD<sub>600</sub> of ~0.5. 6 µl of FM 4-64 dye (Molecular Probes) from a stock of 2 mg/ml in DMSO were added to 250 µl of cells, and the cells were incubated at 30°C for 1 h on a rotating wheel. The cells were washed twice with fresh YPD, resuspended in 5 ml of YPD and incubated on a rotating wheel at 30°C for 2-3 h. Cells were harvested by centrifugation and visualized by confocal microscopy.

### **2.14.3 Staining mitochondria with MitoTracker Red**

Mitochondria were stained with MitoTracker Red CMXRos according to the manufacturer's instructions (Molecular Probes). Essentially, cells were grown in 10 ml of YPD overnight at 30°C, subcultured into fresh YPD, and grown to an OD<sub>600</sub> of ~1.0. Cells were resuspended in prewarmed (30°C) YPD containing MitoTracker Red CMXRos at 200 nM made from a stock solution of 1 mM in DMSO and incubated at 30°C on a rotating wheel for 45 min. The cells were resuspended in fresh prewarmed (30°C) YPD, incubated for 1 h at 30°C and visualized by confocal microscopy.

## **2.15 Cytoskeleton disruption**

### **2.15.1 Actin depolymerization**

Cells were grown in 10 ml of YPD overnight at 30°C, subcultured into fresh YPD and grown to an OD<sub>600</sub> of ~0.2. Latrunculin A (Molecular Probes) was added to the cells to a final concentration of 100 µM from a stock of 200 mM in DMSO. Cells were incubated for 15 min at room temperature and then stained with rhodamine-phalloidin (Section 2.13.1) to confirm disruption of actin.

### **2.15.2 Microtubule depolymerization**

Cells were grown overnight in 10 ml of YPD at 30°C, subcultured into fresh YPD to an OD<sub>600</sub> of 0.2 and then grown to an OD<sub>600</sub> of ~0.4. Nocodazole was added to a final concentration of 2.5 µg/ml from a stock of 5 mg/ml in DMSO. Cells were grown at 30°C for approximately 2 h, at which time approximately 95% of the cells arrested at the large-

budded stage. Immunofluorescence microscopy with anti-tubulin antibodies was used to confirm disruption of microtubules.

## 2.16 Antibody production

Antibodies were raised in guinea pigs against proteins of interest as follows.

DNA fragments were cloned into pGEX-4T-1 downstream and in-frame to the ORF for GST. Plasmids were transformed into *E. coli DH5 $\alpha$*  or *BL21* cells (Table 2-5). Synthesis of fusion proteins was induced by addition of IPTG to a final concentration of 1 mM to growing cells (OD<sub>600</sub> of ~0.5). Cells were incubated in the presence of IPTG for 2-3 h at 37°C, harvested by centrifugation, resuspended, and lysed by sonication bursts of 30 sec using a Branson Sonifier 250 (duty 30%, output control 3). Cell debris was pelleted by centrifugation. Fusion proteins in the supernatant were purified according to the Recombinant Protein Purification Handbook (GE Healthcare). Thrombin protease was used to digest fusion proteins according to the manufacturer's instructions (GE Healthcare).

Proteins were further purified by gel electrophoresis according to Harlow and Lane (1988). Proteins were separated on 10% SDS-PAGE gels. Gels were stained in 0.05% Coomassie Brilliant Blue R-250 in water for 10 to 15 min and destained in water. Gel fragments containing a protein of interest were excised and placed into dialysis tubing. Elution buffer (0.2 M Tris-acetate, pH 7.4, 1% SDS, 10 mM DTT) was added to the tubing at a concentration of 10 ml per g of wet gel. Proteins were eluted from the gel by electrophoresis at 50 V overnight at 4°C in 50 mM Tris-HCl, pH 7.4, 0.1% SDS. The eluate was placed into 2 to 3 new dialysis tubings and dialyzed against 4 L of 50 mM

ammonium bicarbonate once at room temperature and three times at 4°C. The protein solution was then frozen at -80°C and dried by lyophilization. Lyophilized protein was resuspended in a minimal volume of water, and the protein concentration was measured as described in Section 2.6.3.

Animals were immunized according to Harlow and Lane (1988). Proteins were adjusted to a concentration of 500 µg/ml and mixed with an equal volume of Freund's complete or incomplete adjuvant for primary and subsequent injections, respectively. Guinea pigs were injected with 0.4 ml of antigen suspension containing 80 µg of protein at several sites subcutaneously every 6 weeks. Bleeds were taken 10 days after each injection. Serum was separated from cells in clotted blood by centrifugation at  $2,000 \times g$  for 15 min at room temperature. Serum was stored at -20°C in aliquots. The presence of specific antibodies in serum was determined by immunoblotting.

### **2.16.1 Production of antibodies to *YlInp1p***

The plasmid pGEX-4T-1-YIINP1 was constructed as follows. The ORF for *YlInp1p* was amplified by PCR using primers 1862 and 1863 containing EcoRI and SalI recognition sequences, respectively. The amplified fragment was digested with EcoRI and SalI and ligated into the corresponding sites of pGEX-4T-1 to produce the plasmid pGEX-4T-1-YIINP1. Antibodies to *YlInp1p* were raised in guinea pigs T20 and T21 as described in Section 2.16 and partially purified by immunodepletion versus a lysate of *Ylinp1Δ* cells (performed by Elena Savidov, Department of Cell Biology, University of Alberta).

### **2.16.2 Production of antibodies to Pex3Bp**

The plasmid pGEX-4T-1-PEX3B was constructed as follows. The ORF for Pex3Bp was amplified by PCR from the plasmid pTC3-PEX3B using primers 2892 and 2893 containing EcoRI and Sall recognition sequences, respectively. The amplified fragment was digested with EcoRI and Sall and ligated into the corresponding sites of pGEX-4T-1 to produce the plasmid pGEX-4T-1-PEX3B. Antibodies to Pex3Bp were raised in guinea pigs V12 and V13 as described in Section 2.16 and affinity-purified by Elena Savidov, Department of Cell Biology, University of Alberta.

### **2.17 Computer-assisted DNA and protein sequence analysis**

Query protein sequences were compared to sequences deposited in protein databases using the Basic Blast program of the National Center for Biotechnology Information (<http://blast.ncbi.nlm.nih.gov/Blast.cgi>) and aligned using the ClustalW program (<http://www.ebi.ac.uk/Tools/clustalw2>). Protein sequences were analyzed using Génolevures (<http://www.genolevures.org>), the *Saccharomyces* Genome Database (<http://www.yeastgenome.org>), ExPASy Proteomics tools (<http://ca.expasy.org/tools/>), and the CBS prediction servers (<http://www.cbs.dtu.dk/services/TMHMM-2.0/>). DNA sequences were analyzed using Visual Cloning 3.2 (Redasoft).

### CHAPTER 3

#### **YLINP1P IS A PEROXISOMAL MEMBRANE PROTEIN REQUIRED FOR PEROXISOME RETENTION IN *YARROWIA LIPOLYTICA***

A version of this chapter has previously been published as “Peroxisomal peripheral membrane protein Ylinp1p is required for peroxisome inheritance and influences the dimorphic transition in the yeast *Yarrowia lipolytica*” (Jinlan Chang, Andrei Fagarasanu, and Richard A. Rachubinski. 2007. *Eukaryotic Cell* 6:1528-1537). Reprinted with permission.

### 3.1 Overview

In this chapter, we report the identification and characterization of *YInp1p*, the orthologue of *S. cerevisiae* Inp1p, from the dimorphic yeast *Y. lipolytica*.

Most peroxisomes are anchored at the periphery of cells of *Y. lipolytica*. 4D in vivo video microscopy showed that at cell division, approximately half of the anchored peroxisomes in the mother cell are dislodged individually from their static positions and transported to the bud. Peroxisome motility is dependent on the actin cytoskeleton. *YInp1p* is a peripheral PMP that affects partitioning of peroxisomes between mother cell and bud. In cells lacking *YInp1p*, most peroxisomes are transferred to the bud, with only a few remaining in the mother cell. In cells overproducing *YInp1p*, peroxisomes are preferentially retained in the mother cell, resulting in buds almost devoid of peroxisomes. Our results are consistent with a role for *YInp1p* in anchoring peroxisomes in cells. *YInp1p* also has a role in the dimorphic transition in *Y. lipolytica*, as cells lacking the *YINP1* gene more readily than wild-type cells convert from the yeast form to the mycelial form in oleic acid-containing medium, the metabolism of which requires peroxisome activity.

### 3.2 Peroxisome dynamics in wild-type *Y. lipolytica* cells

To begin to investigate peroxisome inheritance in *Y. lipolytica*, we first observed the distribution and movement of peroxisomes in wild-type *E122* cells using 4D in vivo video microscopy. The peroxisomal  $\beta$ -oxidation enzyme 3-ketoacyl-CoA thiolase (Pot1p) was genomically tagged with GFP (Pot1p-GFP) by homologous recombination with a PCR-based integrative transformation of *E122* to make the strain *E122/POT1-GFP* in

which peroxisomes are fluorescently labeled. Incubation of *E122/POT1-GFP* cells for 16 h in YPBO medium containing oleic acid, the metabolism of which requires functional peroxisomes, yielded 30 to 40 fluorescent punctate structures characteristic of peroxisomes per cell on average (Figure 3-1 A and B). Peroxisomes in both mother cells and buds were observed by video microscopy to be highly mobile (Figure 3-1 B and Movie 3-S1). The maximum velocities of anterograde and retrograde movement were determined to be approximately the same (0.41  $\mu\text{m}/\text{sec}$  and 0.39  $\mu\text{m}/\text{sec}$ , respectively). Peroxisomes in the mother cell were seen to oscillate at the cell cortex for a period, and then suddenly alter their positions. Peroxisomes would often gather, and then separate. When peroxisomes entered the bud from the mother cell, they would first arrive at the middle of the bud and, following a small amount of movement there, move to the bud tip and then return to the middle of the bud. Peroxisomes were also frequently observed to return from the bud to the mother cell, an event never observed in wild-type *S. cerevisiae* cells (Fagarasanu et al., 2005; Fagarasanu et al., 2006).

### **3.3 Peroxisome movement in *Y. lipolytica* is dramatically reduced by depolymerization of actin but not of microtubules**

Peroxisome movement involves actin in the yeast *S. cerevisiae* and in plants but uses microtubules in mammalian cells. When *E122/POT1-GFP* cells were treated with the actin-disrupting toxin, latrunculin A, peroxisomes exhibited greatly reduced movement and oscillated in position at the cortex of both mother cell and bud (Figure 3-2 C and Movie 3-S2). In contrast, treatment of cells with the microtubule inhibitor

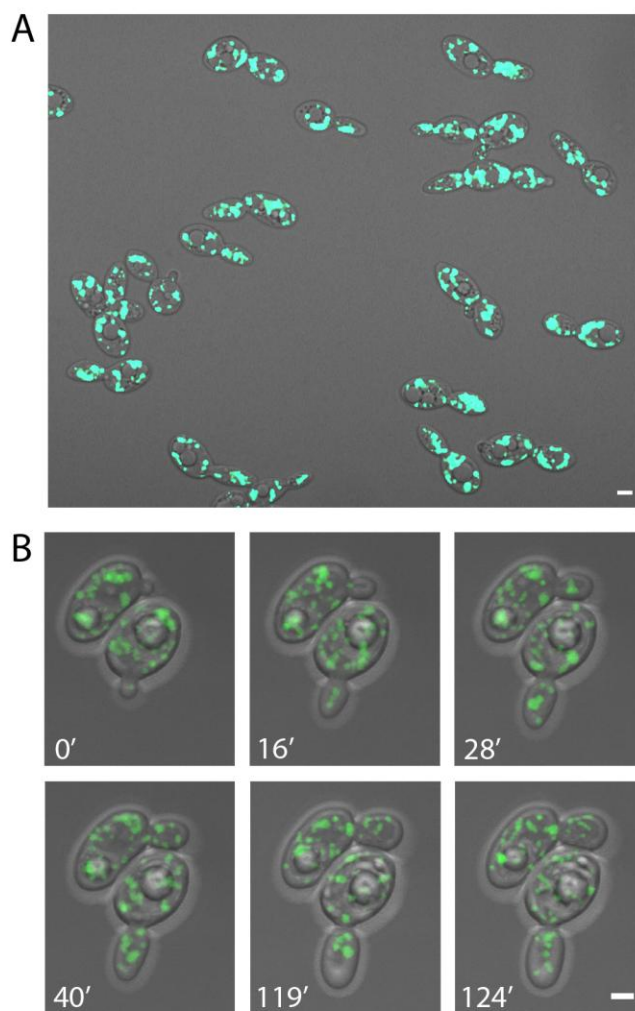


**Figure 3-1. Peroxisome dynamics in *Y. lipolytica*.** (A) Wild-type cells expressing genomically encoded Pot1p-GFP to fluorescently label peroxisomes were grown in glucose-containing YPD medium and then transferred to oleic acid-containing YPBO medium and incubated for 16 h. Fluorescent images were captured by confocal microscopy. In this static picture, peroxisomes are seen to be evenly distributed between mother cell and bud. (B) The strain used in (A) was analyzed by 4D in vivo video microscopy. Representative frames from Movie 3-S1 show the specific movements of peroxisomes. One peroxisome already present in the small bud of the cell at bottom at the start of the movie (0') was observed later to return to the mother cell. At 16 min, one peroxisome in the cell at top entered the bud. Additional peroxisomes entered this bud one by one between 16 min and 90 min. During this period, peroxisomes in the bud sometimes clustered at the center of the bud (28') and later separated (40'), and some peroxisomes returned to the mother cell. Before cytokinesis, some peroxisomes from both mother cell and bud relocated to the mother-bud neck region (119') and then redistributed (124'). Bars, 2  $\mu$ m.

nocodazole seemingly did not affect peroxisome movement, although by 120 min of treatment, most cells arrested with a single large bud (Figure 3-2 D and Movie 3-S3). Staining of cells with rhodamine-phalloidin to detect actin and with anti-tubulin antibodies confirmed disruption of actin and microtubules by latrunculin A and nocodazole, respectively (Figure 3-2 A and B).

In *S. cerevisiae*, the actin cytoskeleton consists of distinct patches and cables that orient toward the bud neck and tip. In filamentous fungi such as *Aspergillus nidulans* and *Neurospora crassa*, actin cables are not observed; however, actin patches that localize to actively growing or emerging hyphal tips and at sites of septation are seen (Xiang and Plamann, 2003). In *Y. lipolytica*, actin cables are also not observed, but actin patches are present, and their distribution during the cell cycle is similar to that described for actin patches in *S. cerevisiae* (Gausmann et al., 1999). Cells stained with rhodamine-phalloidin to detect actin showed actin patches at sites of polarized growth (Figure 3-2 A and E). Peroxisomes were closely apposed to, but did not colocalize with, actin patches (Figure 3-2 E).

The movement of peroxisomes in wild-type, latrunculin A-treated, and nocodazole-treated cells was also analyzed using 3D kymographs (Figure 3-3 A) that were constructed by overlapping the last 100 projections, which corresponds to 20 min of real time of Movies 3-S1, 3-S2 and 3-S3, respectively. Static peroxisomes are seen as fluorescent columns, while mobile peroxisomes are seen as fluorescent spots that change position with time. Mobile peroxisomes were often observed in wild-type and nocodazole-treated cells, while latrunculin A-treated cells showed mostly fluorescent columns, each indicative of a static peroxisome (Figure 3-3 A). The tracking of

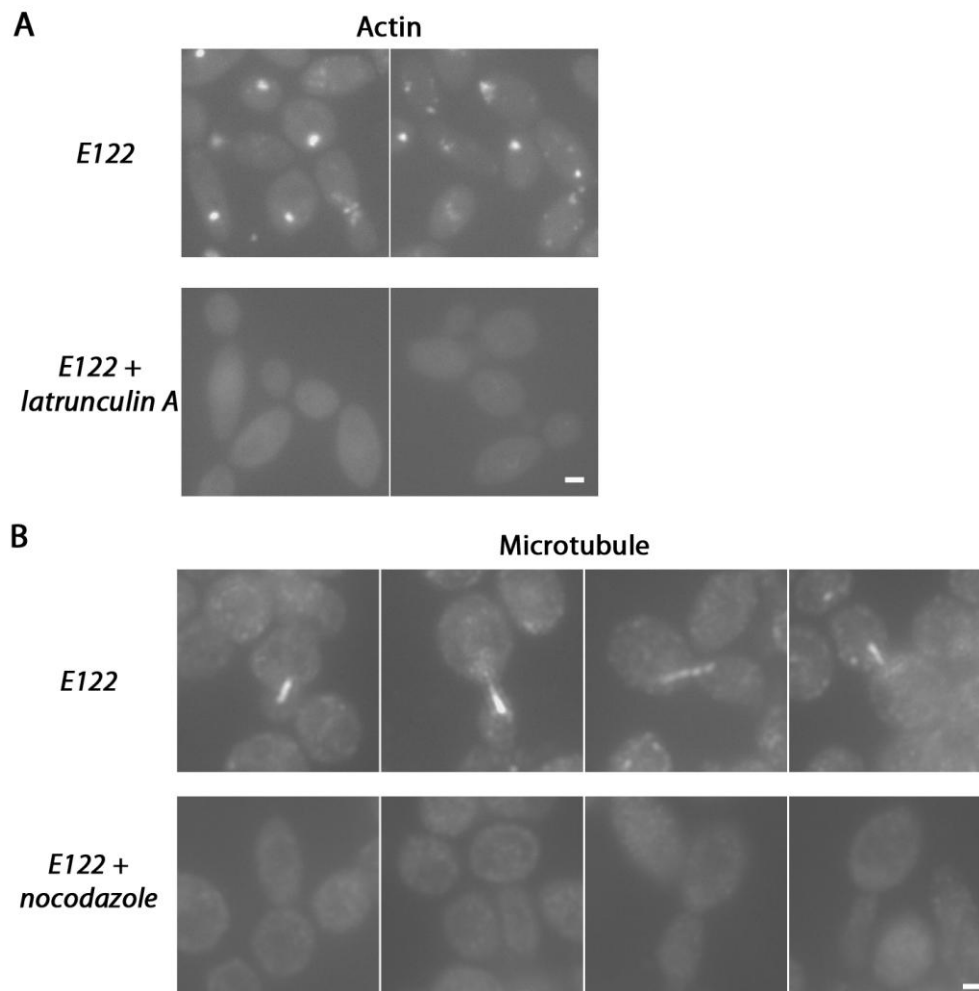
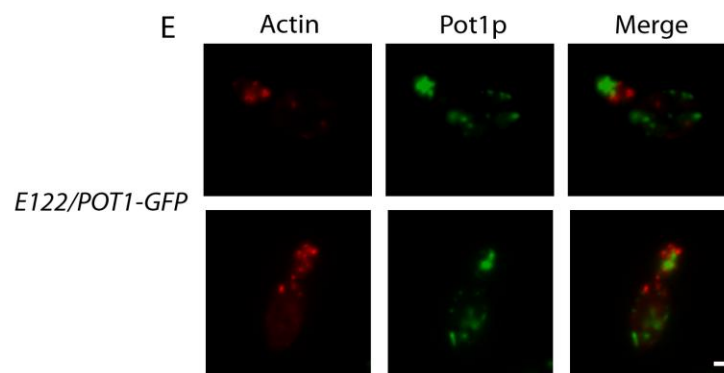
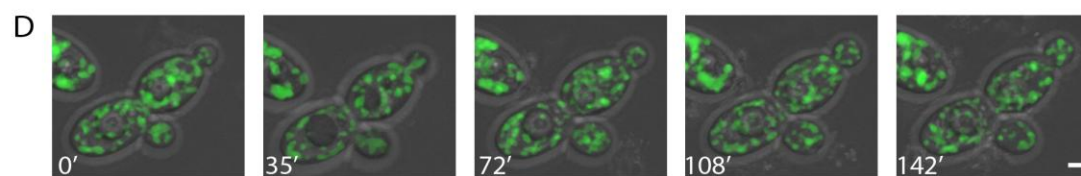
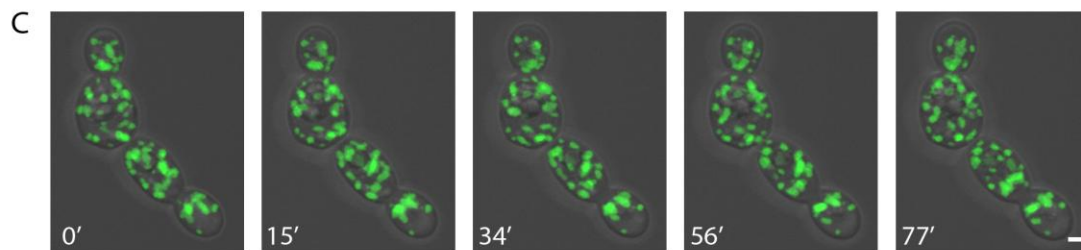


**Figure 3-2. Actin is involved in peroxisome dynamics.** (A) actin depolymerization by treatment with the actin-disrupting toxin latrunculin A. (B) microtubule depolymerization by treatment with the microtubule inhibitor nocodazole. (C-D) Treatment of cells with latrunculin A (C) but not with nocodazole (D) abolishes the dynamic movements of peroxisomes. Although cells grew more slowly following treatment with nocodazole, peroxisomes were still recruited to buds as normal. Representative frames from Movies 3-S2 and 3-S3 are presented in (C) and (D), respectively. (E) Peroxisomes do not colocalize with actin patches. Wild-type cells synthesizing genomically encoded Pot1p-GFP were grown in YPD medium and then transferred to YPBO medium for 16 h. Actin was detected by staining with rhodamine-phalloidin and visualized by epifluorescence microscopy. Bars, 2  $\mu$ m.



randomly selected, individual peroxisomes in wild-type, latrunculin A-treated and nocodazole-treated cells during the last 20 min of Movies 3-S1, 3-S2 and 3-S3 is presented in Figure 3-3 B.

We calculated the mean velocities of peroxisomes in wild-type, latrunculin A-treated and nocodazole-treated cells (Figure 3-3 C). The mean velocities of peroxisomes in wild-type and nocodazole-treated cells are similar and are approximately twice that of peroxisomes in latrunculin A-treated cells. Within each group of cells, there is no difference in mean velocity between mother cell and bud.

### **3.4 *Y*Inp1p is a peripheral membrane protein of peroxisomes**

A requirement for actin in peroxisomal movement within and between cells of *Y. lipolytica* led us to speculate that *Y. lipolytica* might use mechanisms for peroxisome inheritance similar to those used by *S. cerevisiae*. Inp1p is a peripheral membrane protein of peroxisomes that was shown to be required for peroxisome inheritance in *S. cerevisiae* (Fagarasanu et al., 2005). A search of protein databases with the GENEINFO(R) BLAST Network Service of the National Center for Biotechnology Information revealed one protein encoded by ORF *YALIOF31229g* of the *Y. lipolytica* genome with extensive sequence similarity to Inp1p. Hereafter, the protein encoded by ORF *YALIOF31229g* is termed *Y*Inp1p and its encoding gene as *Y*INP1. Inp1p and *Y*Inp1p exhibit 11.6% amino acid identity and 19.9% amino acid similarity (Figure 3-4).

Confocal fluorescence microscopy was used to determine the localization of a genomically encoded fluorescent chimera of *Y*Inp1p and GFP (*Y*Inp1p-GFP).

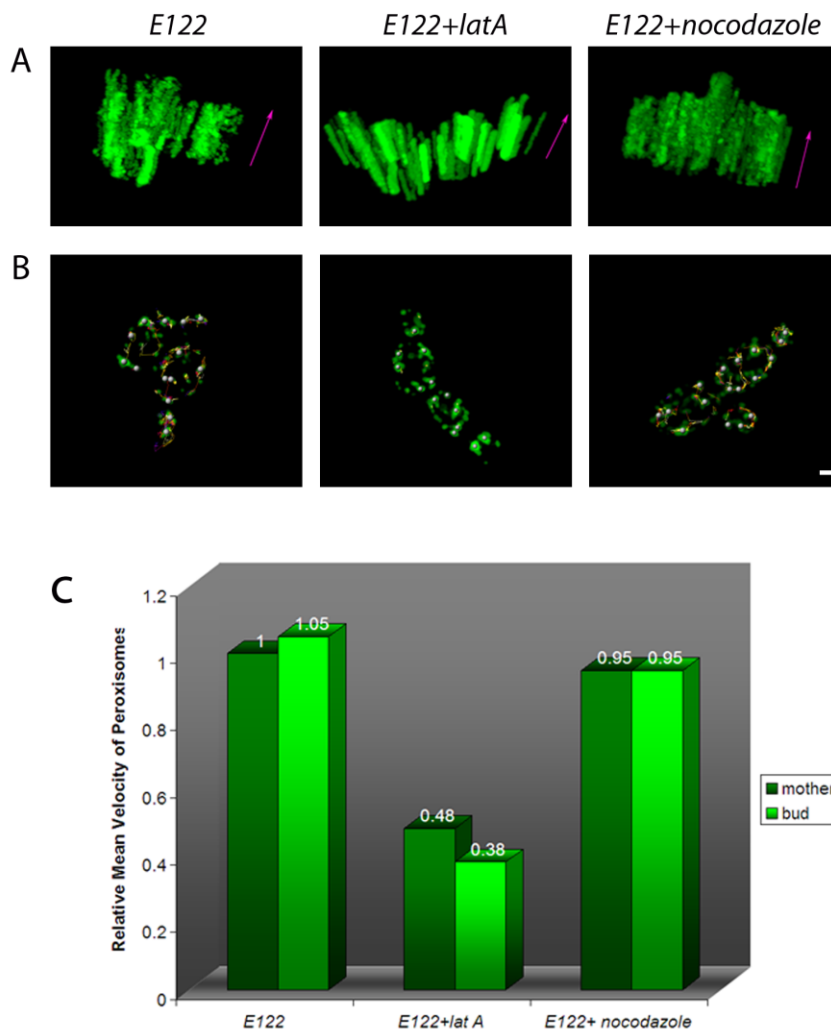


**Figure 3-3. Quantification of peroxisome mobility.** (A) 100 projections corresponding to the last 20 min of Movies 3-S1, 3-S2 and 3-S3 were analyzed with Imaris 4.1, and 3D models were constructed. The  $z$ -axis (purple arrows) represents time. A peroxisome that maintains its  $x$ - $y$  position for the period of time considered and which is essentially immobile is represented by a fluorescent column. A mobile peroxisome is represented by fluorescent spots that have different  $x$ - $y$  positions in time. (B) Tracking peroxisomes in untreated, latrunculin A-treated and nocodazole-treated wild-type cells synthesizing genomically encoded Pot1p-GFP. Randomly selected peroxisomes under each condition were tracked by analyzing the last 100 projections of Movies 3-S1, 3-S2 and 3-S3 with Imaris 4.1. The trajectories of individual peroxisomes are shown as different colored lines. Bar, 2  $\mu$ m. (C) Peroxisomes in latrunculin A-treated cells exhibit reduced mobility. The velocities of individual peroxisomes across individual time points were measured using Imaris 4.1, and an average velocity was obtained for each peroxisome. The average velocities of individual peroxisomes under a given condition were in turn averaged to obtain the mean velocity of peroxisomes under that condition. The mean velocity of peroxisomes under a given condition is expressed relative to the mean velocity of peroxisomes of the untreated wild-type strain, which is taken as 1.

```

ScInp1p MVLSRGETKKNSVRLTAKQE-KKQOSTFQTLKQSLKLSNNKKLKQDS---TQHSNDTNKS 56
YlInp1p MLSKKPSLSDLDATLAHKRELEHMPTEQERTILFDHDLSQLIQFSIPAGAMRRHTQOLEGN 60

ScInp1p VKAKKNGTSSKKTGTQRKRISTORFSLFTYG-----NVQVMNSFVPIH 99
YlInp1p RQTSSFAPGSELANVQLRSRPGSRCASGTYASSISSGATLTEPDEADPNLDFWEQLPPVH 120

ScInp1p NDIPNSSCIR-----RNSQVSANNVTESGVSFNDTQSQDSQNTIKLKFTSLMAKGP 151
YlInp1p CAISERIVAHGRFQVFTLHNDKVTYIKCGDAVQAALPKLRLWRTSLSQFTFFQPIPGRYW 180

ScInp1p -----IEIYQICTGFDKLKENIAPFQKSSKASSHGHVWNYLSIGRHGDIVHPVLPKLOI 206
YlInp1p RVELFRSTYKLTADDLRMALEQSCCELDQIKAPELEGAKEEYIENYLDQLIPEHDLKEKL 240

ScInp1p TRLNGAGFKYFISFYNP---ERYWEIEFLPLISQSQSELENSVKAFENVISKICQFISHIN 263
YlInp1p VSLNPNNSCYIPPPKEKDEDETKVEDDNTVEEVRTNGGELNMDFLASQIDNLSIPTHYD 300

ScInp1p EG----ATIGNNES-----LSDKFKLPPTSDIEPPNTEIINN----- 296
YlInp1p SEEHDLETIGSASSPYSSLLSPSPSPPYSSLSLQSSFDLDSANSTLSDSWDISGHLQPS 360

ScInp1p -----DDNDDDDDNYDDDLNYLLDEEYEQCTDNSFSVISN 334
YlInp1p KYDELFASSSSTLDDIIETFVVEDADQNDGDISVDISDHLARSDITASSPSARFPEKPK 420

ScInp1p TCSNLNASFLYFSDPTDAVSIS---INEAFKNAIRRTAPVLNIPIAAP----- 379
YlInp1p LTERLSQVTLKRSVSQLQLOISPRTPDQEFQRQLMSSPLPAKITPQRQASAGVLGSSEKP 480

ScInp1p --SIHSKOQNKRYSS-----YFFIDSPPYLQDRHRRFQRRSISGLGDL----- 420
YlInp1p RSPIDARSARKEYTTGASAVAFGLRHPPFARWNNILETETMKFRSMDDDWLEINIDSD 540

ScInp1p ----
YlInp1p VPTP 544

```

**Figure 3-4. Sequence alignment of *S. cerevisiae* Inp1p (*ScInp1p*) with the hypothetical *YlInp1p* encoded by the ORF *YALI0F31229g* of the *Y. lipolytica* genome.** Amino acid sequences were aligned with the use of the ClustalW program (<http://www.ebi.ac.uk/clustalw/>). Identical residues (black) and similar residues (gray) in the two proteins are shaded. Similarity rules: G = A = S; A = V; V = I = L = M; I = L = M = F = Y = W; K = R = H; D = E = Q = N; and S = T = Q = N. Dashes represent gaps.

Peroxisomes were decorated by a plasmid-encoded fluorescent chimera (mRFP-SKL) of monomeric red fluorescent protein (mRFP) and the peroxisome targeting signal 1, Ser-Lys-Leu (SKL). *YInp1p*-GFP colocalized with mRFP-SKL to punctate structures characteristic of peroxisomes (Figure 3-5 A).

Antibodies raised against *YInp1p* specifically recognize an ~80-kDa polypeptide in whole-cell lysates prepared from wild-type strain *E122* but not from the *Yinp1Δ* strain. (Figure 3-5 B). Why *YInp1p* exhibits a difference between its predicted molecular mass of ~60 kDa and its ~80-kDa molecular mass determined by SDS-PAGE remains unknown.

Subcellular fractionation also showed *YInp1p* to be peroxisomal. Similar to the peroxisomal protein thiolase (Pot1p), *YInp1p* preferentially localized to a  $20,000 \times g$  (20KgP) fraction enriched for peroxisomes and mitochondria (Figure 3-5 C). Isopycnic density gradient centrifugation of the 20KgP fraction indicated that *YInp1p* coenriched with Pot1p and not with the mitochondrial protein, Sdh2p (Figure 3-5 D).

Organelle extraction was used to determine the intraperoxisomal location of *YInp1p* (Figure 3-5 E). Peroxisomes were subjected to hypotonic lysis in dilute alkali Tris buffer, followed by ultracentrifugation to yield a supernatant (Ti8S) fraction enriched for matrix proteins and a pellet (Ti8P) fraction enriched for membrane proteins. Similarly to the peroxisomal integral membrane protein Pex2p, *YInp1p* preferentially localized to the Ti8P fraction and not to the Ti8S fraction like the matrix protein Pot1p. The Ti8P was then extracted with alkali  $\text{Na}_2\text{CO}_3$  and subjected to ultracentrifugation. *YInp1p* fractionated to the supernatant ( $\text{CO}_3\text{S}$ ) fraction, consistent with it being a

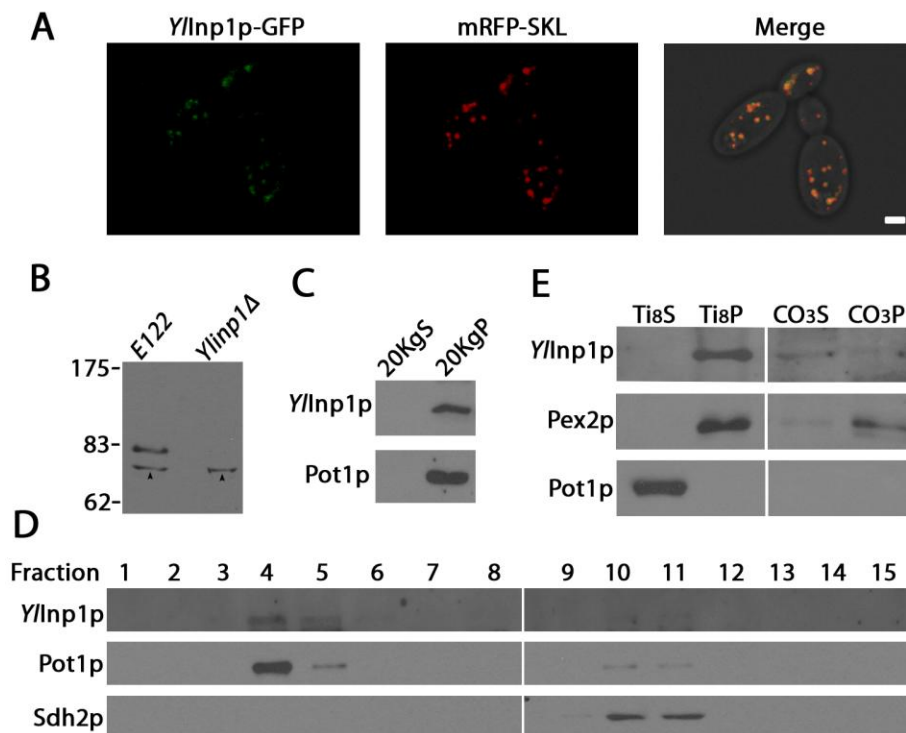


**Figure 3-5. *Ylnp1p* is a peripheral membrane protein of peroxisomes.** (A) *Ylnp1p*-GFP colocalizes with mRFP-SKL to punctate structures characteristic of peroxisomes by confocal microscopy. The right panel presents the merged image of the left and middle panels in which colocalization of *Ylnp1p*-GFP and mRFP-SKL is shown in yellow. Bar, 2  $\mu$ m. (B) Immunoblot analysis of whole-cell lysates of the wild-type strain *E122* and the deletion strain *Ylnp1Δ* probed with anti-*Ylnp1p* antibodies. Arrowheads point to a nonspecific immunoreactive polypeptide present in the lysates of both *E122* and *Ylnp1Δ* cells. (C) *Ylnp1p* localizes to the 20KgP subcellular fraction enriched for peroxisomes. Immunoblot analysis of equivalent portions of the 20KgS and 20KgP subcellular fractions from wild-type *E122* cells was performed with antibodies to *Ylnp1p* and to the peroxisomal matrix enzyme thiolase (Pot1p). (D) *Ylnp1p* cofractionates with peroxisomes. Organelles in the 20KgP fraction were separated by isopycnic centrifugation on a discontinuous sucrose gradient. Fractions were collected from the bottom of the gradient, and equal portions of each fraction were analyzed by immunoblotting. Fractions enriched for peroxisomes and mitochondria were identified by immunodetection of Pot1p and Sdh2p, respectively. (E) Purified peroxisomes were ruptured by treatment with Ti8 buffer and subjected to ultracentrifugation to obtain a supernatant fraction, Ti8S, enriched for matrix proteins and a pellet fraction, Ti8P, enriched for membrane proteins. The Ti8P fraction was treated further with alkali Na<sub>2</sub>CO<sub>3</sub> and separated by ultracentrifugation into a supernatant fraction (CO<sub>3</sub>S) enriched for peripherally associated membrane proteins and a pellet fraction (CO<sub>3</sub>P) enriched for integral membrane proteins. Equivalent portions of each fraction were analyzed by immunoblotting. Immunodetection of Pot1p and Pex2p marked the fractionation profiles of a peroxisomal matrix and integral membrane protein, respectively.

peripheral membrane protein, and not to the pellet (CO<sub>3</sub>P) fraction, as did Pex2p (Figure 3-5 D).

### **3.5 Peroxisome inheritance is impaired in cells lacking or overexpressing *YIINP1***

In wild-type *Y. lipolytica* cells, peroxisomes are essentially evenly distributed between mother cell and bud (Figure 3-1 A and B). In contrast, in *Ylinp1Δ* cells lacking the *YIINP1* gene, most peroxisomes are not retained within the mother cell and are transferred to the bud, where they tend to cluster (Figure 3-6 A and Movie 3-S4). Mother cells without peroxisomes are rarely observed in the *Ylinp1Δ* strain, which contrasts with the situation in *S. cerevisiae* where most *inp1Δ* mother cells fail to retain peroxisomes (Fagarasanu et al., 2005). The small number of peroxisomes remaining in *Ylinp1Δ* mother cells is not evenly distributed, as peroxisomes in these mother cells prefer to localize near the bud-neck region, thereby leaving the tip region distal to the bud without peroxisomes (Figure 3-6 B). Quantification showed that 94% of wild-type mother cells retained peroxisomes at their tips distal to the bud, in contrast to only 32% of *Ylinp1Δ* mother cells (Figure 3-6 B).

The number of peroxisomes transferred from mother cell to bud is greatly reduced in cells overproducing *YInp1p* (Figure 3-7). Only 56% of cells overproducing *YInp1p* contained peroxisomes at the bud tips. In contrast, 97% of the wild-type cells had peroxisomes at the bud tips (Figure 3-7).

Calculation of the mean velocities of peroxisomes showed that peroxisomes in *Ylinp1Δ* cells are on average more mobile than those of wild-type cells. In contrast,

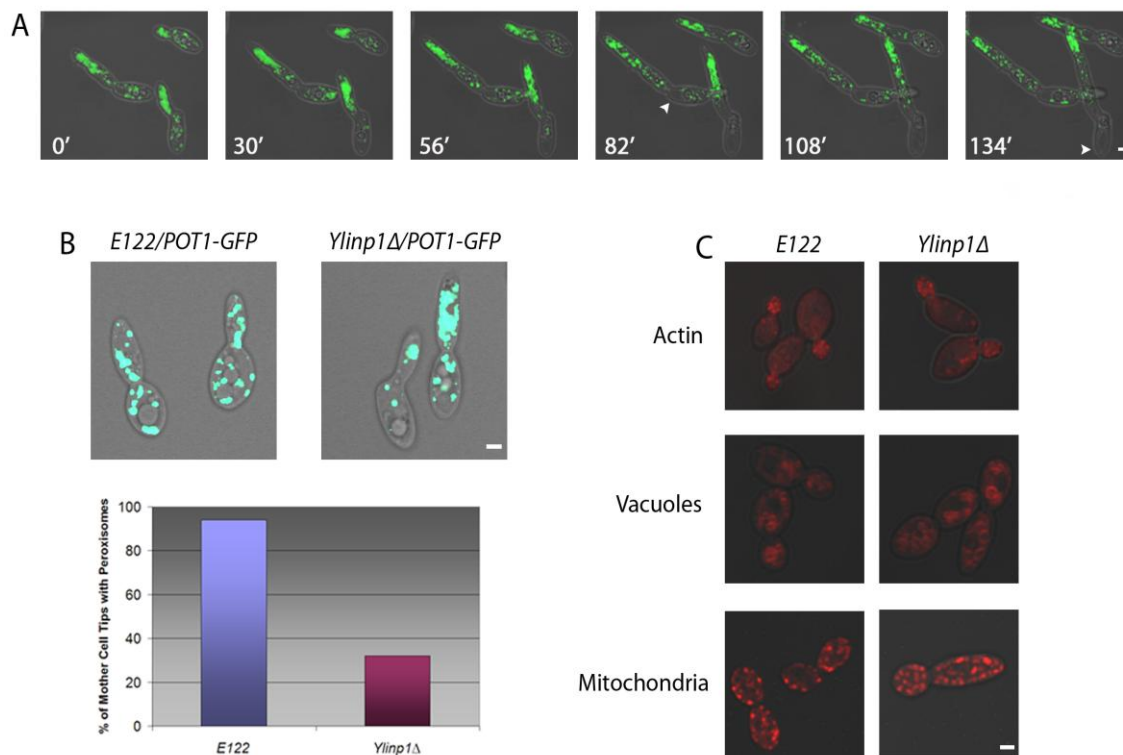


**Figure 3-6. Deletion of the *YIINP1* gene affects specifically peroxisome inheritance.**

(A) Peroxisomes of the *Ylinp1Δ* strain were fluorescently labeled with genomically encoded Pot1p-GFP. Cells were grown for 16 h in YPD medium, transferred to YPBO medium for 16 h and then visualized at room temperature on a LSM 510 META confocal microscope specially modified for 4D in vivo video microscopy. Representative frames from Movie 3-S4 show the specific movements of peroxisomes in the *Ylinp1Δ* strain. At the start of the movie (0'), cells already exhibit pseudohyphal characteristics, and peroxisomes are observed in mother cells and preferentially in buds. Continued video imaging showed that peroxisomes continue to move from mother cells to buds and localize to bud tips opposite mother cells (30' to 133'). Mother cells are largely, but not completely, devoid of peroxisomes. Arrowheads point to tips of mother cells distal to the site of bud emergence that are devoid of peroxisomes. (B) The wild-type strain *E122* and the deletion strain *Ylinp1Δ* expressing genomically integrated *POT1-GFP* were grown for 16 h in YPD medium and transferred to YPBO medium for 16 h. Fluorescence images were captured by confocal microscopy. Peroxisome inheritance was quantified as the percentage of mother cells retaining peroxisomes at their tips distal to the site of bud emergence. (C) Deletion of the *YIINP1* gene does not affect actin structure or the inheritance of organelles other than peroxisomes. Wild-type *E122* and *Ylinp1Δ* cells synthesizing Pot1p-GFP were grown in YPD medium. Actin was stained with rhodamine-phalloidin, vacuoles with the fluorophore FM 4-64, and mitochondria with MitoTracker. Images were captured by confocal microscopy. Bars, 2  $\mu$ m.

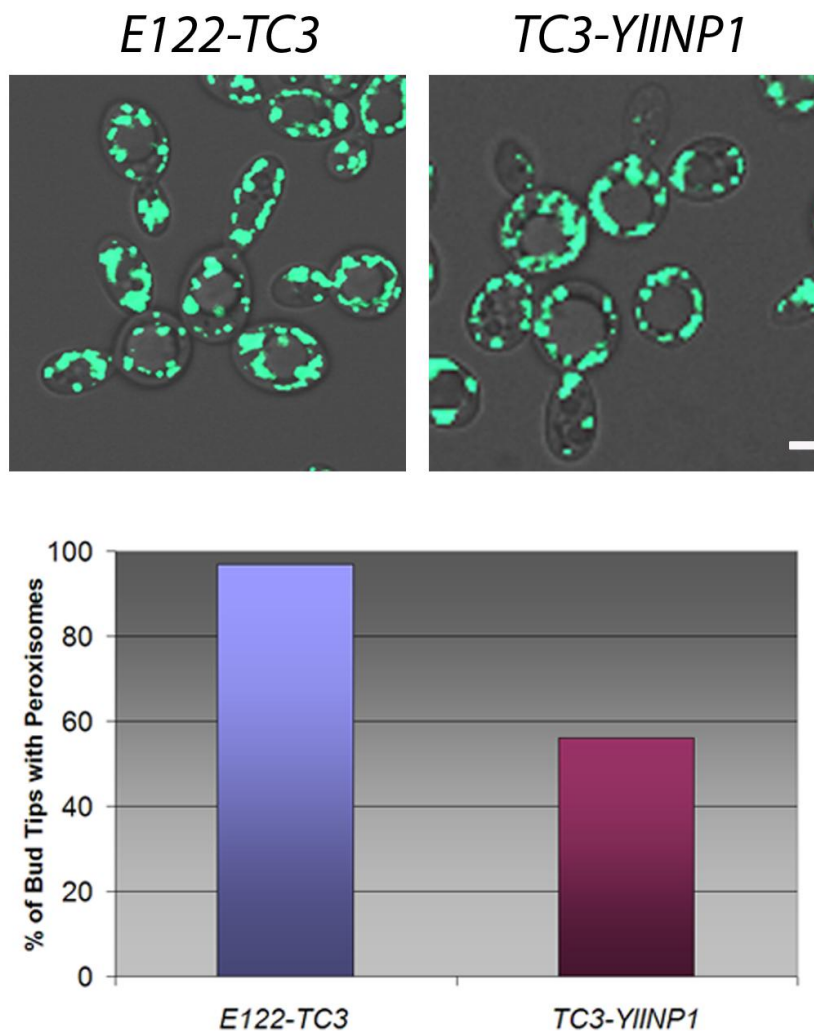


**Figure 3-7. *YIINP1* overexpression leads to peroxisome retention in mother cells.** The strain *E122/POT1-GFP* was transformed with the empty plasmid pTC3 or with pTC3 containing the *YIINP1* gene for overexpression of *YIINP1*. Cells were grown in YND medium and then transferred to and incubated in oleic acid-containing YNO medium for 16 h. Images were captured by confocal microscopy. Quantification of peroxisome retention by mother cells is reported as the percentage of bud tips containing peroxisomes. Bar, 2  $\mu$ m.

peroxisomes in cells overexpressing *YIINP1* are less mobile than those of wild-type cells (Figure 3-8 and Movies 3-S5, 3-S6 and 3-S7).

### **3.6 The structure of actin and the inheritance of other organelles are unaffected in *Ylinp1*Δ cells**

The impairment in peroxisome inheritance in *Ylinp1*Δ cells could be due theoretically to some pleiotropic effect resulting from a compromised actin cytoskeleton. We analyzed the organization of the actin cytoskeleton in wild-type cells and cells lacking *Ylinp1p* by staining with rhodamine-phalloidin (Figure 3-6 C). Actin organization is unchanged in *Ylinp1*Δ cells.

To test if *Ylinp1p* is required specifically for peroxisome inheritance, we compared the partitioning of other organelles in wild-type and *Ylinp1*Δ cells. The inheritance of both vacuoles and mitochondria was unimpaired in *Ylinp1*Δ cells (Figure 3-6 C).

Moreover, *Ylinp1*Δ cells did not exhibit a growth defect in YPD medium, suggesting that *Ylinp1p* is not required for the polarized distribution of secretory vesicles.

### **3.7 *Ylinp1*Δ cells readily undergo the dimorphic transition from yeast to hyphal form**

Yeast strains compromised in peroxisome biogenesis usually demonstrate a reduced ability to use oleic acid as the sole source of carbon. However, *Ylinp1*Δ cells did not exhibit an overall growth defect in oleic acid-containing YPBO medium compared to

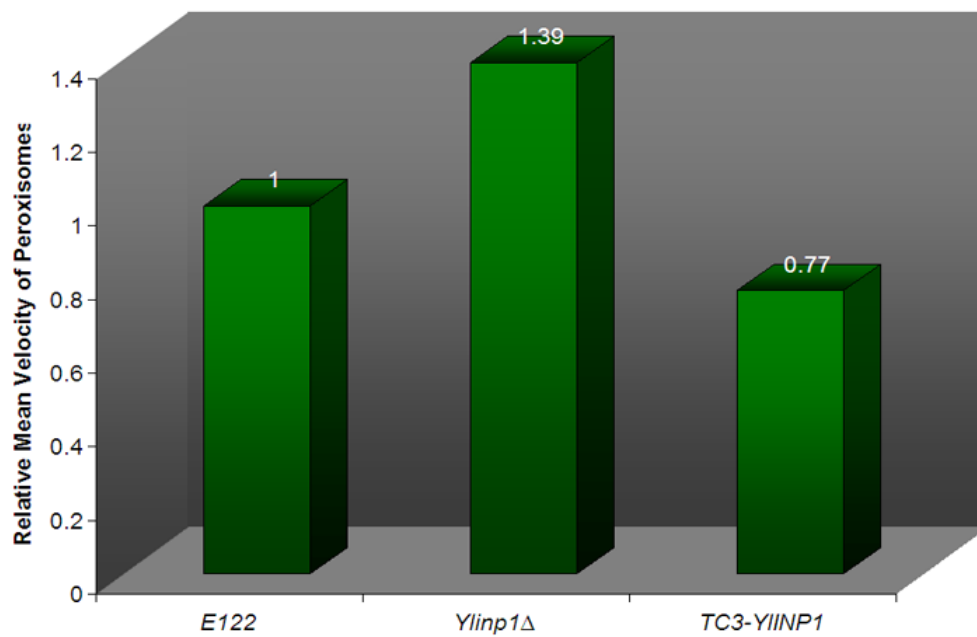


**Figure 3-8. Deletion or overexpression of the *YIINP1* gene affects peroxisome mobility.** The mean velocities of peroxisomes in wild-type *E122/POT1-GFP*, *Ylinp1Δ/POT1-GFP*, and *YIINP1*-overexpressing (*TC3-YIINP1/POT1-GFP*) cells were determined as described in the legend to Figure 3-3 C.

the wild-type strain. However, *Ylinp1* $\Delta$  cells did show altered cell morphology compared to wild-type cells under the same conditions. *Y. lipolytica* undergoes a developmentally regulated dimorphic transition from the yeast form to the mycelial form (Rodriguez and Domingues, 1984). No dimorphic transition was observed in wild-type *E122* or *Ylinp1* $\Delta$  cells immediately upon transfer from YPD to YPBO medium (Figure 3-9, 0 h). *E122* cells did not undergo substantial conversion to the hyphal form even after 48 h incubation in YPBO medium (Figure 3-9). In contrast, *Ylinp1* $\Delta$  cells already began to show evidence of the dimorphic transition by 2 h of incubation in YPBO, and all *Ylinp1* $\Delta$  cells were in pseudohyphal or hyphal form by 24 h to 48 h incubation in YPBO medium (Figure 3-9).

### **3.8 Discussion**

#### **3.8.1 Peroxisome inheritance in the yeast *S. cerevisiae***

The distribution of organelles has to be closely controlled during cell division to ensure their faithful segregation between the two resulting cells. Eukaryotic cells that divide by fission usually ensure the accurate inheritance of their organelles by evenly distributing them in the mitotic cell cytoplasm. The cytokinetic machinery that divides the cell into two equally sized daughter cells would thus apportion the organelles evenly between the resultant cells (Warren and Wickner 1996; Fagarasanu et al., 2007). In contrast to cells that divide by median fission, budding yeast must actively and vectorially deliver half of its organelles to the growing bud, while retaining the remaining organelles in the mother cell (Rosanese and Click, 2001). This feature makes budding yeast more amenable to studies of organelle inheritance, since it facilitates the molecular

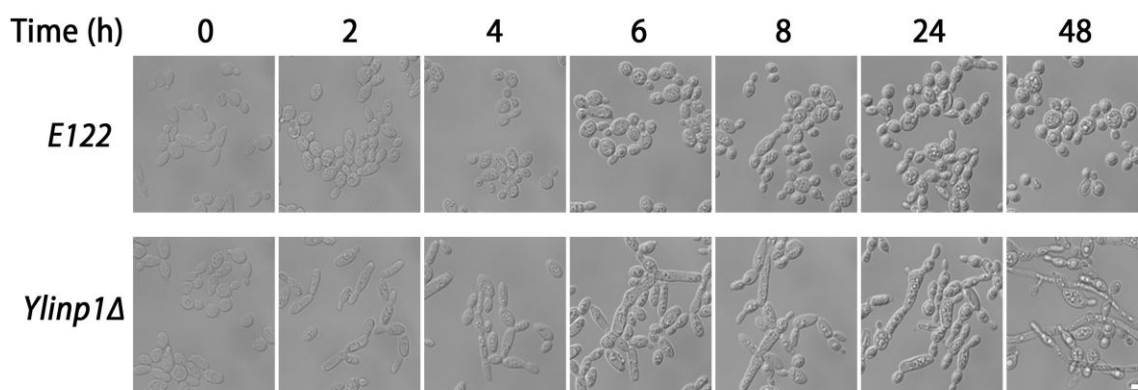


**Figure 3-9. Deletion of the *YIINP1* gene affects the dimorphic transition.** Wild-type *E122* and *Ylinp1Δ* cells were grown in YPD medium for 16 h and then transferred to and incubated in YPBO medium. Samples were removed from YPBO at the times indicated and visualized by microscopy. Bar, 5  $\mu$ m.

dissection of organelle inheritance into distinct processes such as retention of organelles in the mother cell, transport of organelles to the daughter cell and retention of delivered organelles within daughter cells.

Much progress in our understanding of how peroxisomes partition at cell division has come from studies of the budding yeast *S. cerevisiae*. In *S. cerevisiae*, peroxisome dynamics follows a well defined sequence of events during the cell cycle (Hoepfner et al., 2001; Fagarasanu et al., 2005; Fagarasanu et al., 2006; Fagarasanu et al., 2007). Most peroxisomes are immobilized at the cell periphery, a process dependent on the peroxisomal membrane protein Inp1p (Fagarasanu et al., 2005). During bud growth, half of the maternal peroxisomes are recruited one by one from their static cortical positions and are transported to the bud. The movement of peroxisomes is powered by the class V myosin, Myo2p, which is recruited to the peroxisomal membrane via its peroxisome-specific receptor, Inp2p (Hoepfner et al., 2001; Fagarasanu et al., 2006). In the bud, Myo2p remains initially attached to Inp2p, which results in the majority of peroxisomes being localized at sites of growth, where Myo2p normally accumulates. Even at cytokinesis, a few peroxisomes in the bud are still engaged by Myo2p and are thus relocated to the mother bud-neck region, whereas the rest remain anchored at the bud cortex, in preparation for the ensuing cell cycle (Fagarasanu et al., 2006).

### **3.8.2 Peroxisome movement in *Y. lipolytica* is actin-dependent**

As reported in this chapter, we analyzed peroxisome dynamics in the dimorphic yeast *Y. lipolytica*. As in *S. cerevisiae*, most peroxisomes in *Y. lipolytica* are anchored at the cell periphery. Half of these anchored peroxisomes are then dislodged one at a time

from their static positions and transported to the daughter cell. We have shown that peroxisome motility in *Y. lipolytica* is dependent on the actin cytoskeleton.

### 3.8.3 A role for *YInp1p* in peroxisome retention

We were interested in identifying molecular players implicated in peroxisome inheritance in *Y. lipolytica*. A search of *Y. lipolytica* protein databases retrieved one protein of unknown function encoded by the ORF *YALI0F31229g* that exhibits extensive sequence similarity to *S. cerevisiae* Inp1p. We designated this protein as *YInp1p*. We showed *YInp1p* to be a peripheral membrane protein of peroxisomes involved in peroxisome inheritance. In cells lacking *YInp1p*, most peroxisomes were transferred to the bud, with only a few being left in the mother cell. In contrast, in cells overproducing *YInp1p*, peroxisomes are preferentially retained in the mother cell, resulting in buds almost devoid of peroxisomes. These imbalances in peroxisome inheritance resemble the ones observed in *S. cerevisiae* cells either lacking or overproducing Inp1p, respectively. However, the phenotypes observed in *Y. lipolytica* strains are not as severe as the ones displayed by the corresponding *S. cerevisiae* strains. For example, we rarely observed mother cells lacking peroxisomes in *Yinp1Δ* cells or buds devoid of peroxisome in cells overexpressing *YInp1p*, as was observed in *S. cerevisiae* (Fagarasanu et al., 2005; Fagarasanu et al., 2006). We offer three possible explanations for why *Y. lipolytica* strains display milder phenotypes as compared to their corresponding *S. cerevisiae* strains. First, on average, *Y. lipolytica* contains more peroxisomes per cell than does *S. cerevisiae* (30-40 peroxisomes per cell for *Y. lipolytica* in induced condition as opposed to 10 peroxisomes per cell for *S. cerevisiae*), which makes the attainment of an extreme

phenotype less probable in *Y. lipolytica* than in *S. cerevisiae*. Second, other as yet unidentified peroxisomal proteins might function in a manner similar to *YInp1p* to promote the retention of peroxisomes. This potential functional redundancy would preclude the development of a more dramatic phenotype in cells lacking *YInp1p* alone. Third, the de novo synthesis of peroxisomes may be a more rapid process in *Y. lipolytica* than it is in *S. cerevisiae*. The production of new peroxisomes would tend to mitigate the imbalances caused by the lack or overproduction of *YInp1p* and thus help to alleviate the corresponding phenotypes in *Y. lipolytica* as compared to *S. cerevisiae*.

All our observations support a role for *YInp1p* in peroxisome retention, as previously suggested for *S. cerevisiae* *Inp1p*. Most probably *YInp1p* functions as a link between peroxisomes and an anchoring cortical structure. As expected for a protein that would link peroxisomes to an anchoring cortical structure, deletion of the *YIINP1* gene leads to peroxisomes that are more mobile than those of wild-type cells, while overexpression of *YIINP1* leads to peroxisomes that are largely localized to the cell cortex and less mobile than peroxisomes of wild-type cells. Even though the existence of anchoring devices suited to retain various organelles in the mother cell has long been proposed, their molecular composition has remained undetermined. Interestingly, retention of mitochondria within *S. cerevisiae* mother cells has been shown to be dependent on the actin cytoskeleton (Yang et al., 1999). However, actin patches did not colocalize with cortically immobilized peroxisomes of *Y. lipolytica*. Moreover, the treatment of wild-type *Y. lipolytica* cells with the actin-disrupting toxin latrunculin A did not result in the detachment of cortical peroxisomes from their static locations. Taken

together, these findings suggest that actin is not involved in the retention of peroxisomes at the cell cortex in *Y. lipolytica*.

#### **3.8.4 *YInp1p* is involved in the dimorphic transition in *Y. lipolytica***

*Y. lipolytica* is a dimorphic fungus that is able to alternate between a unicellular yeast form and a distinct mycelial form (hyphae and pseudohyphae). Interestingly, in contrast to wild-type cells, *Ylinp1Δ* cells were observed to undergo substantial conversion from the yeast to the hyphal form when grown in oleic acid as the sole available carbon source. Usually, filamentous growth is an adaptive strategy employed by non-motile microorganisms to forage through the environment for scarce nutrients. By restricting growth to the filament tip, cells are able to probe a large volume without investing in a great body mass (Kron, 1997). Cell type switching in dimorphic fungi is known to be modulated by environmental factors, such as nutrient availability (Kron, 1997; Sanchez-Martinez and Perez-Martin, 2001). Why do cells lacking *YInp1p* readily undergo a dimorphic transition to hyphae when grown under conditions requiring peroxisomes? One possibility is that *Ylinp1Δ* cells are inefficient in metabolizing fatty acids and thus perceive the availability of fatty acids as the sole carbon source as a state of nutrient deprivation. *YInp1p* is not required for peroxisome assembly, as *Ylinp1Δ* cells contain peroxisomes by microscopic analysis. Moreover, these peroxisomes are functional, due to their ability to import proteins targeted by either the PTS1 or the PTS2 signal (our unpublished data). However, *YInp1p* regulates peroxisome dynamics, which serves a dual purpose. First, it allows peroxisomes to assume correct positioning during cell division, which is required to endow both resulting cells with an equitable number of

peroxisomes. Second, it is needed to disperse peroxisomes within cells, thereby increasing their metabolic efficiency (Yan et al., 2005). Lack of *YInp1p* affects the segregation of peroxisomes both within and between cells. In cells lacking *YInp1p*, peroxisomes are clustered at the bud tip, leaving other parts of the budded cell almost devoid of peroxisomes. This accumulation of the majority of the peroxisome population at a unique location within cells is likely to result in a decrease in the efficiency of peroxisomal functions. Moreover, the uneven distribution of peroxisomes in cells lacking *YInp1p* is likely to trigger the production of new peroxisomes. It has been shown that most of the components essential for peroxisome biogenesis in *Y. lipolytica* are also required for the dimorphic transition from the yeast to the mycelial form and for the delivery of mycelial-form specific proteins to the plasma membrane (Titorenko et al., 1997). Thus, activation of the peroxisome-manufacturing machinery might also result in a drastic effect on cell morphology. Collectively, these observations would suggest that *YInp1p* plays an indirect role in regulating dimorphism through its regulation of peroxisome distribution. However, at this time, a direct effect of *YInp1p* on cell morphogenesis cannot be excluded.

In closing, in this chapter we presented evidence demonstrating that the peroxisomal peripheral membrane protein *YInp1p* is directly involved in the inheritance of peroxisomes in *Y. lipolytica*. *YInp1p* probably functions as a peroxisome-retention factor, tethering peroxisomes to putative anchoring structures that line the cell periphery (Fagarasanu et al., 2005).

## CHAPTER 4

### **A ROLE FOR THE PEX3 PROTEIN FAMILY IN PEROXISOME MOTILITY IN *YARROWIA LIPOLYTICA***

A version of this chapter has been previously published as “Pex3 peroxisome biogenesis proteins function in peroxisome inheritance as class V myosin receptors” (Jinlan Chang, Fred D. Mast, Andrei Fagarasanu, Dorian A. Rachubinski, Gary A. Eitzen, Joel B. Dacks, and Richard A. Rachubinski. 2009. *The Journal of Cell Biology* 187:2233-2246). Reprinted with permission.

## 4.1 Overview

We have identified and characterized a novel peroxisomal protein, Pex3Bp, of the yeast *Y. lipolytica*. In this chapter, we present results showing that Pex3Bp and members of the Pex3 protein family of peroxisome biogenic factors in general function in peroxisome motility and inheritance.

In *S. cerevisiae*, the class V myosin motor, Myo2p, interacts specifically with its peroxisomal receptor, Inp2p, to move peroxisomes along actin from mother cell to bud. However, homologues of Inp2p are not readily identifiable outside the *Saccharomycetaceae* family, which raises questions as to what might constitute a general mechanism of peroxisome inheritance in cells. We have taken advantage of the presence of a paralogue, Pex3Bp, of the early acting peroxisome biogenesis factor Pex3p in the yeast *Y. lipolytica* to demonstrate an unexpected role for Pex3 proteins in peroxisome inheritance. Both Pex3Bp and Pex3p are peroxisomal integral membrane proteins that function as peroxisomal receptors for class V myosin through direct interaction with the myosin globular tail. In cells lacking Pex3Bp, peroxisomes are preferentially retained by the mother cell, while most peroxisomes gather and are transferred en masse to the bud in cells overexpressing Pex3Bp or Pex3p. Our results reveal an unprecedented role for members of the Pex3 protein family in peroxisome motility and inheritance in addition to their well established role in peroxisome biogenesis at the ER. Our results point to a temporal link between peroxisome formation and inheritance and delineate a general mechanism of peroxisome inheritance in eukaryotic cells.

#### **4.2 The *Y. lipolytica* genome encodes a paralogue of Pex3p designated Pex3Bp**

Pex3 proteins are peroxisomal integral membrane proteins that act early in the peroxisome biogenic cascade. A search of protein databases using the Basic Blast program of the National Center for Biotechnology Information (NCBI) showed that *Y. lipolytica* is unique in having both Pex3p and a paralogue of Pex3p (XP\_501103). This uncharacterized paralogue of Pex3p has previously been designated as Pex3Bp (Kiel et al., 2006), and we have retained this convention here. Pex3Bp is predicted to be 395 amino acids in length, 36 amino acids shorter than Pex3p, with a molecular weight of 44,350 Da (Figure 4-1). Pex3p and Pex3Bp share 29.8% amino acid identity and 26.2% amino acid similarity. Like Pex3p between amino acids 11 to 28, Pex3Bp is predicted to have one transmembrane domain between amino acids 12 to 30 (<http://www.cbs.dtu.dk/services/TMHMM-2.0/>).

#### **4.3 Pex3Bp is an integral membrane protein of peroxisomes**

Because of the extensive similarity between Pex3p and Pex3Bp, we examined whether Pex3Bp, like Pex3p, is localized to peroxisomes. We showed using confocal microscopy that a chimera of Pex3Bp tagged at its C-terminus with monomeric red fluorescent protein (Pex3Bp-mRFP) colocalized with a GFP-tagged chimera of the peroxisomal matrix protein thiolase (Pot1p-GFP) to punctate structures characteristic of peroxisomes (Figure 4-2 A). Subcellular fractionation showed that Pex3Bp-mRFP, like Pot1p, localized preferentially to a 20,000 × *g* pellet fraction (20KgP) enriched for peroxisomes and not a 20,000 × *g* supernatant fraction (20KgS) enriched for cytosol (Figure 4-2 B). Peroxisomes in the 20KgP fraction were hypotonically lysed by

```

Pex3p  M-DFFRRHQKKVLALVGVALSSYLEFTDYVKKKFFETIQGRSSERTAKQNLRRRFEQNOOD 59
Pex3Bp MLQSLNRNKKRLAVSTGLIAYAVVVISYTTKRLIEKQEQKLEERAKERLQQLFAQTONE 60

Pex3p  ADETIMAILSSLTTPVMERYPVDQIKAEIQSKRRPTDRVLALESSTSSSATAQTVPTMTS 119
Pex3Bp AAFHTASVLPOLCEQIMEFVAVEKIAEQONMRAEKRRKQNMDDDKHSVLSLGTETTASM 120

Pex3p  GATEEGEKSKTQLWQDLKRTTISRAFSLVYADALLIFFTRLQNLILGRNRYVNSVVALAQ 179
Pex3Bp ADGQ--KMSKIQLWDELKIESLTRIVTLLYCVSLLNYLIRLQTNIVGRKRYON-----E 172

Pex3p  QGREGNAEGRVAPSPFGDLADMGYFGDLGSSSSFGETIVDPDLDEQYLTFSWWLLNEGWVS 239
Pex3Bp AGPAG-----ATYDMSLEQCYT----WLLTRGWKS 198

Pex3p  LSERVEEAVRRVWDPVSPKAEELGFDELSELTGRTOMLIDRPLNPSPLNFLSOLLPPREQ 299
Pex3Bp VVDNVRRSVQQVFTGVNPRONLSLDEFATLLKRVQTLVNSEPYSTTPNTFLTSLPPREL 258

Pex3p  EEYVLAQ-NPSDTAAPIVGPTRLRLLDETADEFESPNAAEVIERLVHSGLSVFMCKLAVT 358
Pex3Bp EQLRLEKEKQSLSPNYTYGSPLKDLVEESAQHIOSPQGMSSERAIIDQSFKVFLEKVNES 318

Pex3p  FGATPADSGS-----PYPVVLPTAKVKLPSILANMAROAGGMAOGSPGVENEYIDV 409
Pex3Bp QYVNPSTGGKRIAVGALQPPILSGGPKVKVLASLLSVATROSSVISHAQP---NPYVDA 375

Pex3p  MNQVOELTSFSAVVYSSFDWAL 431
Pex3Bp INSVAEYNGLCAVIYSSFEQ-- 395

```

**Figure 4-1. Sequence alignment of Pex3p with the hypothetical protein Pex3Bp encoded by the *Y. lipolytica* genome.** Amino acid sequences were aligned with the use of the ClustalW program (<http://www.ebi.ac.uk/Tools/clustalw2>). Identical residues (black) and similar residues (gray) in the two proteins are shaded. Similarity rules: G = A = S; A = V; V = I = L = M; I = L = M = F = Y = W; K = R = H; D = E = Q = N; and S = T = Q = N. Dashes represent gaps.

incubation in dilute alkali Tris buffer and subjected to centrifugation to yield a supernatant (Ti8S) enriched for matrix proteins and a pellet (Ti8P) enriched for membrane proteins (Figure 4-2 C). Pex3Bp-mRFP localized almost exclusively to the Ti8P fraction like the known peroxisomal integral membrane protein Pex2p (Eitzen et al., 1996) and in contrast to the soluble peroxisomal matrix enzyme Pot1p, which was found only in the Ti8S fraction. The Ti8P fractions were then extracted with alkali sodium carbonate and subjected to centrifugation (Figure 4-2 C). This treatment releases proteins associated with, but not integral to, membranes (Fujiki et al., 1982). Under these conditions, Pex3Bp-mRFP fractionated with Pex2p to the pellet fraction enriched for integral membrane proteins. Isopycnic density gradient centrifugation of the 20K<sub>g</sub>P fraction of wild-type *E122* cells indicated that Pex3Bp co-enriched with Pot1p and not with the mitochondrial protein, Sdh2p (Figure 4-3). Collectively, these data demonstrate that Pex3Bp is an integral membrane protein of peroxisomes.

The potential for functional redundancy between Pex3p and Pex3Bp may have prevented the identification of Pex3Bp as a bona fide peroxin involved in peroxisome biogenesis in *Y. lipolytica* in screens employing random mutagenesis and negative selection for growth on medium containing oleic acid as sole carbon source and whose metabolism requires functional peroxisomes. Consistent with this possibility, the deletion strain *pex3BΔ* was only marginally retarded in growth compared to the wild-type strain *E122* when spotted as serial dilutions onto agar medium containing oleic acid (Figure 4-2 D). This is in stark contrast to the *pex3Δ* strain, which shows no growth. The slightly retarded growth of the *pex3BΔ* strain in the presence of oleic acid is consistent with a

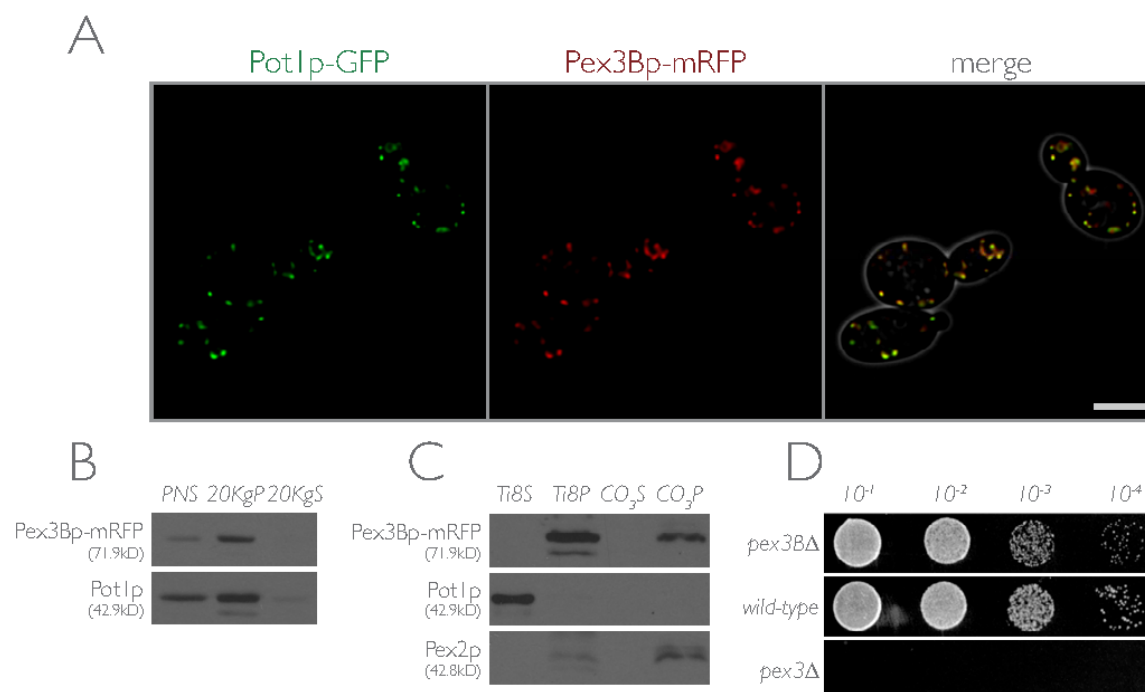


**Figure 4-2. Pex3Bp is a peroxisomal integral membrane protein.** (A) Pex3Bp-mRFP colocalizes with the peroxisomal chimeric reporter Pot1p-GFP to punctate structures characteristic of peroxisomes by confocal microscopy. The right panel presents the merged image of the left and middle panels, with colocalization of Pex3Bp-mRFP and Pot1p-GFP shown in yellow. Bar, 5  $\mu$ m. (B) Pex3Bp-mRFP localizes to the 20KgP subcellular fraction enriched for peroxisomes. Immunoblot analysis of equivalent portions of the PNS, 20KgP and 20KgS subcellular fractions from cells expressing Pex3Bp-mRFP was performed with antibodies to mRFP and to the peroxisomal matrix enzyme thiolase (Pot1p). (C) Pex3Bp exhibits the characteristics of an integral membrane protein. The 20KgP fraction from cells expressing Pex3Bp-mRFP was treated with Ti8 buffer to lyse peroxisomes and then subjected to centrifugation to yield a supernatant fraction (Ti8S) enriched for matrix proteins and a pellet fraction (Ti8P) enriched for membrane proteins. The Ti8P fraction was further treated with alkali Na<sub>2</sub>CO<sub>3</sub> and separated by centrifugation into a supernatant fraction (CO<sub>3</sub>S) enriched for peripheral membrane proteins and a pellet fraction (CO<sub>3</sub>P) enriched for integral membrane proteins. Equivalent portions of each fraction were analyzed by immunoblotting. Immunodetection of Pot1p and Pex2p marked the fractionation profiles of a peroxisomal matrix and integral membrane protein, respectively. (D) *pex3BΔ* cells exhibit slightly retarded growth on oleic acid medium. Cells of the wild-type strain *E122* and of the deletion strains *pex3BΔ* and *pex3Δ* were grown to mid-log phase in liquid YPD, incubated in liquid YPBO for 1 day, spotted at dilutions of 10<sup>-1</sup> to 10<sup>-4</sup> on YPBO agar, and grown for 2 days at 30°C.

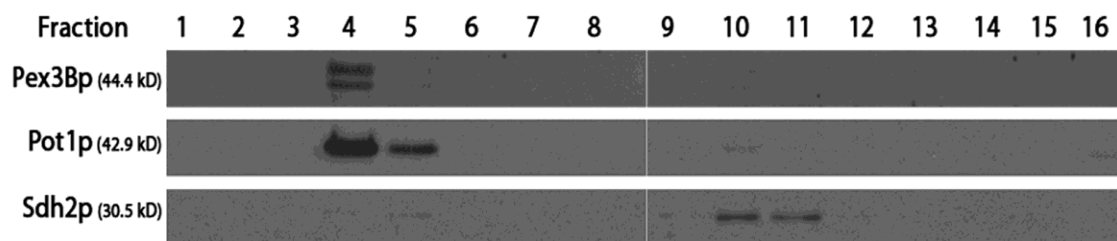


**Figure 4-3. Pex3Bp cofractionates with peroxisomes.** Organelles in the 20KgP fraction from wild-type *E122* cells were separated by isopycnic centrifugation on a discontinuous sucrose gradient. Fractions were collected from the bottom of the gradient, and equal volumes of each fraction were separated by SDS-PAGE and analyzed by immunoblotting with antibodies to the indicated proteins. Fractions enriched for peroxisomes and mitochondria were identified by immunodetection of Pot1p and Sdh2p, respectively.

possible regulatory role of Pex3Bp in peroxisome morphology, division or inheritance rather than in peroxisome assembly per se (Yan et al., 2005).

#### **4.4 Deletion of the *PEX3B* gene affects peroxisome morphology**

To investigate a possible role for Pex3Bp in peroxisome biogenesis, we used confocal microscopy to track both the subcellular localization of the fluorescent peroxisomal marker chimera Pot1p-GFP and the morphology of peroxisomes containing Pot1p-GFP in *pex3BΔ* cells. Wild-type cells and *pex3BΔ* cells were observed over time following a shift from glucose-containing YPD medium to oleic acid-containing YPBO medium. Peroxisomes increase in size and number with a switch from a fermentative carbon source like glucose to a nonfermentative carbon source like oleic acid, which is metabolized exclusively by peroxisomes.

At the time of transfer from YPD to YPBO medium, wild-type cells had numerous (~20-40) punctate peroxisomes that increased both in size and number with time of incubation in YPBO medium (Figure 4-4 A). In contrast, the morphology and numbers of peroxisomes were highly heterogenous in *pex3BΔ* cells. As time of incubation in YPBO increased, *pex3BΔ* cells exhibited hyperelongated, tubular-reticular peroxisomes, suggesting an imbalance between peroxisome growth and fission in *pex3BΔ* cells. Peroxisome number in *pex3BΔ* cells varied from as low as 1 to 2 peroxisomes per cell to numbers of peroxisomes comparable to those observed in wild-type cells. The percentage of *pex3BΔ* cells containing elongated peroxisomes increased with time of incubation in oleic acid-containing medium, so that by 10 h of incubation in YPBO, approximately 90% of *pex3BΔ* cells contained tubular-reticular peroxisomes (Figure 4-4

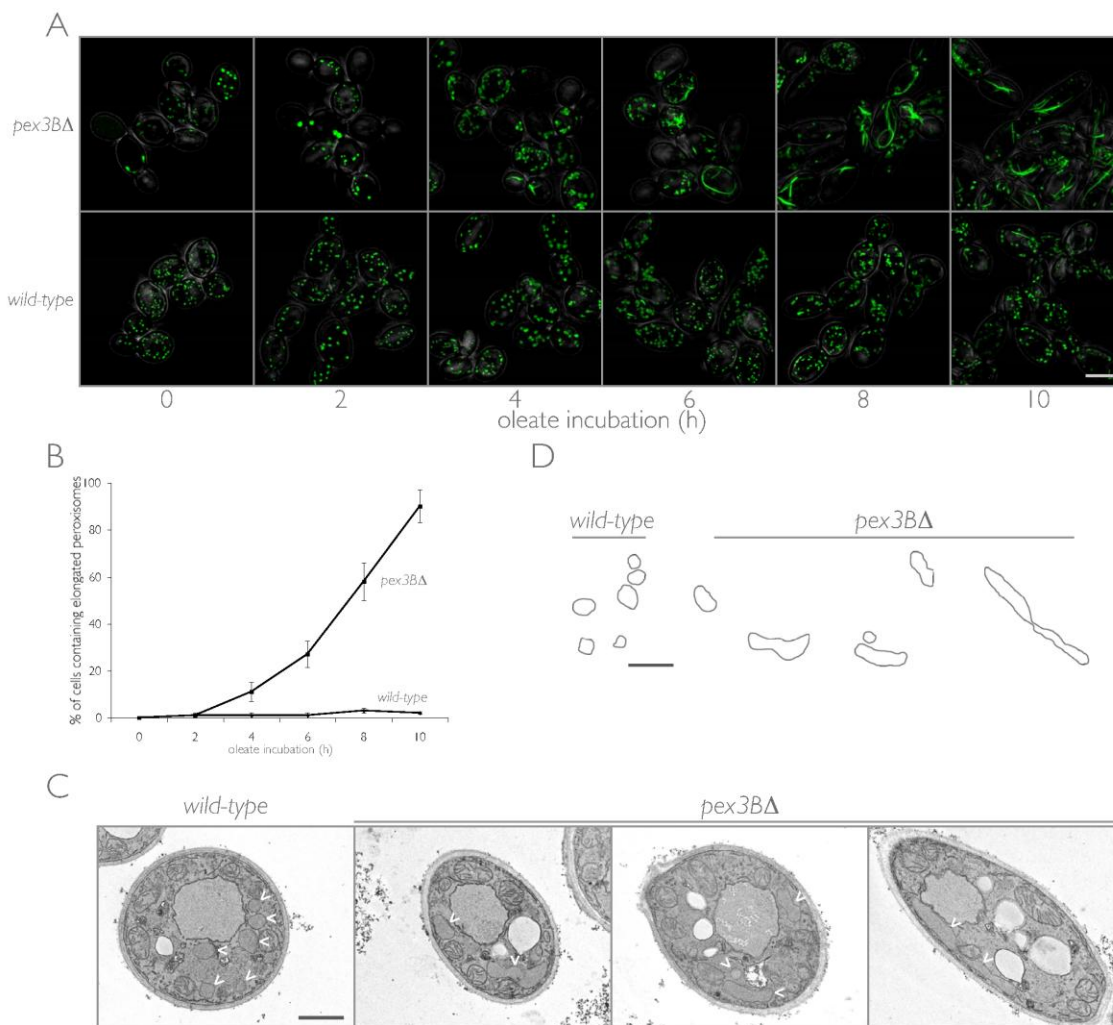


**Figure 4-4. Deletion of the *PEX3B* gene affects peroxisome morphology.** (A) Wild-type and *pex3BA* cells expressing genomically integrated *POT1-GFP* were grown in glucose-containing YPD for 16 h and then transferred to oleic acid-containing YPBO. Fluorescent images of cells at different times of incubation in YPBO were captured by confocal microscopy and deconvolved. Bar, 5  $\mu$ m. (B) Cells lacking Pex3Bp contain elongated peroxisomes. An elongated peroxisome was functionally defined as being 2  $\mu$ m or greater in length along its long axis. Graphic results are the means and SEMs of 3 independent experiments. (C) Ultrastructure of wild-type *E122* and *pex3BA* cells. Cells were cultured in YPD for 16 h, transferred to YPBO for 10 h, and then fixed and processed for EM. Arrowheads point to individual peroxisomes. Bar, 1  $\mu$ m. (D) Tracings of individual peroxisomes in the electron micrographs of cells presented in (C). Bar, 1  $\mu$ m.

B). The percentage of wild-type cells containing elongated peroxisomes never exceeded 1-2%. Furthermore, the reduced numbers of peroxisomes and the elongated peroxisome morphology seen in *pex3BΔ* cells correlated with a noticeable absence of peroxisomes from buds in these cells. Thin section transmission EM showed the typical spherical peroxisomal profiles of wild-type cells (Figure 4-4 C and D). In contrast, *pex3BΔ* cells contained peroxisomes that were vermiform in appearance and were reduced in number, with typically 1 or 2 peroxisomal profiles observed per section as compared to 5 or more profiles in a section of a wild-type cell (Figure 4-4 C and D). The elongated peroxisomes in *pex3BΔ* cells often exhibited a long to short axis ratio in excess of 10 to 1. These elongated peroxisomes differ in appearance from other elongated peroxisomes previously observed, for example, in *S. cerevisiae* cells lacking the dynamin-related protein Vps1p, which contain elongated peroxisomes with a beads-on-a-string appearance (Hoepfner et al., 2001), or *S. cerevisiae* cells overexpressing the peroxisomal membrane protein Pex11p controlling peroxisomal division, which often show two peroxisomes connected by a thin tubule, somewhat like a dumbbell (Erdmann and Blobel, 1995).

#### **4.5 Deletion of the *PEX3B* gene affects specifically peroxisome inheritance**

The absence of punctate peroxisomes in many of the buds of *pex3BΔ* cells (Figure 4-4 A and Figure 4-5 A) led us to speculate that Pex3Bp might have a role in partitioning peroxisomes between mother cell and bud at cell division. We previously showed that peroxisome inheritance in *Y. lipolytica* is an active process with *YInp1p*-mediated retention of peroxisomes in cells and directed transport of peroxisomes along actin filaments to growing buds (Chapter 3). We quantified a defect in peroxisome inheritance

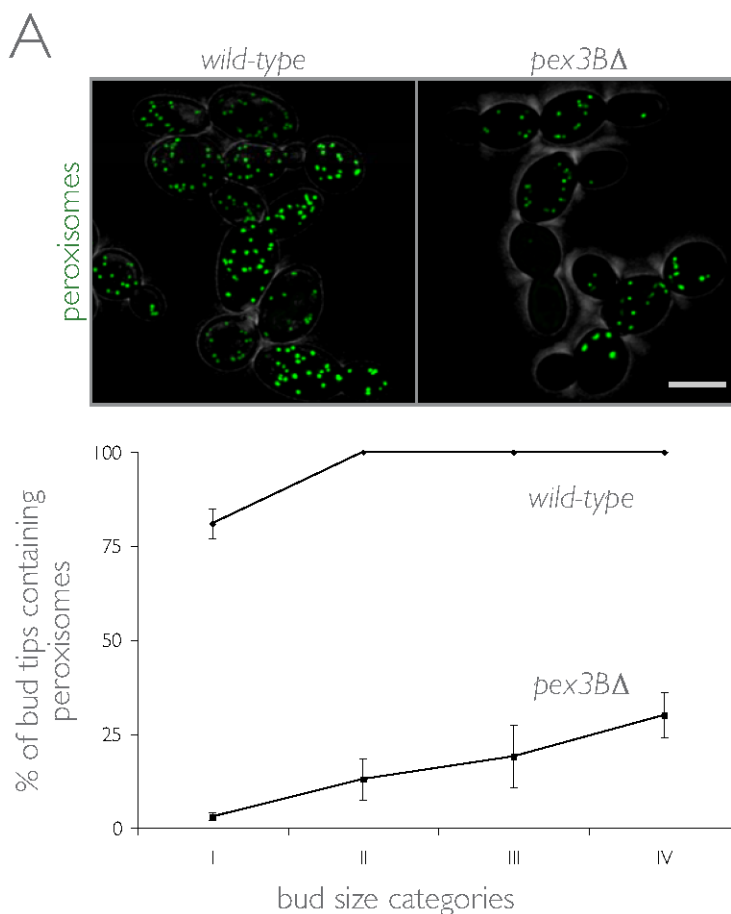
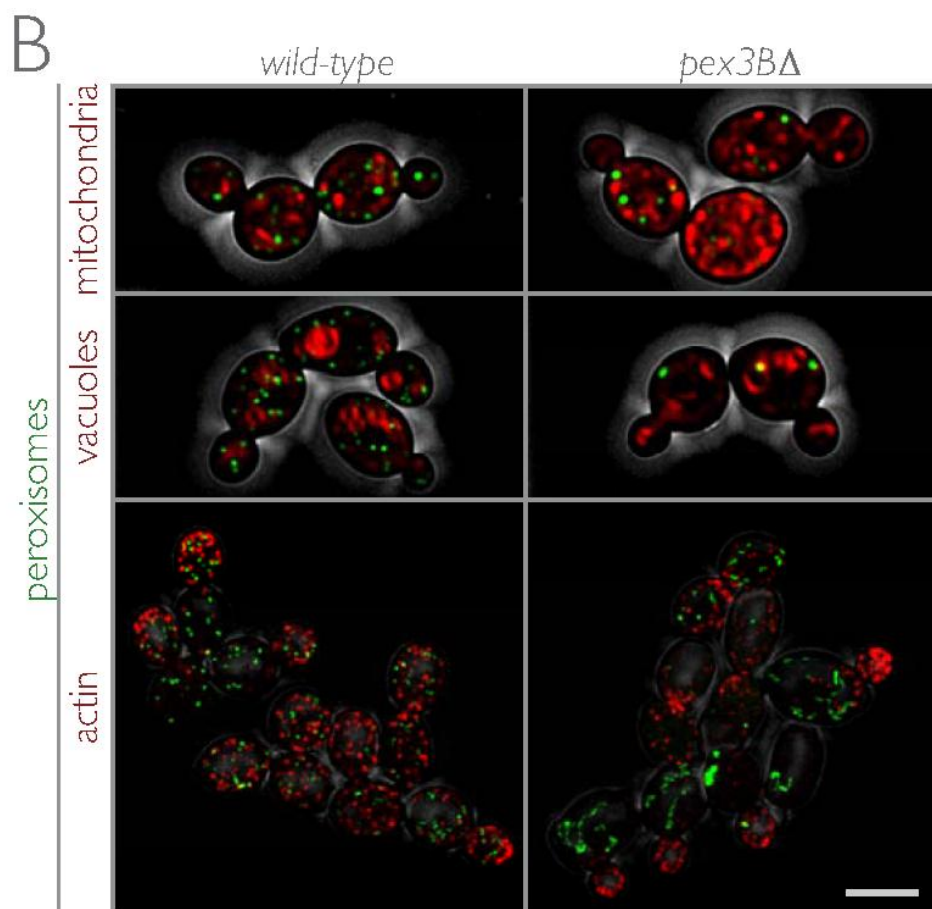


**Figure 4-5. Deletion of the *PEX3B* gene affects specifically peroxisome inheritance.**

(A) Wild-type and *pex3Δ* cells expressing genomically integrated *POT1-GFP* were grown in YPD for 16 h and then transferred to YPBO for 2 h. Fluorescent images of randomly chosen fields of cells were acquired as a stack by confocal microscopy and deconvolved. Buds were sized according to four categories relative to the volume of the mother cell. The percentages of bud tips containing peroxisomes at each size category were plotted. Quantification was performed on at least 50 budded cells from each category. Graphic results are the means and SEMs of 3 independent experiments. Bar, 5  $\mu$ m. (B) Deletion of the *PEX3B* gene does not affect the actin structure of cells or the inheritance of vacuoles or mitochondria. Wild-type and *pex3Δ* cells synthesizing Pot1p-GFP were grown in YPD. Mitochondria were stained with Mitotracker dye, vacuoles were stained with the fluorophore FM 4-64 and actin was stained with rhodamine-phalloidin. Images were captured by confocal microscopy. Bar, 5  $\mu$ m.



in *pex3 $\Delta$*  cells (Figure 4-5 A). When *pex3 $\Delta$*  cells were incubated in oleic acid-containing YPBO medium for 2 h, only 3%, 13%, 19% and 26% of bud tips in the respective categories I, II, III and IV (from smallest to largest in size) contained peroxisomes. In wild-type cells, 81% of bud tips in category I and 100% of bud tips in categories II, III and IV contained peroxisomes. Lack of Pex3Bp specifically affected the inheritance of peroxisomes, as both vacuoles and mitochondria showed normal inheritance in *pex3 $\Delta$*  cells (Figure 4-5 B). Actin organization in wild-type and *pex3 $\Delta$*  cells was similar, with rhodamine-phalloidin staining showing actin patches at sites of polarized growth in both wild-type and *pex3 $\Delta$*  cells (Figure 4-5 B).

#### **4.6 Peroxisome dynamics in *pex3 $\Delta$* cells**

Our observations suggested a link between altered peroxisome morphology and defective peroxisome inheritance in *pex3 $\Delta$*  cells. We investigated this possible link by imaging wild-type and *pex3 $\Delta$*  cells expressing *POT1-GFP* by 4D confocal microscopy (Figure 4-6). Peroxisomes in wild-type cells were active and exhibited both directed and saltatory movements (Figure 4-6 A and Movie 4-S1; see also Chapter 3). Peroxisome inheritance occurred soon after bud formation, with peroxisomes being delivered to the bud and becoming associated with bud tips and then evenly distributed in the bud. Retrograde movement of peroxisomes from bud to mother could also be detected, and the traffic of peroxisomes between mothers and buds remained bidirectional until cytokinesis, whereupon a new bud emerged and the cycle continued. The saltatory movement of peroxisomes was more apparent in buds than mothers. Peroxisome partitioning led to peroxisomes evenly distributed between mothers and buds, with some

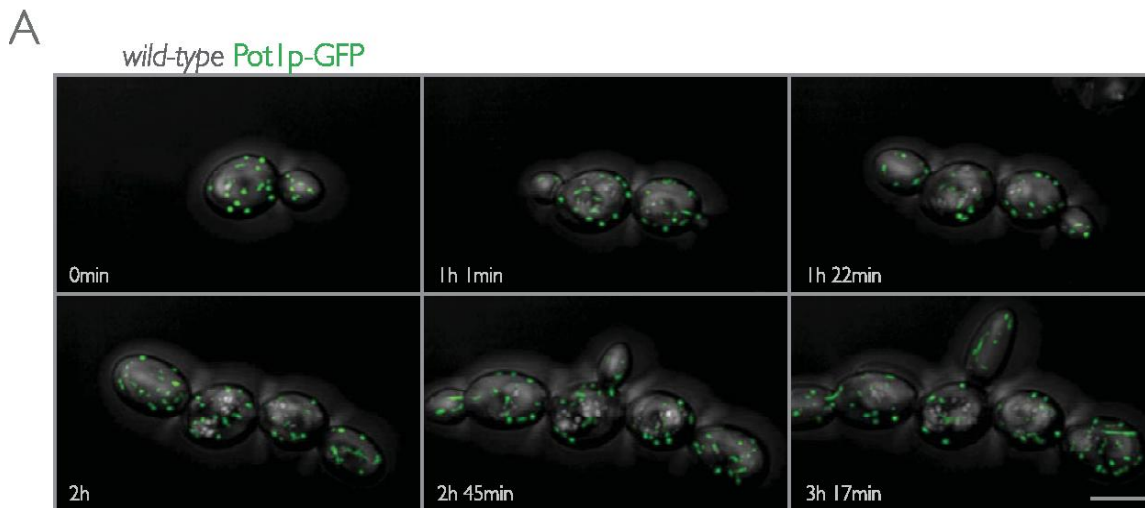
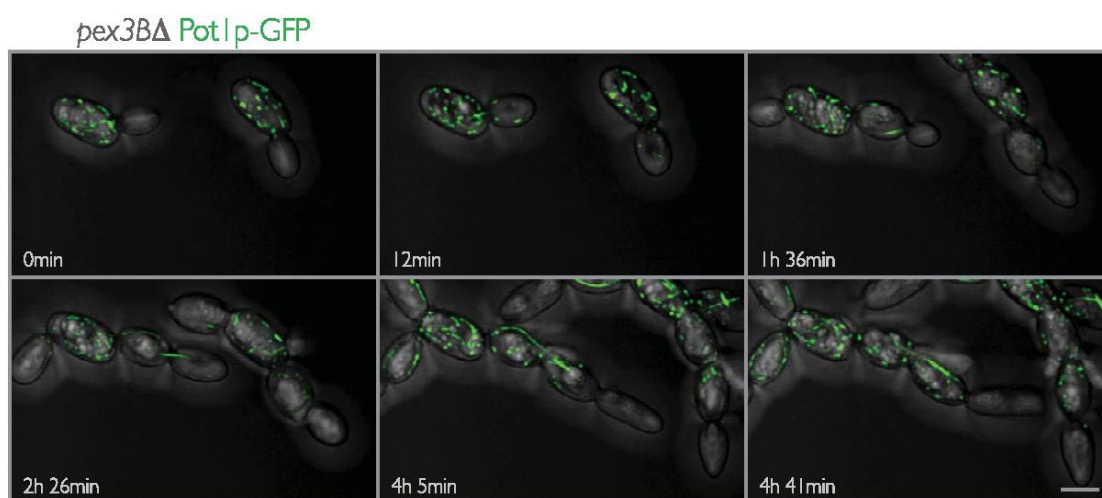
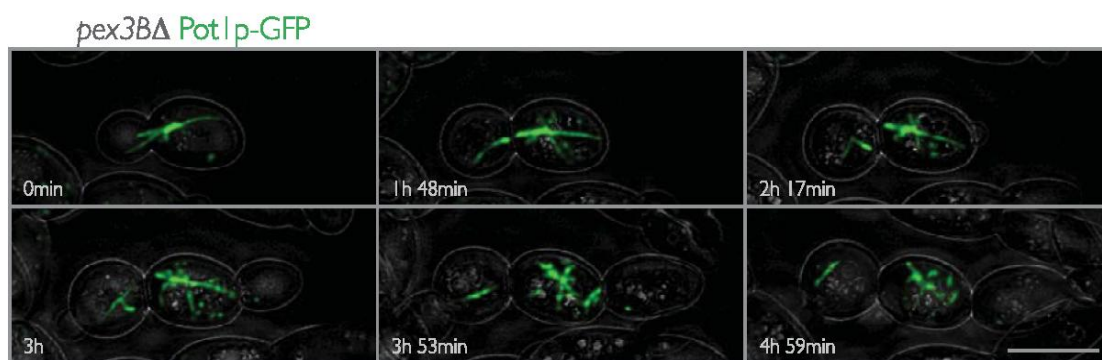


**Figure 4-6. Peroxisome dynamics in wild-type and *pex3B*Δ cells.** Peroxisomes were fluorescently labeled with genomically encoded Pot1p-GFP. Cells were grown for 16 h in YPD, transferred to YPBO for 6 h, and visualized at 28°C (A-B) or 23°C (C) with an LSM 510 confocal microscope specifically modified for 4D in vivo microscopy. (A) Wild-type *E122/POT1-GFP* strain. Representative frames from Movie 4-S1 show the specific movements and division of peroxisomes through several cell divisions. The emergence of new buds is followed by the vectorial transfer of a portion of peroxisomes from the mother cell to the bud, where they initially associate with the bud tip and then evenly distribute in the bud. Bar, 5 μm. (B-C) *pex3B*Δ/*POT1-GFP* strain. (B) Representative frames from Movie 4-S2 display the specific movements and morphogenesis of peroxisomes in *pex3B* cells. At the start of the movie (0 min), both buds lack peroxisomes. By 12 min, several peroxisomes have entered the buds but have failed to associate with the bud tips. Subsequently, many peroxisomes undergo a morphogenic transition, becoming elongated and tubular-reticular in appearance. These peroxisomes sometimes straddle the mother-bud neck (2 h 26 min). Also, peroxisome inheritance does not keep pace with cell division, as many buds are devoid of peroxisomes at later time points (4 h 5 min and 4 h 41 min). Bar, 5 μm. (C) Representative frames from Movie 4-S3 display the inability of a tubular-reticular peroxisome to divide except through cytokinesis. A tubular-reticular peroxisome is seen initially straddling the mother-bud neck (0 min). At 1 h 48 min, the peroxisome is cut in two by constriction of the septin ring, concluding cytokinesis. A second scission event occurs at 3 h 53 min with the conclusion of cytokinesis between the mother cell and the bud to her right inheriting only one peroxisome. Subsequent buds fail to inherit peroxisomes (4 h 49 min). Bar, 5 μm.

B



C



peroxisomes being mobile and others being anchored.

In *pex3 $\Delta$*  cells, peroxisomes lacked saltatory movements, and their inheritance was delayed or abolished (Figure 4-6 B and Movie 4-S2). Peroxisomes did not enter the bud until it was approximately half the size of the mother cell and quickly ceased their movements in the bud, failing to reach the bud tip. Many peroxisomes in *pex3 $\Delta$*  cells also became elongated and assumed a tubular-reticular appearance and were either anchored to the cell cortex or found sliding along the cortex. Sometimes the elongated peroxisomes were found straddling the mother-bud neck junction. We also observed that the elongated peroxisomes in *pex3 $\Delta$*  cells rarely divided but rather were severed by cytokinesis because of their straddling the mother-bud junction (Figure 4-6 C and Movie 4-S3). Interestingly, the peroxisome inheritance defect in *pex3 $\Delta$*  cells led to buds lacking peroxisomes but now exhibiting de novo peroxisome biogenesis (Movie 4-S2). Pot1p-GFP accumulated cytosolically in these buds and then was imported into discrete, newly formed punctae.

#### **4.7 Peroxisome inheritance by buds depends on a class V myosin motor in *Y.***

##### ***lipolytica***

Class V myosins are conserved motor proteins. These motor proteins associate with the actin cytoskeleton through their N-terminal motor domain and with the transporting cargo through their C-terminal globular domain. *S. cerevisiae* has two class V myosins, Myo2p and Myo4p. Most organelles, including peroxisomes, are carried to the bud by Myo2p in *S. cerevisiae*. A search of the *Y. lipolytica* genome revealed one class V myosin encoded by the ORF, *YAL10E00176g*. This class V myosin functions in peroxisome

transport to buds, as overexpression of its cargo-binding domain (amino acids 1092-1594) led to large reductions in the number of peroxisomes transferred from mother cell to bud (Figure 4-7 A). In overexpressing cells, only 25% of small buds and 62% of large buds contained peroxisomes, while 90% of small buds and 100% of large buds of wild-type cells contained peroxisomes (Figure 4-7 A). Interestingly, overexpressing cells grew more slowly than wild-type cells (Figure 4-7 B), suggesting that the unique class V myosin in *Y. lipolytica* may be involved in the transport of other organelles, including secretory vesicles, which are also carried by Myo2p in *S. cerevisiae* (Pashkova et al., 2006).

#### **4.8 A candidate *Y. lipolytica* Inp2p orthologue, YALI0E03124p, is not the peroxisome-specific receptor for myosin V**

Peroxisomes in *S. cerevisiae* are transported by the myosin V motor protein, Myo2p, through its direct interaction with the peroxisomal protein Inp2p (Fagarasanu et al., 2006). Inp2p shows no obvious homology to Pex3Bp. We therefore searched the *Y. lipolytica* genome for a possible Inp2p orthologue. A Position-Specific Iterated (PSI)-Blast (Altschul et al., 1997) of three iterations using the *S. cerevisiae* protein Inp2p as a bait sequence identified the protein encoded by the ORF *YALI0E03124g* as a possible Inp2p orthologue in *Y. lipolytica*. We tested YALI0E03124p for two critical criteria of a peroxisome-specific receptor for myosin V: specific localization to peroxisomes and direct interaction with myosin V. YALI0E03124p did not localize to peroxisomes and, under conditions in which cells were incubated in oleic acid, targeted to regions of the cell that appeared to be elements of the secretory pathway (Figure 4-8). Furthermore, in a

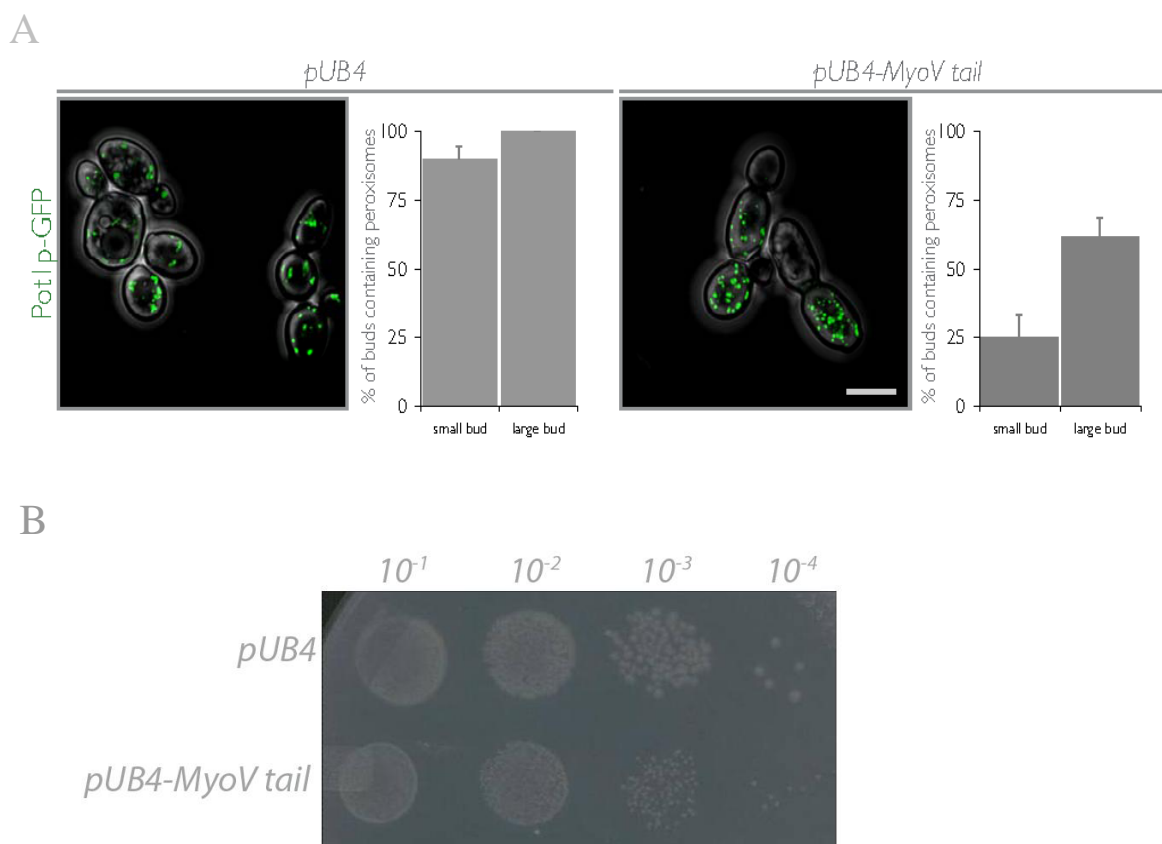


**Figure 4-7. Peroxisome movement depends on class V myosin.** (A) Peroxisome inheritance is reduced by overexpression of the *Y. lipolytica* class V myosin cargo-binding tail. Wild-type strain *E122* expressing genomically encoded Pot1p-GFP to fluorescently label peroxisomes was transformed with the empty plasmid pUB4 or with pUB4 expressing the globular tail domain (amino acids 1092-1594) of *Y. lipolytica* class V myosin under the control of the oleic acid-inducible *POT1* promoter. Cells were grown in YPD supplemented with hygromycin B and then transferred to and incubated in oleic acid-containing YPBO supplemented with hygromycin B for 6 h. Fluorescent images of randomly chosen fields of cells were acquired as a stack by confocal microscopy and then deconvolved. Buds were sized as “small” or “large”. The percentages of buds containing peroxisomes in each size category are presented. Quantification was performed on at least 50 budded cells from each category. Graphic results are the means and SEMs of 3 independent experiments. Bar, 5  $\mu\text{m}$ . (B) Cells overexpressing the globular tail of class V myosin exhibit slower growth than wild-type cells. Wild-type strain *E122* transformed with the empty plasmid pUB4 or with pUB4 expressing the globular tail domain (amino acids 1092-1594) of *Y. lipolytica* class V myosin under the control of the oleic acid-inducible *POT1* promoter was grown to mid-log phase in liquid YPD supplemented with hygromycin B, spotted at dilutions of  $10^{-1}$  to  $10^{-4}$  on YPBO agar supplemented with hygromycin B, and grown for 2 days at  $30^\circ\text{C}$ .

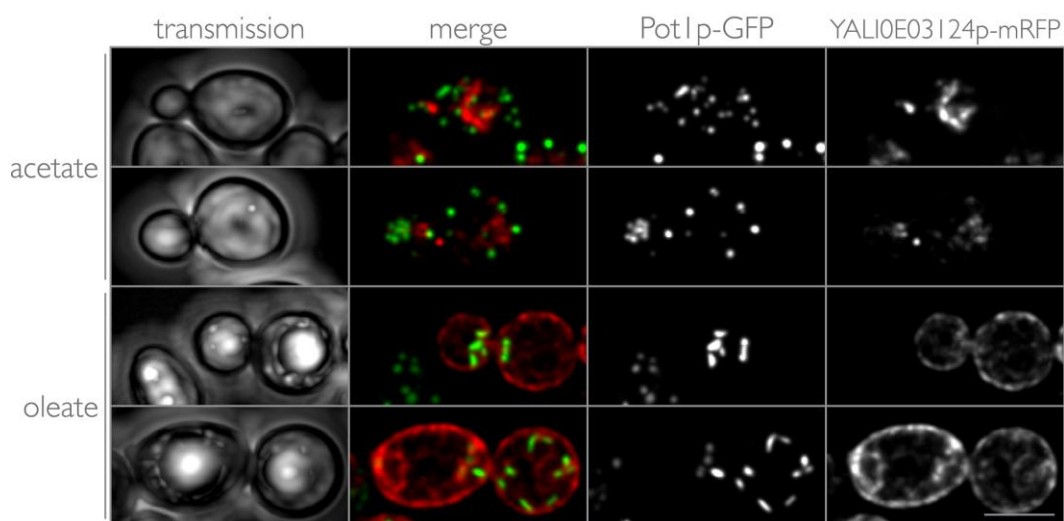


**Figure 4-8. A candidate *Y. lipolytica* Inp2p orthologue, YALI0E03124p, does not localize to peroxisomes.** The chimeric protein YALI0E03124p-mRFP whose expression is under the control of the oleic acid-inducible promoter *POT1* was imaged in the wild-type strain *E122* expressing genomically integrated Pot1p-GFP to fluorescently label peroxisomes. YALI0E03124p-mRFP did not localize to punctate peroxisomes, and when cells were incubated in oleic acid-containing medium, YALI0E03124p-mRFP exhibited a pattern typical of protein localization to the ER and secretory system. The top panels show representative images of cells grown in medium containing acetate, the bottom panels show representative images of cells grown in medium containing oleic acid. Bar, 5  $\mu\text{m}$ .

GST pull-down assay, recombinant MBP-YALIOE03124p did not interact with GST fused to the cargo-binding tail of the class V myosin of *Y. lipolytica* (GST-YIMyoV) (Figure 4-9 B), ruling out a direct interaction between the two proteins.

#### **4.9 Pex3Bp and Pex3p interact directly with the globular tail of the *Y. lipolytica* class V myosin**

Because *pex3BΔ* cells exhibit a defective peroxisome inheritance phenotype similar to that exhibited by *inp2Δ* cells of *S. cerevisiae*, we performed a split-ubiquitin membrane yeast two-hybrid analysis to test the ability of Pex3Bp to interact with the globular tail domain (amino acids 1092-1594) of the *Y. lipolytica* class V myosin (Figure 4-9 A). A strong interaction was detected between Pex3Bp and the globular tail domain of the class V myosin. Interestingly, Pex3p also showed a detectable interaction with the globular tail domain of the class V myosin. Interactions between Pex3Bp and Pex3p, Pex3Bp and itself, and Pex3p and itself were also observed.

If members of the Pex3p protein family are bona fide peroxisomal receptors for the *Y. lipolytica* class V myosin, we expect them to interact directly with the class V myosin. Since two-hybrid analysis does not differentiate between direct and bridged protein interactions, we performed a pull-down assay using recombinant Pex3Bp and Pex3p fused to maltose binding protein (MBP) and the *Y. lipolytica* class V myosin tail fused to glutathione-S-transferase (GST) made in *E.coli* (Figure 4-9 B). MBP-Pex3Bp was pulled down by GST-*Y. lipolytica* myosin V (GST-YIMyoV). MBP-Pex3Bp was also pulled down by a GST fusion to the tail domain of *S. cerevisiae* class V myosin, Myo2p (GST-ScMyoV), but to a lesser extent than by GST-YIMyoV. Appreciable

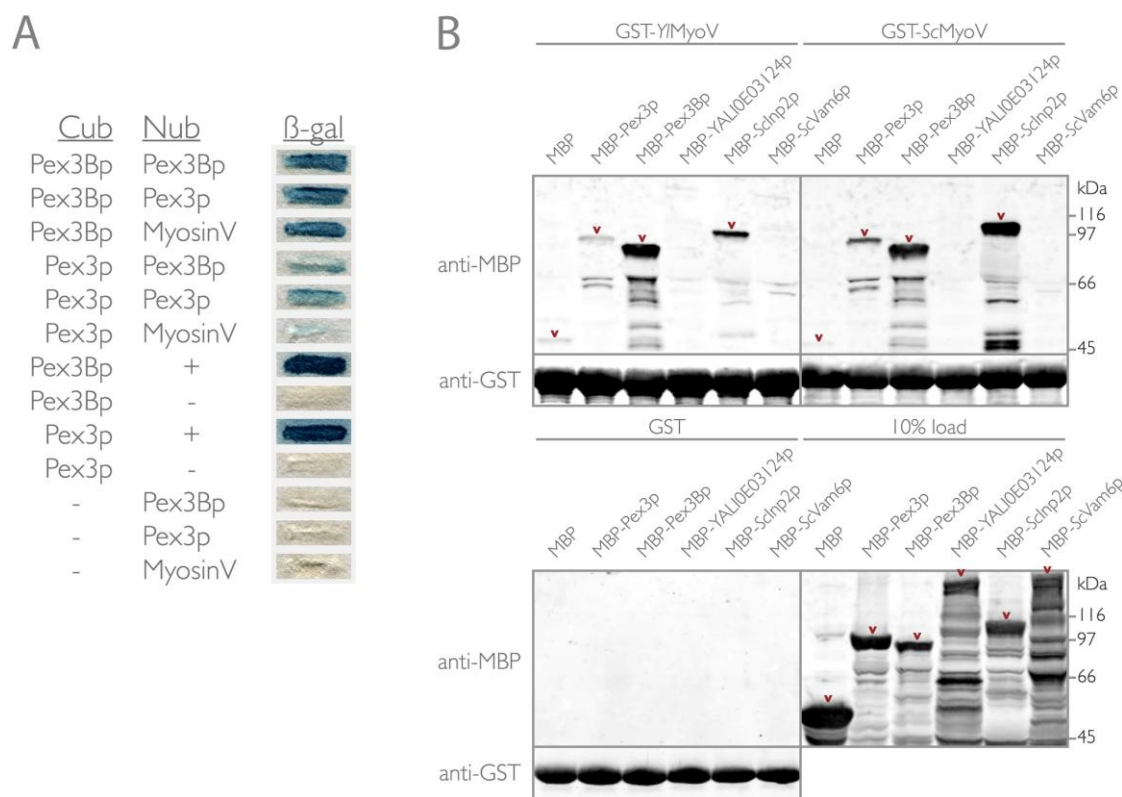


**Figure 4-9. Pex3Bp and Pex3p interact directly with the cargo-binding tail of *Y. lipolytica* class V myosin.** (A) Split-ubiquitin membrane yeast two-hybrid analysis. Cells of the *S. cerevisiae* strain *DSY-1* synthesizing Cub protein fusions to Pex3Bp or Pex3p and NubG protein fusions to Pex3Bp, Pex3p or the globular tail of the class V myosin of *Y. lipolytica* (amino acids 1092-1594) were tested for their ability to interact with each other by a  $\beta$ -galactosidase filter detection assay. A positive interaction is detected by the production of blue color. The color intensities of positive (+) and negative (-) controls are indicated. (B) Glutathione sepharose beads containing GST fused to the cargo-binding tail of the class V myosin of *Y. lipolytica* (GST-YIMyoV), the cargo-binding tail of the class V myosin, Myo2p, of *S. cerevisiae* (GST-ScMyoV), or GST alone were incubated with extracts of *E. coli* synthesizing MBP, MBP-Pex3p, MBP-Pex3Bp, MBP-YALI0E03124p, MBP-ScInp2p or MBP-ScVam6p. Bound proteins, as well as 10% of input proteins, were analyzed by immunoblotting with anti-MBP antibodies. Total GST-YIMyoV, GST-ScMyoV or GST protein levels were visualized by immunoblotting with anti-GST antibodies. Arrowheads highlight MBP or MBP fusion proteins.

amounts of MBP-Pex3p were also pulled down by both GST-YIMyoV and GST-ScMyoV; however, this interaction was not as strong as that observed between MBP-Pex3Bp and GST-YIMyoV or GST-ScMyoV. These results confirmed the results of yeast two-hybrid analysis and ruled out a requirement for additional proteins in the interaction between Pex3Bp or Pex3p and myosin V.

#### **4.10 Peroxisome dynamics in *pex3B*Δ cells overexpressing *PEX3B* or *PEX3***

Delivery of peroxisomes from mother cell to bud by an actin-myosin based system mediated through the interactions of myosin V with Pex3Bp and Pex3p suggested that overexpression of Pex3Bp or Pex3p should result in the disproportionate segregation of peroxisomes to the bud, as has been observed for overexpression of the peroxisomal class V myosin receptor, Inp2p, in *S. cerevisiae* (Fagarasanu et al., 2006). To test this prediction, we used 4D in vivo confocal microscopy to image *pex3B*Δ cells containing fluorescently labeled peroxisomes and overexpressing *PEX3B* or *PEX3* (Figure 4-10). Rather than the elongated tubular-reticular peroxisomes observed in *pex3B*Δ cells, peroxisomes in cells overexpressing *PEX3B* appeared bulbous and globular (Figure 4-10 A and Figure 4-11 A, Movie 4-S4). These peroxisomes clustered initially near the bud-neck region and, despite their large size, were successively delivered through several cell divisions to each newly formed bud. We also detected de novo peroxisome formation occurring in the mother cells devoid of peroxisomes (Movie 4-S4). Surprisingly, these de novo made peroxisomes were also transferred to newly formed buds, demonstrating the fidelity of the mechanism of peroxisome inheritance. Time-lapse 4D confocal microscopy of *pex3B*Δ cells containing fluorescently labeled peroxisomes and

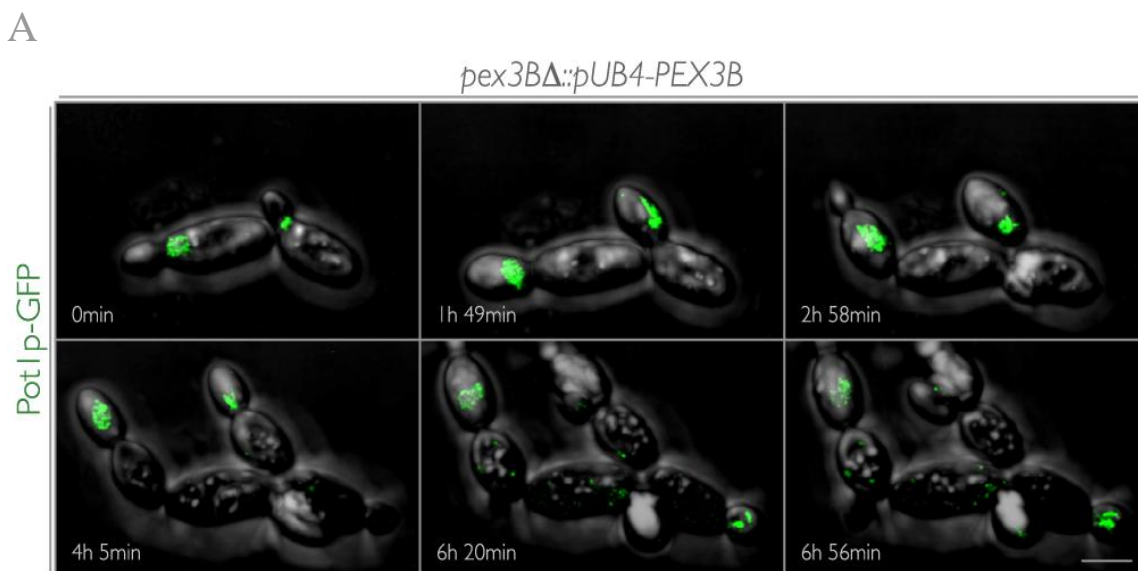
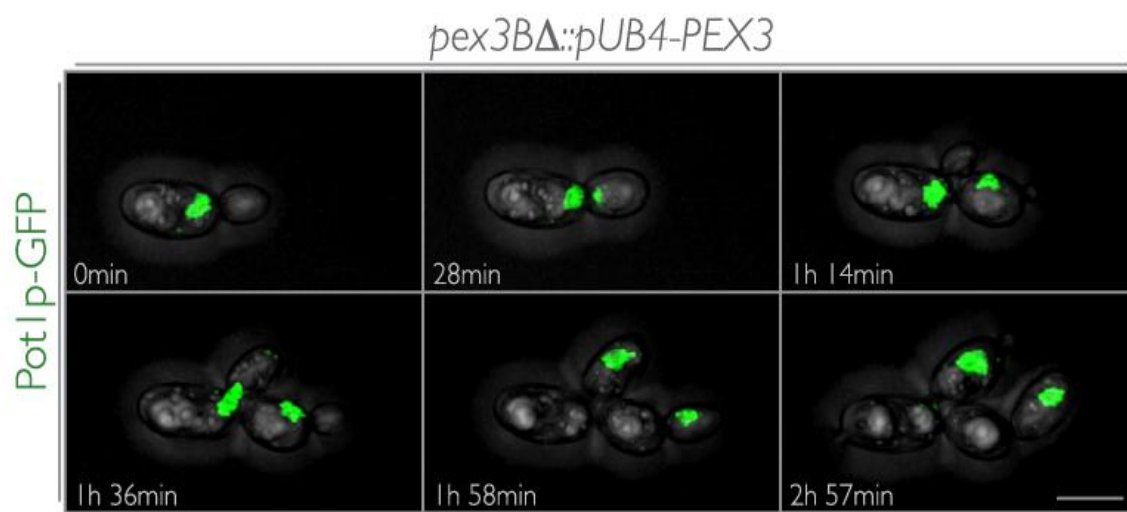


**Figure 4-10. Peroxisome dynamics in *pex3BΔ* cells overexpressing *PEX3B* or *PEX3*.** (A) *pex3BΔ* cells containing peroxisomes labeled with Pot1p-GFP and the plasmid pUB4 expressing *PEX3B* under the control of the oleic acid-inducible *POT1* promoter were grown for 16 h in YPD supplemented with hygromycin B, then transferred to oleic acid-containing YPBO supplemented with hygromycin B for 6 h, and visualized at 23°C with an LSM 510 confocal microscope specifically modified for 4D *in vivo* microscopy. Representative frames from Movie 4-S4 show the specific movements of peroxisomes and their inheritance from mother cell to bud. At 0 min, two large peroxisome clusters are initially located next to the mother-bud neck. By 1 h 49 min, these peroxisomes have been transferred to their respective buds, and by 4 h 5 min, the cycle is repeated, with the peroxisomes now residing in the granddaughters of the original mother cells. De novo synthesis of peroxisomes can also be detected by the reappearance of fluorescent punctae in mother cells that had transferred their original peroxisome complement to their buds. These de novo formed peroxisomes are also vectorially transferred to newly formed buds (6 h 20 min). The formation of peroxisomes and subsequent transfer to buds continue (6 h 56 min). Bar, 5 μm. (B) *pex3BΔ* cells containing peroxisomes labeled with Pot1p-GFP and the plasmid pUB4 expressing *PEX3* under the control of the oleic acid-inducible *POT1* promoter were grown and imaged as in (A). Representative frames from movie 4-S5 show the specific movements of peroxisomes and their inheritance from mother cell to bud. At 0 min, one large peroxisome cluster is initially located near the mother-bud neck. By 28 min, the peroxisome cluster is split in two by cytokinesis. As new buds emerge, these peroxisome clusters are transferred to the new buds. Several single peroxisomes can be seen at the bud tip by 1 h 36 min. As the buds continue to grow, the peroxisome clusters also move to the bud tips. Bar, 5 μm.

B



overexpressing *PEX3* also showed that peroxisomes were preferentially transferred to daughter cells, leaving the mother cells without peroxisomes (Figure 4-10 B and Movie 4-S5). Our data confirm the role of Pex3Bp and Pex3p in peroxisome inheritance as the peroxisomal receptor for myosin V.

#### **4.11 Overexpression of *PEX3B* or *PEX3* restores peroxisome inheritance to buds in *pex3BΔ* cells**

To better understand the relationship between Pex3p and Pex3Bp and further explore their relative functions in peroxisome biogenesis and/or in modulating peroxisome morphology and inheritance, Pex3p and Pex3Bp were reciprocally overexpressed in cells of their respective deletion backgrounds. Cells harboring plasmid encoding *PEX3* or *PEX3B* under the control of the oleic acid-inducible *POT1* promoter were incubated in oleic acid-containing YPBO medium and imaged by confocal and electron microscopy (Figure 4-11 A and B). Control strains containing empty plasmid presented the mutant phenotypes of *pex3Δ* and *pex3BΔ* cells, i.e. an absence of punctate peroxisomes and mislocalization of matrix proteins to the cytosol in *pex3Δ* cells and tubular-reticular peroxisomes and compromised peroxisome inheritance in *pex3BΔ* cells (Figure 4-11 A). Overexpression of Pex3Bp failed to complement the mutant phenotype of *pex3Δ* cells, while overexpression of Pex3p in either *pex3Δ* or *pex3BΔ* cells resulted in the appearance of large globular peroxisome clusters in addition to individual punctate peroxisomes (Figure 4-11 A). Overexpression of Pex3Bp in *pex3BΔ* cells also resulted in the formation of globular peroxisome clusters, which were often located near the mother-

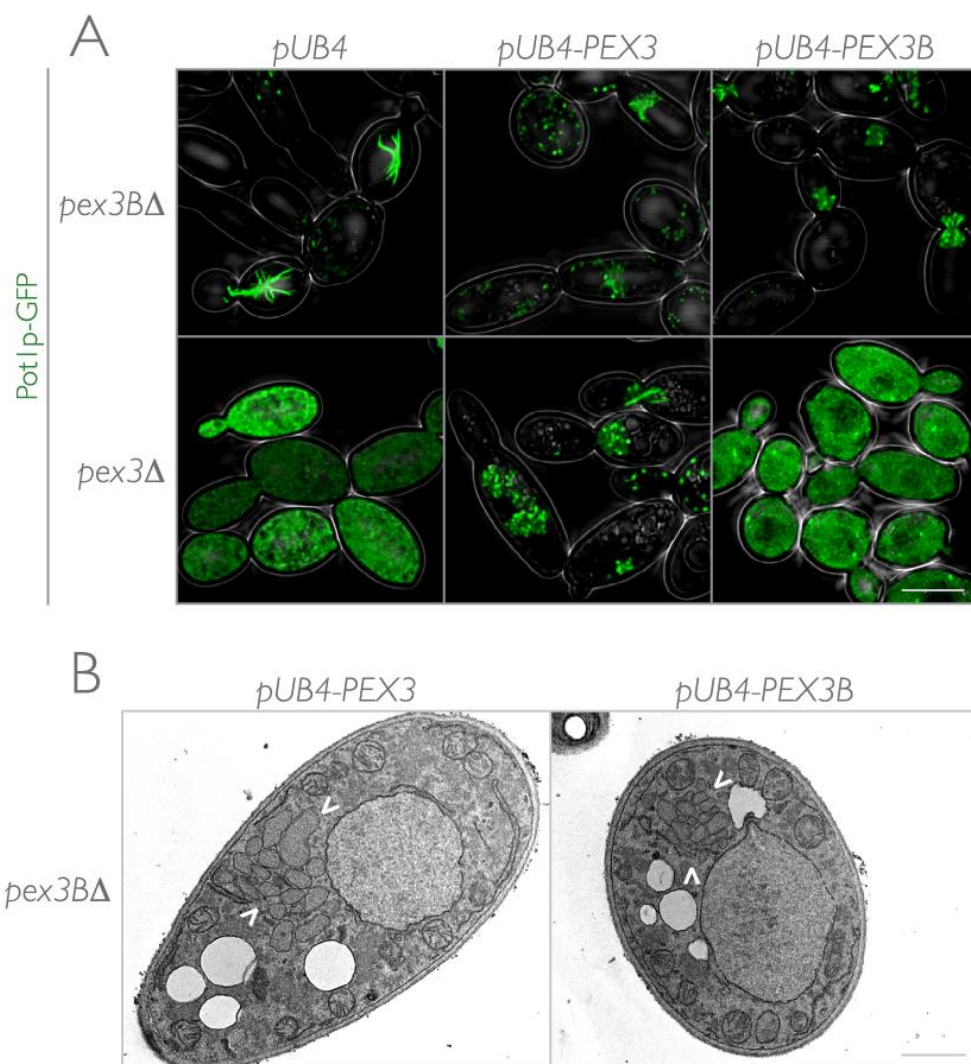
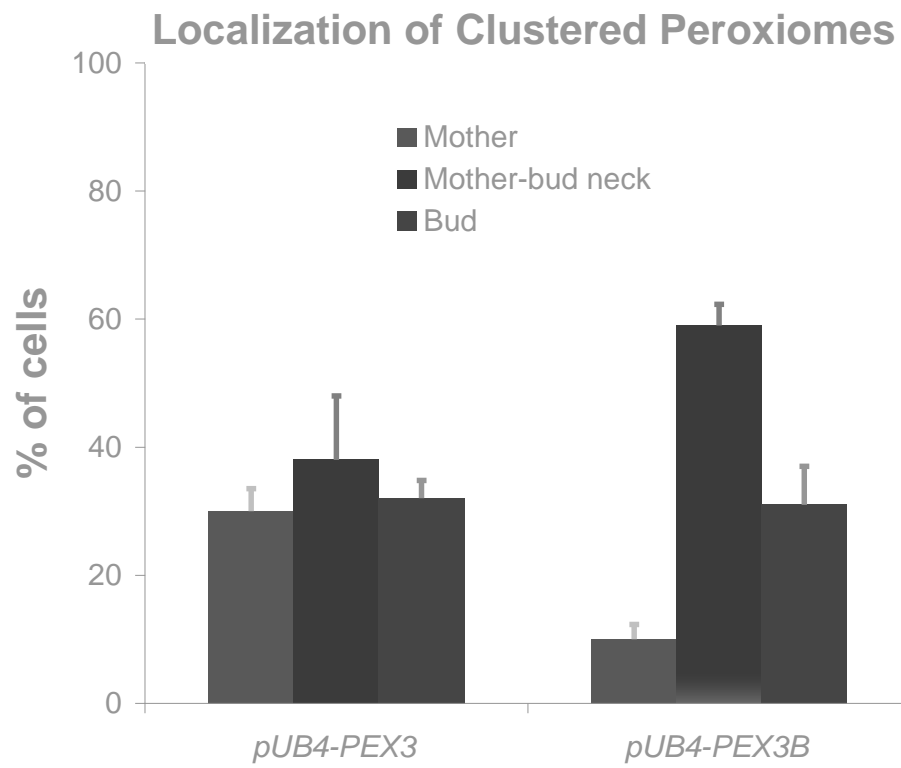


**Figure 4-11. Overexpression of *PEX3* can substitute for *Pex3Bp* in peroxisome inheritance.** (A) *pex3BΔ* and *pex3Δ* cells expressing genomically integrated Pot1p-GFP were transformed with empty plasmid *pUB4* or *pUB4* containing *PEX3* or *PEX3B* for overexpression in oleic acid-containing medium. Cells were grown in YPD supplemented with hygromycin B and then transferred to and incubated for 6 h in oleic acid-containing YPBO supplemented with hygromycin B. Fluorescent images of cells were captured by confocal microscopy and deconvolved. Bar, 5  $\mu\text{m}$ . (B) Ultrastructure of *pex3BΔ* cells overexpressing *PEX3* or *PEX3B*. Cells were cultured as in A and then fixed and processed for EM. Bar, 1  $\mu\text{m}$ . (C) Quantification of the localization of clustered peroxisomes in *pex3BΔ* cells overexpressing *PEX3* or *PEX3B*. The percentages of cells containing clustered peroxisomes in the mother, the bud-neck region or the bud are presented. Quantification was performed on at least 50 cells with large buds defined as in Figure 4-7 A. Graphic results are the means and SEMs of 3 independent experiments.

C



bud neck region or in the bud itself (Figure 4-11 A). That the large globular structures observed by fluorescence microscopy do in fact represent primarily clusters of small peroxisomes was confirmed by EM for *pex3BΔ* cells overexpressing *PEX3* or *PEX3B* (Figure 4-11 B) and *pex3Δ* cells overexpressing *PEX3* (data not shown), as has been observed previously (Bascom et al., 2003). The *pex3BΔ* strain overexpressing *PEX3* also exhibited a peroxisome segregation phenotype (Figure 4-11 A). Quantification showed that the clustered peroxisomes localized preferentially near the bud-neck region or in the bud in *pex3BΔ* cells overexpressing *PEX3*, although to a lesser extent than in the *pex3BΔ* strain overexpressing *PEX3B* (Figure 4-11 C). Our data demonstrate that Pex3Bp overexpression in *pex3Δ* cells cannot reestablish the wild-type peroxisome phenotype. However, both Pex3p and Pex3Bp can function in the transfer of peroxisomes from mother cells to buds through a direct interaction with myosin V. Pex3p and Pex3Bp may also share some functions that remain undefined, namely with respect to their roles in regulating peroxisome morphology.

## 4.12 Discussion

### 4.12.1 The putative Inp2p orthologue, YALI0E03124p, is not the peroxisome-specific myosin V receptor of *Y. lipolytica*

Eukaryotic cells have evolved specific mechanisms for the faithful segregation of their organelles, including peroxisomes, during cell division. In general, organelle inheritance requires an expansion of the organelle population prior to cell division, retention of approximately half of the expanded organelle population by the mother cell, a cytoskeletal track for organelle movement from mother cell to daughter cell, a motor to

carry the organelle along the cytoskeletal track, and an organelle-specific receptor that selectively recognizes the motor. Together, this highly orchestrated program permits the cell to temporally and spatially regulate the inheritance of one type of organelle from the inheritance of other types of organelle.

In *S. cerevisiae*, peroxisome inheritance relies on the actin cytoskeleton and is governed by the actions of two antagonistic proteins, Inp1p and Inp2p. Inp1p acts as a peroxisome-specific retention factor, tethering peroxisomes to putative anchoring structures within the mother cell and the bud (Fagarasanu et al., 2005), while Inp2p is the peroxisome-specific receptor for Myo2p (Fagarasanu et al., 2006), the class V myosin motor responsible for the directed traffic of most organelles from mother cell to bud in *S. cerevisiae* (Hoepfner et al., 2001).

As in *S. cerevisiae*, peroxisome movement and inheritance in *Y. lipolytica* are dependent on the actin cytoskeleton (Chang et al., 2007). *Y. lipolytica* also contains a homologue of Inp1p, which functions in peroxisome retention through its anchoring of peroxisomes to the cell cortex (Chang et al., 2007). Our interrogation of the *Y. lipolytica* genome revealed the presence of a single class V myosin gene in *Y. lipolytica* in contrast to the two class V myosin genes, *MYO2* and *MYO4*, in *S. cerevisiae*. Here we showed that the unique class V myosin of *Y. lipolytica* is required for the transfer of peroxisomes from mother cell to bud. However, interrogation of the *Y. lipolytica* genome revealed no strong candidate homologue of Inp2p, the peroxisome-specific myosin V receptor in *S. cerevisiae*. A putative Inp2p homologue, YALI0E03124p, was identified by iterative PSI blast analysis, but it was shown neither to bind myosin V nor be localized to peroxisomes, two expected requirements for a peroxisome-specific receptor for myosin

V. Nevertheless, the similarities in peroxisome inheritance between *S. cerevisiae* and *Y. lipolytica* and our results showing that overexpression of the myosin V cargo binding domain leads to reduced transfer of peroxisomes from mother cell to bud led us to predict the presence of a peroxisome-specific receptor for the class V myosin of *Y. lipolytica*.

#### **4.12.2 Pex3p and its paralogue, Pex3Bp, function as peroxisome-specific receptors for the class V myosin of *Y. lipolytica***

Surprisingly, we found that the early acting peroxisome biogenesis protein, Pex3p, and its paralogue Pex3Bp, function as peroxisome-specific receptors for the class V myosin of *Y. lipolytica*. Several lines of evidence support this conclusion: 1) Pex3p and Pex3Bp are integral membrane proteins of peroxisomes, fulfilling the spatial specificity requirement for a peroxisome-specific receptor. 2) Deletion of the *PEX3B* gene results in the inability of cells to properly segregate peroxisomes, leaving many buds devoid of peroxisomes, a phenotype observed in *S. cerevisiae* cells lacking *INP2* (Fagarasanu et al., 2006). Also, the lack of saltatory, vectorial movements of peroxisomes seen in *pex3BΔ* cells is consistent with an uncoupling of peroxisomes from the myosin V motor. 3) Pex3p and Pex3Bp interact directly with myosin V, thus satisfying the requirement for a direct connection between the motor and its organelle receptor. Interestingly, we also detected an interaction between Pex3p or Pex3Bp and Myo2p, the myosin V motor protein that transports peroxisomes in *S. cerevisiae*. Likewise, Inp2p was found to bind the myosin V of *Y. lipolytica* (Figure 4-9 B). These interactions are consistent with the idea that conserved patches on the surfaces of cargo-binding domains of myosin Vs from different organisms serve to bind specific cargoes (Pashkova et al., 2006). It is tempting to

speculate that there exists a conserved interorganismal patch for peroxisome receptors on the surface of class V myosin tails. 4) Overexpression of Pex3p or Pex3Bp leads to preferential partitioning of peroxisomes to buds, leaving many mother cells without peroxisomes. Likewise, overexpression of Inp2p also leads to the concentration of the peroxisome population in buds and increased numbers of mother cells without peroxisomes (Fagarasanu et al., 2006). 5) The failure to correctly segregate peroxisomes in cells either lacking or overexpressing Pex3Bp activates de novo peroxisome biogenesis in the empty buds and mother cells, respectively (Movies 4-S2 and 4-S4). This is similar to what is observed in mutants of vacuole inheritance in which buds without vacuoles are rapidly able to form new vacuolar structures de novo, thereby allowing the bud to develop and go on to produce daughter cells of its own (Weisman et al., 1987; Raymond et al., 1990; Gomes De Mesquita et al., 1997).

#### **4.12.3 How *Y. lipolytica* and *S. cerevisiae* differ in peroxisome inheritance**

Although the overall process of peroxisome inheritance is similar in *S. cerevisiae* and *Y. lipolytica*, there are differences. First, the localization of Pex3p (Bascom et al., 2003) or Pex3Bp to peroxisomes is not polarized, i.e. it is not preferentially associated with those peroxisomes that are inherited, as is the case for Inp2p (Fagarasanu et al., 2006). This might suggest that it is not the levels of Pex3p or Pex3Bp that dictate the segregation fate of peroxisomes, but rather that Pex3p or Pex3Bp could be activated via a posttranslational modification, such as phosphorylation, which would enable it to engage the class V myosin motor. *S. cerevisiae* Vac17p, the vacuole-specific receptor for Myo2p, has been shown to be phosphorylated at multiple sites, important both for its activation

and its targeting to degradation (Peng and Weisman, 2008; Bartholomew and Hardy, 2009). We also cannot exclude the presence of a regulatory protein that governs the interaction between Pex3p or Pex3Bp and myosin V. A requirement for additional regulatory subunits in the receptor-myosin transport complex has been postulated previously (Ishikawa et al., 2003; Weisman, 2006).

Interestingly, both Inp2p and Vac17p in *S. cerevisiae* function exclusively as the adaptor molecules for Myo2p on peroxisomes and vacuoles, respectively, without apparently performing any other metabolic or biogenic function in their respective organelles (Ishikawa et al., 2003; Fagarasanu et al., 2006). This has led to the view that organelle-specific receptors for myosins are devoted solely to organelle motility and are thus able to fluctuate during the cell cycle without altering the metabolic efficiency of organelles (Fagarasanu et al., 2007). However, this view has recently been challenged by the discovery of Ypt31p/Ypt32p as the receptor for post-Golgi secretory vesicles (Lipatova et al., 2008). The Ypt31p/Ypt32p GTPase functional pair plays a major role in the budding of trans Golgi-derived vesicles. Its other role in recruiting Myo2p to vesicle membranes therefore links temporally the biogenesis of secretory vesicles with their bud-destined transport. Similarly, members of the Pex3p family appear to be multifunctional, having roles in de novo peroxisome biogenesis and in regulating peroxisome morphology and inheritance.

#### **4.12.4 Members of the Pex3p family may be multifunctional**

With the demonstration of a role for the Pex3 protein family in peroxisome inheritance, several exciting possibilities arise. For example, it is tempting to speculate

that Pex3 proteins are part of a mechanism that ensures the preferential transfer of new peroxisomal material to daughter cells. If Pex3 proteins are involved in both the production of peroxisomes at the ER and the recruitment of myosin to their membranes, the newly formed peroxisomal vesicles would probably be admirably equipped to harness the robust anterograde-directed machinery to promote their transfer to the bud. Therefore, we may have unraveled a mechanism that relates the age of peroxisomes with their segregation fates. Importantly, through their specific metabolic functions, peroxisomes are exposed to potentially damaging reactive oxygen species (Smith and Aitchison, 2009). It is well accepted that oxidized proteins are important factors in replicative aging (Macara and Mili, 2008). The proposed model wherein newer peroxisomal material is preferentially inherited by the daughter cell would predict that oxidatively damaged peroxisomal proteins accumulate in the mother cell, explaining in part how deleterious material is differentially retained by the aging cell. Since the Pex3 family of proteins is highly conserved throughout the eukaryotes, the temporal connection between peroxisome biogenesis and their motility might be a common mechanism in peroxisome inheritance. Notably, it has previously been observed that overproduction of Pex3p in *S. cerevisiae* cells leads to the transfer of all peroxisomes to the growing bud (Tam et al., 2005). However, deletion of the *PEX3* gene in any organism studied so far has led to a complete loss of peroxisomes, and therefore the presence of two members of the Pex3 protein family in *Y. lipolytica* may have offered an “evolutionary” window of opportunity for the direct observation of a heretofore unknown contribution of Pex3 proteins to peroxisome motility.

#### **4.12.5 Pex3Bp's action in peroxisome division**

While our findings readily show that the Pex3 protein family is involved in peroxisome inheritance, we have not resolved the cellular mechanisms leading to the observed imbalance of peroxisome division in Pex3Bp deletion and Pex3p/Pex3Bp overexpression strains. Elongation of peroxisomes in cells lacking Pex3Bp might be caused indirectly by the inefficiency of the association of myosin V with the peroxisomal membrane. Cytoskeletal tracks and motor proteins are known to exert tensions on organelle membranes, thus assisting in organelle fission (Schrader and Fahimi, 2006). It has been suggested previously that the pulling forces exerted by the machinery that propels the bud-directed movement of peroxisomes on the one hand and peroxisome retention mechanisms on the other act on the membranes of peroxisomes to sever them (Fagarasanu et al., 2007; Motley and Hettema, 2007). The clustering of peroxisomes seen in cells overexpressing Pex3Bp or Pex3p might be explained by our two-hybrid data, which showed that Pex3Bp and Pex3p can interact with themselves and with each other. This would allow peroxisomes to associate with one another via protein interactions in trans. Further studies are needed to determine how the interactions between Pex3p, Pex3Bp and myosin V function in the recruitment of division and/or other inheritance factors to the peroxisomal membrane and whether these interactions contribute to the overall morphology of peroxisomes. These studies would also help to elucidate how peroxisome biogenesis, division and inheritance are linked.

In closing, we demonstrated an unexpected role for the early acting Pex3 peroxisome biogenesis proteins in peroxisome inheritance and motility through their direct coupling of peroxisomes to the myosin V motor protein. Our studies reveal a

general mechanism of peroxisome inheritance and point to a temporal link between peroxisome formation and inheritance mediated through the Pex3 proteins.

**CHAPTER 5**

**PERSPECTIVES**

## 5.1 Synopsis

In this thesis, I present the results of our studies of peroxisome dynamics and inheritance in the yeast *Y. lipolytica*. We showed that peroxisome motility is driven along the actin cytoskeleton by the unique class V myosin of *Y. lipolytica*. We described two novel peroxisomal proteins, *YInp1p* and *Pex3Bp*, involved in peroxisome inheritance. These two proteins function antagonistically. *YInp1p* functions in peroxisome retention at the cell cortex, whereas *Pex3Bp*, a paralogue of *Pex3p*, functions as the peroxisome-specific receptor for the class V myosin of *Y. lipolytica*. We also established that *Pex3p* of *Y. lipolytica* is a multifunctional protein, having roles not only in de novo peroxisome formation from the ER but also in peroxisome motility and inheritance.

## 5.2 Future research on *YInp1p*

*YInp1p* is a peripheral membrane protein of peroxisomes involved in peroxisome inheritance. Since *YInp1p*'s primary role is in anchoring peroxisomes to the cell cortex, it would be reasonable to expect that *YInp1p* is localized to the cytosolic surface of the peroxisomal membrane. *YInp1p* therefore may act to bridge peroxisomes to an unknown cortical anchor. Immunoprecipitation of complexes containing *YInp1p* followed by mass spectrometry would identify *YInp1p*'s interaction partners both at the peroxisome membrane and at the cell cortex.

Mother cells of the *S. cerevisiae inp1Δ* mutant strain are often devoid of peroxisomes, while in an *Inp1p* overexpressing strain, the buds usually lack peroxisomes (Fagarasanu et al., 2005). These extremes of phenotype are rarely observed in *Y. lipolytica*. We propose that unidentified peroxisomal proteins might function similarly to

*YInp1p* to help anchor peroxisomes to the cell cortex. It would be of interest to define these proteins and determine their relationships to *YInp1p*.

Peroxisomes are frequently clustered at the bud tips of *Ylinp1Δ* cells, suggesting the involvement of *YInp1p* in separating peroxisomes from one another. Although there is an intrinsic relationship between peroxisome retention and division (Chapter 1), we could not rule out that the functions of *YInp1p* in peroxisome retention and division might be independent. An analysis of the different functional regions of *YInp1p* would provide greater understanding of how *YInp1p* acts in its different roles. It would also be interesting to examine a possible interaction between *YInp1p* and proteins involved in peroxisome division, including, for example, Pex11 protein family members, DRPs or the *Y. lipolytica* homologue of Fis1p.

Although some *Inp1p* is expressed throughout the cell cycle in *S. cerevisiae*, its expression oscillates and peaks at the G2-M transition (Fagarasanu et al., 2005; Fagarasanu et al., 2007). This suggests that peroxisome retention varies in strength during the various stages of the cell cycle. To better understand how the different molecular players coordinate their activities during peroxisome inheritance, it will be important to measure the expression levels of *YInp1p* during the cell cycle. One caveat to such studies is that it is difficult to synchronize the movement of *Y. lipolytica* through the cell cycle in contrast to *S. cerevisiae*, which is easily synchronized by addition of the mating pheromone,  $\alpha$ -factor.

### 5.3 Future research on Pex3Bp

We showed that both Pex3p and Pex3Bp function as peroxisome-specific receptors for the class V myosin of *Y. lipolytica*. If Pex3p and Pex3Bp function together in a receptor complex, Pex3Bp is probably the dominant partner for a number of reasons. First, Pex3Bp interacts more strongly than Pex3p with the globular tail domain of the class V myosin as shown by both yeast two-hybrid analysis and protein pull-down assays. Second, only *pex3BΔ* cells exhibit compromised peroxisome inheritance, as *pex3Δ* cells lack any vestige of peroxisomes. Third, although *pex3BΔ* cells overexpressing Pex3p show compromised peroxisome segregation, the phenotype is milder than that of *pex3BΔ* cells overexpressing Pex3Bp (Chapter 4).

Like Pex3p (Bascom et al., 2003), Pex3Bp is an integral PMP and predicted to have one transmembrane domain near its N-terminus (amino acids 12-30). Since Pex3Bp functions as a motor receptor on the peroxisomal membrane, it is presumably anchored at the membrane by its N-terminal transmembrane domain, leaving most of the protein exposed to the cytosol. Protease protection experiments could be performed to confirm the topology of Pex3Bp.

Class V myosins are highly conserved from yeasts to mammals. If Pex3Bp is the key component of the receptor complex for the class V myosin of *Y. lipolytica*, it must share some features common to other class V myosin receptors. Vac17p and Inp2p are two well characterized receptors of class V myosin, Myo2p, of *S. cerevisiae* (Ishikawa et al., 2003; Fagarasanu et al., 2005), while melanophilin found on melanosomes is the only characterized myosin Va receptor in mammals (Wu et al., 2002). These receptors all possess two putative coiled-coil domains of about 30 amino acids each in length.

Likewise, Pex3Bp also contain two predicted coiled-coil domains of about the same size. Pex3p, on the other hand, is predicted to contain only one coiled-coil domain located immediately after its transmembrane domain. It would be interesting to determine whether the predicted coiled-coil domains of Pex3Bp are involved in its interaction with the class V myosin.

In addition to the defect in peroxisome inheritance, *pex3BA* cells also display hyperelongated peroxisomes during induction on oleic acid. Some *pex3BA* cells have fewer and larger peroxisomes than wild-type cells, indicating that Pex3Bp is also involved in peroxisome division. As discussed in Section 4.12.5, the elongation of peroxisomes in cells lacking Pex3Bp could be caused indirectly by an inefficiency in the association of myosin V with the peroxisomal membrane. However, a direct effect of Pex3Bp on peroxisome division cannot be excluded. If Pex3Bp is implicated directly in peroxisome division, it might function in peroxisome constriction, downstream of the Pex11 proteins and upstream of DRPs, because the elongated peroxisomes of *pex3BA* cells do not show extensive evidence of constriction by electron microscopy. Pex16p of *Y. lipolytica* has been shown to control the peroxisomal membrane constriction from within peroxisomes (Guo et al., 2007). Whether Pex3Bp cooperates with Pex16p, or functions independently, in peroxisome constriction requires further investigation. Moreover, the possible interactions of Pex3Bp with Pex11 proteins or DRPs should be investigated to gain further insight into how peroxisomes divide.

Pex3Bp is the paralogue of Pex3p, which has an established role in the de novo formation of peroxisomes. Considering how closely related Pex3Bp and Pex3p are in sequence, it would not be surprising that Pex3Bp might also function in de novo

peroxisome biogenesis. However, deletion of *PEX3* in *Y. lipolytica* leads to peroxisome deficiency (Bascom et al., 2003), excluding the possibility that Pex3p and Pex3Bp are completely functionally redundant in regard to their roles in peroxisome formation. To investigate a possible role for Pex3Bp in peroxisome biogenesis per se, one could first introduce a plasmid library of randomly mutated *pex3* mutant genes into a *pex3Δ/pex3BΔ* strain containing fluorescent peroxisomes labeled with Pot1p-GFP. Next, *PEX3B* would be expressed in those strains expressing a *pex3* mutant that fails to import Pot1p-GFP correctly to see if *PEX3B* could functionally complement for the *pex3* defect in peroxisome biogenesis. The mechanism by which Pex3Bp achieves this functional complementation would then be the focus of continued investigation.

#### 5.4 Future research on Pex3p

Pex3p is generally considered as acting early in peroxisome biogenesis and being responsible for de novo peroxisome biogenesis from the ER. The findings presented in Chapter 4 show that Pex3p in *Y. lipolytica* also contributes to the ultimate event of peroxisome biogenesis, peroxisome inheritance, as the receptor for the class V myosin. A role for Pex3p in peroxisome inheritance as the anchor for Inp1p on the membrane of peroxisomes of *S. cerevisiae* has recently been shown (Munck et al., 2009). Protein interaction studies could determine whether Pex3p interacts with Inp2p in *S. cerevisiae* and whether Pex3p interacts with *YlInp1p* in *Y. lipolytica*. It is interesting to speculate that Pex3p acts as a molecular switch between Inp1p (*YlInp1p*) and Inp2p (Pex3Bp).

The roles of Pex3 proteins in peroxisome biogenesis are summarized in Figure 5-1.

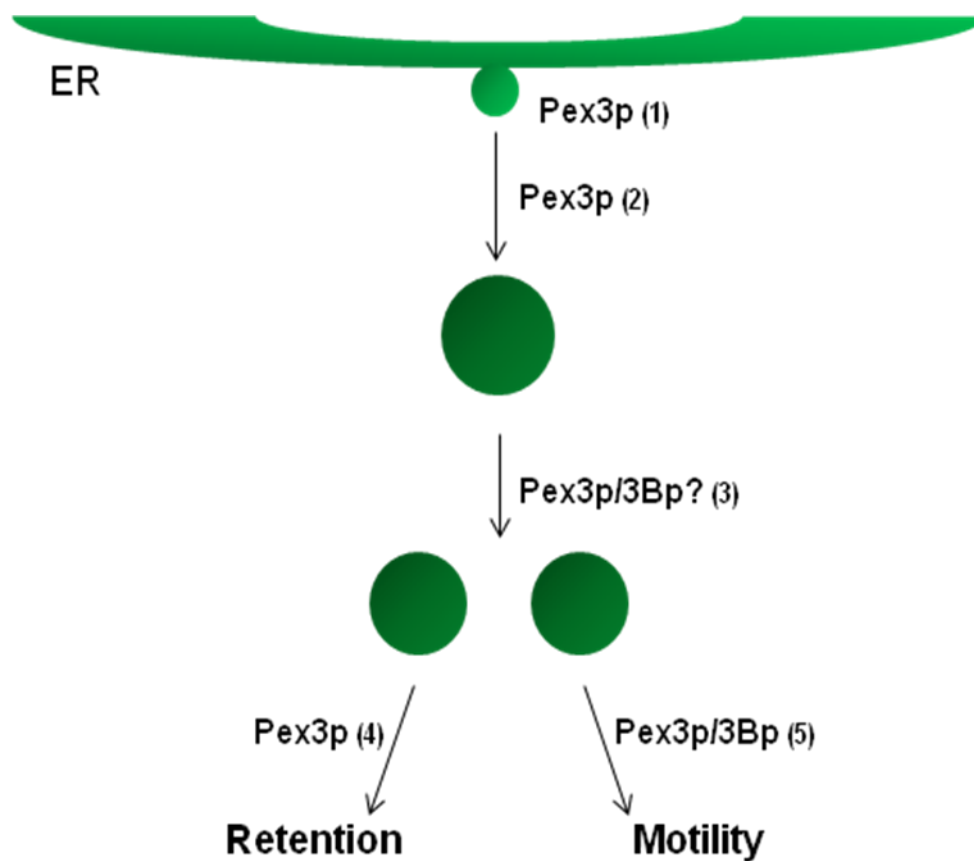


**Figure 5-1. Roles for Pex3 proteins in peroxisome multiplication and inheritance.** (1) Pex3p is involved in the de novo synthesis of peroxisomes from the ER. (2) Pex3p is the docking factor for Pex19p in PMP import. (3) The functions of Pex3p/Pex3Bp in peroxisome division are unclear. (4) Pex3p recruits Inp1p for peroxisome retention in *S. cerevisiae*. (5) Pex3p and Pex3Bp form the peroxisomal receptor complex for myosin V to move peroxisomes in *Y. lipolytica*.

How might Pex3p regulate its various functions? Although peroxisomes are highly dynamic and change dramatically under different environmental conditions, the levels of Pex3p under the same conditions remain essentially unchanged. Therefore, Pex3p is unlikely to adjust its functions through transcriptional regulatory or protein degradative processes. Pex3p might control changes in its function through posttranslational modification, e.g. phosphorylation. Also, Pex3p's capacity to oligomerize could regulate its different functions.

Compared to what is known in yeast, little is known about organelle inheritance in mammalian cells. The long-distance and bidirectional transport of organelles in mammalian cells is usually mediated by microtubules through dynein and kinesin motor proteins, while the localized movement of organelles depends primarily on actin filaments and myosin motors. In melanocytes, microtubule-dependent movement of melanosomes cooperates with myosin Va-dependent movements of melanosomes along actin filaments. This cooperation leads to the peripheral accumulation of melanosomes in melanocytes to facilitate transfer of melanosomes to keratinocytes (Wu et al., 2002). It would be particularly interesting to examine whether Pex3p and myosin Va act together to localize peroxisomes to the cortical region of mammalian cells.

**CHAPTER 6****REFERENCES**

- Adams, A. E. and J. R. Pringle. 1984. Relationship of actin and tubulin distribution to bud growth in wild-type and morphogenetic-mutant *Saccharomyces cerevisiae*. *J. Cell Biol.* 98:934-945.
- Aitchison, J. D., R. K. Szilard, W. M. Nuttley, and R. A. Rachubinski. 1992. Antibodies directed against a yeast carboxyl-terminal peroxisomal targeting signal specifically recognize peroxisomal proteins from various yeasts. *Yeast.* 8:721-734.
- Altmann, K., M. Frank, D. Neumann, S. Jakobs, and B. Westermann. 2008. The class V myosin motor protein, Myo2, plays a major role in mitochondrial motility in *Saccharomyces cerevisiae*. *J. Cell Biol.* 181:119-130.
- Altschul, S. F., T. L. Madden, A. A. Schaffer, J. Zhang, Z. Zhang, W. Miller, and D. J. Lipman. 1997. Gapped BLAST and PSI-BLAST: a new generation of protein database search programs. *Nucleic Acids Res.* 25:3389-3402.
- Ausubel, F. J., R. Brent, R. E. Kingston, D. D. Moore, J. G. Seidman, J. A. Smith, and K. Struhl. 1989. *Current Protocols in Molecular Biology*. Greene Publishing Associates, New York, New York.
- Barnett, P., H. F. Tabak, and E. H. Hettema. 2000. Nuclear receptors arose from pre-existing protein modules during evolution. *Trends Biochem. Sci.* 25:227-228.
- Barth, G. and C. Gaillardin. 1996. *Yarrowia lipolytica*. In: *Non-conventional Yeasts in Biotechnology*. K. Wolf (Ed.). Springer-Verlag, New York, New York. pp. 313-388.
- Bartholomew, C. R. and C. F. Hardy. 2009. p21-activated kinases Cla4 and Ste20 regulate vacuole inheritance in *Saccharomyces cerevisiae*. *Eukaryot. Cell.* 8:560-572.
- Bascom, R. A., H. Chan, and R. A. Rachubinski. 2003. Peroxisome biogenesis occurs in an unsynchronized manner in close association with the endoplasmic reticulum in temperature-sensitive *Yarrowia lipolytica* Pex3p mutants. *Mol. Biol. Cell.* 14:939-957.
- Brade, A. M. Peroxisome Assembly in *Yarrowia lipolytica*. 1992. M.Sc. Thesis, McMaster University, Hamilton, Ontario.

- Bradford, M. M. 1976. A rapid and sensitive method for the quantification of microgram quantities of protein utilizing the principle of protein-dye binding. *Anal. Biochem.* 72:248-254.
- Burnette, W. N. 1981. "Western blotting": electrophoretic transfer of proteins from sodium dodecyl sulfate-polyacrylamide gels to unmodified nitrocellulose and radiographic detection with antibody and radioiodinated protein A. *Anal. Biochem.* 112:195-203.
- Cartier, N., S. Hacein-Bey-Abina, C. C. Bartholomae, G. Veres, M. Schmidt, I. Kutschera, M. Vidaud, U. Abel, L. Dal-Cortivo, L. Caccavelli, N. Mahlaoui, V. Kiermer, D. Mittelstaedt, C. Bellesme, N. Lahlou, F. Lefrère, S. Blanche, M. Audit, E. Payen, P. Leboulch, B. l'Homme, P. Bournès, C. Von Kalle, A. Fischer, M. Cavazzana-Calvo, and P. Aubourg. 2009. Hematopoietic stem cell gene therapy with a lentiviral vector in X-linked adrenoleukodystrophy. *Science.* 326:818-823.
- Chang, J., A. Fagarasanu, and R. A. Rachubinski. 2007. Peroxisomal peripheral membrane protein YInp1p is required for peroxisome inheritance and influences the dimorphic transition in the yeast *Yarrowia lipolytica*. *Eukaryot. Cell.* 6:1528-1537.
- Chang, J., F. D. Mast, A. Fagarasanu, D. A. Rachubinski, G. A. Eitzen, J. B. Dacks, and R. A. Rachubinski. 2009. Pex3 peroxisome biogenesis proteins function in peroxisome inheritance as class V myosin receptors. *J. Cell Biol.* 187:233-246.
- de Duve, C. and P. Baudhuin. 1966. Peroxisomes (microbodies and related particles). *Physiol. Rev.* 46:323-357.
- Dibrov, E., S. Fu, and B. D. Lemire. 1998. The *Saccharomyces cerevisiae* TCM62 gene encodes a chaperone necessary for the assembly of the mitochondrial succinate dehydrogenase (complex II). *J. Biol. Chem.* 273:32042-32048.
- Dujon, B., D. Sherman, G. Fischer, P. Durrens, S. Casaregola, I. Lafontaine, J. de Montigny, C. Marck, C. Neuvéglise, E. Talla, N. Goffard, L. Frangeul, M. Aigle, V. Anthouard, A. Babour, V. Barbe, S. Barnay, S. Blanchin, J.-M. Beckerich, E. Beyne, C. Bleykasten, A. Boisramé, J. Boyer, L. Cattolico, F. Confanioleri, A. de Daruvar, L. Despons, E. Fabre, C. Fairhead, H. Ferry-Dumazet, A. Groppi, F. Hantraye, C. Hennequin, N. Jauniaux, P. Joyet, R. Kachouri, A. Kerrest, R. Koszul, M. Lemaire, I. Lesur, L. Ma, H. Muller, J.-M. Nicaud, M. Nikolski, S. Oztas, O. Ozier-Kalogeropoulos, S. Pellenz, S. Potier, G.-F. Richard, M.-L.

- Straub, A. Suleau, D. Swennen, F. Tekaiia, M. Wésolowski-Louvel, E. Westhof, B. Wirth, M. Zeniou-Meyer, I. Zivanovic, M. Bolotin-Fukuhara, A. Thierry, C. Bouchier, B. Caudron, C. Scarpelli, C. Gaillardin, J. Weissenbach, P. Wincker, and J.-L. Souciet. 2004. Genome evolution in yeasts. *Nature*. 430:35-44.
- Eitzen, G. A. An Analysis of Peroxisome Assembly Mutants of the Yeast *Yarrowia lipolytica*. 1997. Ph.D. Thesis, University of Alberta, Edmonton, Alberta.
- Eitzen, G. A., R. K. Szilard, and R. A. Rachubinski. 1997. Enlarged peroxisomes are present in oleic acid-grown *Yarrowia lipolytica* overexpressing the *PEX16* gene encoding an intraperoxisomal peripheral membrane peroxin. *J. Cell Biol.* 137:1265-1278.
- Eitzen, G. A., V. I. Titorenko, J. J. Smith, M. Veenhuis, R. K. Szilard, and R. A. Rachubinski. 1996. The *Yarrowia lipolytica* gene *PAY5* encodes a peroxisomal integral membrane protein homologous to the mammalian peroxisome assembly factor PAF-1. *J. Biol. Chem.* 271:20300-20306.
- Erdmann, R. and G. Blobel. 1995. Giant peroxisomes in oleic acid-induced *Saccharomyces cerevisiae* lacking the peroxisomal membrane protein Pmp27p. *J. Cell Biol.* 128:509-523.
- Estrada, P., J. Kim, J. Coleman, L. Walker, B. Dunn, P. Takizawa, P. Novick, and S. Ferro-Novick. 2003. Myo4p and She3p are required for cortical ER inheritance in *Saccharomyces cerevisiae*. *J. Cell Biol.* 163:1255-1266.
- Fagarasanu, A., M. Fagarasanu, G. A. Eitzen, J. D. Aitchison, and R. A. Rachubinski. 2006. The peroxisomal membrane protein Inp2p is the peroxisome-specific receptor for the myosin V motor Myo2p of *Saccharomyces cerevisiae*. *Dev. Cell.* 10:587-600.
- Fagarasanu, A., M. Fagarasanu, and R. A. Rachubinski. 2007. Maintaining peroxisome populations: a story of division and inheritance. *Annu. Rev. Cell Dev. Biol.* 23:321-344.
- Fagarasanu, A., F. D. Mast, B. Knoblach, Y. Jin, M. J. Brunner, M. R. Logan, J. N. Glover, G. A. Eitzen, J. D. Aitchison, L. S. Weisman, and R. A. Rachubinski. 2009. Myosin-driven peroxisome partitioning in *S. cerevisiae*. *J. Cell Biol.* 186:541-554.

- Fagarasanu, A. and R. A. Rachubinski. 2007. Orchestrating organelle inheritance in *Saccharomyces cerevisiae*. *Curr. Opin. Microbiol.* 10:528-538.
- Fagarasanu, M., A. Fagarasanu, Y. Y. C. Tam, J. D. Aitchison, and R. A. Rachubinski. 2005. Inp1p is a peroxisomal membrane protein required for peroxisome inheritance in *Saccharomyces cerevisiae*. *J. Cell Biol.* 169:765-775.
- Fang, Y., J. C. Morrell, J. M. Jones, and S. J. Gould. 2004. PEX3 functions as a PEX19 docking factor in the import of class I peroxisomal membrane proteins. *J. Cell Biol.* 164:863-875.
- Farré, J. C. and S. Subramani. 2004. Peroxisome turnover by micropexophagy: an autophagy-related process. *Trends Cell Biol.* 14:515-523.
- Fujiki, Y., A. L. Hubbard, S. Fowler, and P. B. Lazarow. 1982. Isolation of intracellular membranes by means of sodium carbonate treatment: application to endoplasmic reticulum. *J. Cell Biol.* 93:97-102.
- Fujiki, Y., Y. Matsuzono, T. Matsuzaki, and M. Fransen. 2006. Import of peroxisomal membrane proteins: the interplay of Pex3p- and Pex19p-mediated interactions. *Biochim. Biophys. Acta.* 1763:1639-1646.
- Gabalton, T., B. Snel, F. van Zimmeren, W. Hemrika, H. Tabak, and M. A. Huynen. 2006. Origin and evolution of the peroxisomal proteome. *Biol. Direct.* 1:8.
- Gausmann, U., E. Franzl, and C. Kurischko. 1999. Distribution of the actin cytoskeleton during the cell cycle of *Yarrowia lipolytica* and the visualization of the tubulin cytoskeleton by immunofluorescence. *Yeast.* 15:1079-1086.
- Gietz, R. D. and R. A. Woods. 2002. Transformation of yeast by lithium acetate/single-stranded carrier DNA/polyethylene glycol method. *Methods Enzymol.* 350:87-96.
- Gomes de Mesquita, D. S., J. Shaw, J. A. Grimbergen, M. A. Buys, L. Dewi, and C. L. Woldringh. 1997. Vacuole segregation in the *Saccharomyces cerevisiae vac2-1* mutant: structural and biochemical quantification of the segregation defect and formation of new vacuoles. *Yeast.* 13:999-1008.

- Goodman, J. M., S. B. Trapp, H. Hwang, and M. Veenhuis. 1990. Peroxisomes induced in *Candida boidinii* by methanol, oleic acid and *D*-alanine vary in metabolic function but share common integral membrane proteins. *J. Cell Sci.* 97:193-204.
- Grabenbauer, M., K. Satzler, E. Baumgart, and H. D. Fahimi. 2000. Three-dimensional ultrastructural analysis of peroxisomes in HepG2 cells. Absence of peroxisomal reticulum but evidence of close spatial association with the endoplasmic reticulum. *Cell Biochem. Biophys.* 32:37-49.
- Gunkel, K., I. J. van der Klei, G. Barth, and M. Veenhuis. 1999. Selective peroxisome degradation in *Yarrowia lipolytica* after a shift of cells from acetate/oleate/ethylamine into glucose/ammonium sulfate-containing media. *FEBS Lett.* 451:1-4.
- Guo, T., C. Gregg, T. Boukh-Viner, P. Kyryakov, A. Goldberg, S. Bourque, F. Banu, S. Haile, S. Miljevic, K. H. San, J. Solomon, V. Wong, and V. I. Titorenko. 2007. A signal from inside the peroxisome initiates its division by promoting the remodeling of the peroxisomal membrane. *J. Cell Biol.* 177:289-303.
- Guo, T., Y. Y. Kit, J.-M. Nicaud, M. T. Le Dall, S. K. Sears, H. Vali, H. Chan, R. A. Rachubinski, and V. I. Titorenko. 2003. Peroxisome division in the yeast *Yarrowia lipolytica* is regulated by a signal from inside the peroxisome. *J. Cell Biol.* 162:1255-1266.
- Hammond, A. T. and B. S. Glick. 2000. Raising the speed limits for 4D fluorescence microscopy. *Traffic.* 1:935-940.
- Harlow, E. and D. Lane. 1988. *Antibodies: A Laboratory Manual*. Cold Spring Harbor Laboratory, Cold Spring Harbor, New York. pp. 63-70.
- Hettema, E. H., W. Girzalsky, M. van den Berg, R. Erdmann, and B. Distel. 2000. *Saccharomyces cerevisiae* Pex3p and Pex19p are required for proper localization and stability of peroxisomal membrane proteins. *EMBO J.* 19:223-233.
- Hoepfner, D., D. Schildknegt, I. Braakman, P. Philippsen, and H. F. Tabak. 2005. Contribution of the endoplasmic reticulum to peroxisome formation. *Cell.* 122:85-95.

- Hoepfner, D., M. van den Berg, P. Philippsen, H. F. Tabak, and E. H. Hetteema. 2001. A role for Vps1p, actin, and the Myo2p motor in peroxisome abundance and inheritance in *Saccharomyces cerevisiae*. *J. Cell Biol.* 155:979-990.
- Huynh, T. V., R. A. Young, and R. W. Davis. 1985. DNA Cloning: A Practical Approach. IRL Press, Oxford, United Kingdom.
- Innis, M. A. and D. H. Gelfand. 1990. Optimization of PCRs. In: PCR Protocols: A Guide to Methods and Applications. M. A. Innis, D. H. Gelfand, J. J. Sninsky, and T. J. White, (Eds.) Academic Press, San Diego, California. pp. 3-12.
- Ishikawa, K., N. L. Catlett, J. L. Novak, F. Tang, J. J. Nau, and L. S. Weisman. 2003. Identification of an organelle-specific myosin V receptor. *J. Cell Biol.* 160:887-897.
- Issemann, I. and S. Green. 1990. Activation of a member of the steroid hormone receptor superfamily by peroxisome proliferators. *Nature.* 347:645-650.
- Jansen, G. A. and R. J. A. Wanders. 2006. Alpha-oxidation. *Biochim. Biophys. Acta.* 1763:1403-1412.
- Jedd, G. and N.-H. Chua. 2000. A new self-assembled peroxisomal vesicle required for efficient resealing of the plasma membrane. *Nat. Cell Biol.* 2:226-231.
- Kamiryo, T., M. Abe, K. Okazaki, S. Kato, and N. Shimamoto. 1982. Absence of DNA in peroxisomes of *Candida tropicalis*. *J. Bacteriol.* 152:269-274.
- Kelley, R. I. 1983. Review: the cerebrohepatorenal syndrome of Zellweger, morphologic and metabolic aspects. *Am. J. Med. Genet.* 16:503-517.
- Kiel, J.-A., M. Veenhuis, and I. J. van der Klei. 2006. PEX genes in fungal genomes: common, rare or redundant. *Traffic.* 7:1291-1303.
- Kilmartin, J. V. and A. E. Adams. 1984. Structural rearrangements of tubulin and actin during the cell cycle of the yeast *Saccharomyces*. *J. Cell Biol.* 98:922-933.

- Kim, P. K., R. T. Mullen, U. Schumann, and J. Lippincott-Schwartz. 2006. The origin and maintenance of mammalian peroxisomes involves a de novo PEX16-dependent pathway from the ER. *J. Cell Biol.* 173:521-532.
- Knoblach, B. and R. A. Rachubinski. 2010. Phosphorylation-dependent activation of peroxisome proliferator protein PEX11 controls peroxisome abundance. *J. Biol. Chem.* 285:6670-6680.
- Koch, A., M. Thiemann, M. Grabenbauer, Y. Yoon, M. A. McNiven, and M. Schrader. 2003. Dynamin-like protein 1 is involved in peroxisomal fission. *J. Biol. Chem.* 278:8597-8605.
- Koch, A., G. Schneider, G. H. Luers, and M. Schrader. 2004. Peroxisome elongation and constriction but not fission can occur independently of dynamin-like protein 1. *J. Cell Sci.* 117:3995-4006.
- Kovacs, W. J., K. N. Tape, J. E. Shackelford, T. M. Wikander, M. J. Richards, S. J. Fliesler, S. K. Krisans, and P. L. Faust. 2009. Peroxisome deficiency causes a complex phenotype because of hepatic SREBP/Insig dysregulation associated with endoplasmic reticulum stress. *J. Biol. Chem.* 284:7232-7245.
- Kron, S. J. 1997. Filamentous growth in budding yeast. *Trends Microbiol.* 5:450-454.
- Kuravi, K., S. Nagotu, A. M. Krikken, K. Sjollema, M. Deckers, R. Erdmann, M. Veenhuis, and I. J. van der Klei. 2006. Dynamin-related proteins Vps1p and Dnm1p control peroxisome abundance in *Saccharomyces cerevisiae*. *J. Cell Sci.* 119:3994-4001.
- Lazarow, P. B. and Y. Fujiki. 1985. Biogenesis of peroxisomes. *Annu. Rev. Cell Biol.* 1:489-530.
- Li, X. and S. J. Gould. 2003. The dynamin-like GTPase DLP1 is essential for peroxisome division and is recruited to peroxisomes in part by PEX11. *J. Biol. Chem.* 278:17012-17020.
- Lingard, M. J., S. K. Gidda, S. Bingham, S. J. Rothstein, R. T. Mullen, and R. N. Trelease. 2008. *Arabidopsis* PEROXIN11c-e, FISSION1b, and DYNAMIN-RELATED PROTEIN3A cooperate in cell cycle-associated replication of peroxisomes. *Plant Cell.* 20:1567-1585.

- Lingard, M. J. and R. N. Trelease. 2006. Five *Arabidopsis* peroxin 11 homologs individually promote peroxisome elongation, duplication or aggregation. *J. Cell Sci.* 119:1961-1972.
- Lipatova, Z., A. A. Tokarev, Y. Jin, J. Mulholland, L. S. Weisman, and N. Segev. 2008. Direct interaction between a myosin V motor and the Rab GTPases Ypt31/32 is required for polarized secretion. *Mol. Biol. Cell.* 19:4177-4187.
- Lisenbee, C. S., M. Heinze, and R. N. Trelease. 2003. Peroxisomal ascorbate peroxidase resides within a subdomain of rough endoplasmic reticulum in wild-type *Arabidopsis* cells. *Plant Physiol.* 132:870-882.
- Lodish H., A. Berk, C. A. Kaiser, M. Krieger, M. P. Scott, A. Bretscher, H. Ploegh, and P. Matsudaira. 2008. *Molecular and Cell Biology*. Sixth edition. W. H. Freeman, New York, New York. pp. 713-756.
- Macara, I. G. and S. Mili. 2008. Polarity and differential inheritance—universal attributes of life? *Cell.* 135:801-812.
- Maniatis, T., E. F. Fritsch, and J. Sambrook. 1982. *Molecular Cloning: A Laboratory Manual*. Cold Spring Harbor Laboratory, Cold Spring Harbor, New York.
- Marshall, P. A., J. M. Dyer, M. E. Quick, and J. M. Goodman. 1996. Redox-sensitive homodimerization of Pex11p: a proposed mechanism to regulate peroxisomal division. *J. Cell Biol.* 135:123-137.
- Marshall, P. A., Y. I. Krimkevich, R. H. Lark, J. M. Dyer, M. Veenhuis, and J. M. Goodman. 1995. Pmp27 promotes peroxisomal proliferation. *J. Cell Biol.* 129:345-355.
- Matsuzono, Y., N. Kinoshita, S. Tamura, N. Shimozawa, M. Hamasaki, K. Ghaedi, R. J. A. Wanders, Y. Suzuki, N. Kondo, and Y. Fujiki. 1999. Human PEX19: cDNA cloning by functional complementation, mutation analysis in a patient with Zellweger syndrome, and potential role in peroxisomal membrane assembly. *Proc. Natl. Acad. Sci. U. S. A.* 96:2116-2121.
- Motley, A. M. and E. H. Hettema. 2007. Yeast peroxisomes multiply by growth and division. *J. Cell Biol.* 178:399-410.

- Munck, J. M., A. M. Motley, J. M. Nuttall, and E. H. Hetteema. 2009. A dual function for Pex3p in peroxisome formation and inheritance. *J. Cell Biol.* 187:463-471.
- Nagotu, S., R. Saraya, M. Otzen, M. Veenhuis, and I. J. van der Klei. 2008. Peroxisome proliferation in *Hansenula polymorpha* requires Dnm1p which mediates fission but not *de novo* formation. *Biochim. Biophys. Acta.* 1783:760-769.
- Needleman, R. B. and A. Tzagoloff. 1975. Breakage of yeast: a method for processing multiple samples. *Anal. Biochem.* 64:545-549.
- Neuspiel, M., A. C. Schauss, E. Braschi, R. Zunino, P. Rippstein, R. A. Rachubinski, M. A. Andrade-Navarro, and H. M. McBride. 2008. Cargo-selected transport from the mitochondria to peroxisomes is mediated by vesicular carriers. *Curr. Biol.* 18:102-108.
- Novikoff, P. M. and A. B. Novikoff. 1972. Peroxisomes in absorptive cells of mammalian small intestine. *J. Cell Biol.* 53:532-560.
- Nuttley, W. M., A. M. Brade, C. Gaillardin, G. A. Eitzen, J. R. Glover, J. D. Aitchison, and R. A. Rachubinski. 1993. Rapid identification and characterization of peroxisomal assembly mutants in *Yarrowia lipolytica*. *Yeast.* 9:507-517.
- Orth, T., S. Reumann, X. Zhang, J. Fan, D. Wenzel, S. Quan, and J. Hu. 2007. The PEROXIN11 protein family controls peroxisome proliferation in *Arabidopsis*. *Plant Cell.* 19:333-350.
- Pashkova, N., Y. Jin, S. Ramaswamy, and L. S. Weisman. 2006. Structural basis for myosin V discrimination between distinct cargoes. *EMBO J.* 25:693-700.
- Peng, Y. and L. S. Weisman. 2008. The cyclin-dependent kinase Cdk1 directly regulates vacuole inheritance. *Dev. Cell.* 15:478-485.
- Perry, R. J., F. D. Mast, and R. A. Rachubinski. 2009. Endoplasmic reticulum-associated secretory proteins Sec20p, Sec39p, and Dsl1p are involved in peroxisome biogenesis. *Eukaryot. Cell.* 8:830-843.
- Platta, H. W. and R. Erdmann. 2007. Peroxisomal dynamics. *Trends Cell Biol.* 17:474-484.

- Poirier, Y., V. D. Antonenkov, T. Glumoff, and J. K. Hiltunen. 2006. Peroxisomal  $\beta$ -oxidation—a metabolic pathway with multiple functions. *Biochim. Biophys. Acta.* 1763:1413-1426.
- Praefcke, G. J. and H. T. McMahon. 2004. The dynamin superfamily: universal membrane tubulation and fission molecules? *Nat. Rev. Mol. Cell Biol.* 5:133-147.
- Pringle, J. R., A. E. Adams, D. G. Drubin, and B. K. Haarer. 1991. Immunofluorescence methods for yeast. *Methods Enzymol.* 194:565-602.
- Promega Protocols and Applications Guide. 1989/90.
- Pruyne, D., A. Legesse-Miller, L. Gao, Y. Dong, and A. Bretscher. 2004. Mechanisms of polarized growth and organelle segregation in yeast. *Annu. Rev. Cell Dev. Biol.* 20:559-591.
- Raymond, C. K., P. J. O'Hara, G. Eichinger, J. H. Rothman, and T. H. Stevens. 1990. Molecular analysis of the yeast *VPS3* gene and the role of its product in vacuolar protein sorting and vacuolar segregation during the cell cycle. *J. Cell Biol.* 111:877-892.
- Reddy, J. K. and G. P. Mannaerts. 1994. Peroxisomal lipid metabolism. *Annu. Rev. Nutr.* 14:343-370.
- Reumann, S. and A. P. Weber. 2006. Plant peroxisomes respire in the light: some gaps of the photorespiratory C2 cycle have become filled—others remain. *Biochim. Biophys. Acta.* 1763:1496-1510.
- Rodriguez, C. and A. Domingues. 1984. The growth characteristics of *Saccharomycopsis lipolytica*: morphology and induction of mycelium formation. *Can. J. Microbiol.* 30:605-612.
- Rose, M. D., F. Winston, and P. Heiter. 1988. Laboratory Course Manual for Methods in Yeast Genetics. Cold Spring Harbor Laboratory, Cold Spring Harbor, New York.
- Rossanese, O. W., C. A. Reinke, B. J. Bevis, A. T. Hammond, I. B. Sears, J. O'Connor, and B. S. Glick. 2001. A role for actin, Cdc1p, and Myo2p in the inheritance of late Golgi elements in *Saccharomyces cerevisiae*. *J. Cell Biol.* 153:47-62.

- Rottensteiner, H., K. Stein, E. Sonnenhol, and R. Erdmann. 2003. Conserved function of Pex11p and the novel Pex25p and Pex27p in peroxisome biogenesis. *Mol. Biol. Cell.* 14:4316-4328.
- Saiki, R. K. 1990. Amplification of genomic DNA. In: PCR Protocols: A Guide to Methods and Applications. M. A. Innis, D. H. Gelfand, J. J. Sninsky, and T. J. White (Eds.). Academic Press, San Diego, California. pp. 13-21.
- Sanchez-Martinez, C. and J. Perez-Martin. 2001. Dimorphism in fungal pathogens: *Candida albicans* and *Ustilago maydis*—similar inputs, different outputs. *Curr. Opin. Microbiol.* 4:214-221.
- Sanger, F., S. Nicklen, and A.R.Coulson. 1977. DNA sequencing with chain-terminating inhibitors. *Proc. Natl. Acad. Sci. U. S. A.* 74:5463-5467.
- Schott, D., J. Ho, D. Pruyne, and A. Bretscher. 1999. The COOH-terminal domain of Myo2p, a yeast myosin V, has a direct role in secretory vesicle targeting. *J. Cell Biol.* 147:791-808.
- Schrader, M. and H. D. Fahimi. 2006. Growth and division of peroxisomes. *Int. Rev. Cytol.* 255:237-290.
- Schrader, M. and H. D. Fahimi. 2008. The peroxisome: still a mysterious organelle. *Histochem. Cell Biol.* 129:421-440.
- Schrader, M., B. E. Reuber, J. C. Morrell, G. Jimenez-Sanchez, C. Obie, T. A. Stroh, D. Valle, T. A. Schroer, and S. J. Gould. 1998. Expression of PEX11 $\beta$  mediates peroxisome proliferation in the absence of extracellular stimuli. *J. Biol. Chem.* 273:29607-29614.
- Serasinghe, M. N. and Y. Yoon. 2008. The mitochondrial outer membrane protein hFis1 regulates mitochondrial morphology and fission through self-interaction. *Exp. Cell Res.* 314:3494-3507.
- Shapiro, E., W. Krivit, L. Lockman, I. Jambaque, C. Peters, M. Cowan, R. Harris, S. Blanche, P. Bordigoni, D. Loes, R. Ziegler, M. Crittenden, D. Ris, B. Berg, C. Cox, H. Moser, A. Fischer, and P. Aubourg. 2000. Long-term effect of bone-marrow transplantation for childhood-onset cerebral X-linked adrenoleukodystrophy. *Lancet.* 356:713-718.

- Shepard, K. A., A. P. Gerber, A. Jambhekar, P. A. Takizawa, P. O. Brown, D. Herschlag, J. L. DeRisi, and R. D. Vale. 2003. Widespread cytoplasmic mRNA transport in yeast: identification of 22 bud-localized transcripts using DNA microarray analysis. *Proc. Natl. Acad. Sci. U. S. A.* 100:11429-11434.
- Smith, J. J. Maintenance of Peroxisomes in the Yeast *Yarrowia lipolytica*. 2000. Ph.D. Thesis, University of Alberta, Edmonton, Alberta.
- Smith, J. J. and J. D. Aitchison. 2009. Regulation of peroxisome dynamics. *Curr. Opin. Cell Biol.* 21:119-126.
- South, S. T., K. A. Sacksteder, X. Li, Y. Liu, and S. J. Gould. 2000. Inhibitors of COPI and COPII do not block PEX3-mediated peroxisome synthesis. *J. Cell Biol.* 149:1345-1360.
- Spellman, P. T., G. Sherlock, M. Q. Zhang, V. R. Iyer, K. Anders, M. B. Eisen, P. O. Brown, D. Botstein, and B. Futcher. 1998. Comprehensive identification of cell cycle-regulated genes of the yeast *Saccharomyces cerevisiae* by microarray hybridization. *Mol. Biol. Cell.* 9:3273-3297.
- Stagljar, I., C. Korostensky, N. Johnsson, and S. te Heesen. 1998. A genetic system based on split-ubiquitin for the analysis of interactions between membrane proteins *in vivo*. *Proc. Natl. Acad. Sci. U. S. A.* 95:5187-5192.
- Steinberg, S. J., G. Dodt, G. V. Raymond, N. E. Braverman, A. B. Moser, and H. W. Moser. 2006. Peroxisome biogenesis disorders. *Biochim. Biophys. Acta.* 1763:1733-1748.
- Szilard, R. K. and R. A. Rachubinski. 2000. Tetratricopeptide repeat domain of *Yarrowia lipolytica* Pex5p is essential for recognition of the type 1 peroxisomal targeting signal but does not confer full biological activity on Pex5p. *Biochem. J.* 346:177-184.
- Tabak, H. F., J. L. Murk, I. Braakman, and H. J. Geuze. 2003. Peroxisomes start their life in the endoplasmic reticulum. *Traffic.* 4:512-518.
- Tam, Y. Y. C. Early to Late Events in Peroxisome Biogenesis. 2005. Ph.D. Thesis, University of Alberta, Edmonton, Alberta.

- Tam, Y. Y. C., J. C. Torres-Guzman, F. J. Vizeacoumar, J. J. Smith, M. Marelli, J. D. Aitchison, and R. A. Rachubinski. 2003. Pex11-related proteins in peroxisome dynamics: a role for the novel peroxin Pex27p in controlling peroxisome size and number in *Saccharomyces cerevisiae*. *Mol. Biol. Cell.* 14:4089-4102.
- Tam, Y. Y. C., A. Fagarasanu, M. Fagarasanu, and R. A. Rachubinski. 2005. Pex3p initiates the formation of a preperoxisomal compartment from a subdomain of the endoplasmic reticulum in *Saccharomyces cerevisiae*. *J. Biol. Chem.* 280:34933-34939.
- Tang, F., E. J. Kauffman, J. L. Novak, J. J. Nau, N. L. Catlett, and L. S. Weisman. 2003. Regulated degradation of a class V myosin receptor directs movement of the yeast vacuole. *Nature.* 422:87-92.
- Thoms, S., S. Gronborg, and J. Gartner. 2009a. Organelle interplay in peroxisomal disorders. *Trends Mol. Med.* 15:293-302.
- Thoms, S., K.-U. Kalies, and J. Gartner. 2009b. Evidence for Sec61 translocon involvement in peroxisome formation. International Meeting on Peroxisome Research, Institute for Systems Biology, Seattle, Washington (Abstract).
- Titorenko, V. I., H. Chan, and R. A. Rachubinski. 2000. Fusion of small peroxisomal vesicles in vitro reconstructs an early step in the in vivo multistep peroxisome assembly pathway of *Yarrowia lipolytica*. *J. Cell Biol.* 148:29-44.
- Titorenko, V. I., D. M. Ogrydziak, and R. A. Rachubinski. 1997. Four distinct secretory pathways serve protein secretion, cell surface growth, and peroxisome biogenesis in the yeast *Yarrowia lipolytica*. *Mol. Cell. Biol.* 17:5210-5226.
- Titorenko, V. I. and R. A. Rachubinski. 1998. Mutants of the yeast *Yarrowia lipolytica* defective in protein exit from the endoplasmic reticulum are also defective in peroxisome biogenesis. *Mol. Cell. Biol.* 18:2789-2803.
- Towbin, H., T. Staehelin, and J. Gordon. 1979. Electrophoretic transfer of proteins from polyacrylamide gels to nitrocellulose sheets: procedure and some applications. *Proc. Natl. Acad. Sci. U. S. A.* 76:4350-4354.
- van den Bosch, H., R. B. H. Schutgens, R. J. A. Wanders, and J. M. Tager. 1992. Biochemistry of peroxisomes. *Annu. Rev. Biochem.* 61:157-197.

- van Roermund, C. W., H. F. Tabak, M. van den Berg, R. J. A. Wanders, and E. H. Hettema. 2000. Pex11p plays a primary role in medium-chain fatty acid oxidation, a process that affects peroxisome number and size in *Saccharomyces cerevisiae*. *J. Cell Biol.* 150:489-498.
- van der Klei, I. J. and M. Veenhuis. 1997. Yeast peroxisomes: function and biogenesis of a versatile cell organelle. *Trends Microbiol.* 5:502-509.
- van der Klei, I. J. and M. Veenhuis. 2006. Yeast and filamentous fungi as model organisms in microbody research. *Biochim. Biophys. Acta.* 1763:1364-1373.
- Veenhuis, M., M. Mateblowski, W.-H. Kunau, and W. Harder. 1987. Proliferation of microbodies in *Saccharomyces cerevisiae*. *Yeast.* 3:77-84.
- Vida, T. A. and S. D. Emr. 1995. A new vital stain for visualizing vacuolar membrane dynamics and endocytosis in yeast. *J. Cell Biol.* 128:779-792.
- Vizeacoumar, F. J., W. N. Vreden, M. Fagarasanu, G. A. Eitzen, J. D. Aitchison, and R. A. Rachubinski. 2006. The dynamin-like protein Vps1p of the yeast *Saccharomyces cerevisiae* associates with peroxisomes in a Pex19p-dependent manner. *J. Biol. Chem.* 281:12817-12823.
- Wanders, R. J. A. 2004. Peroxisomes, lipid metabolism, and peroxisomal disorders. *Mol. Genet. Metab.* 83:16-27.
- Wanders, R. J. A. and H. R. Waterham. 2006. Peroxisomal disorders: the single peroxisomal enzyme deficiencies. *Biochim. Biophys. Acta.* 1763:1707-1720.
- Warren, G. and W. Wickner. 1996. Organelle inheritance. *Cell.* 84:395-400.
- Weisman, L. S. 2006. Organelles on the move: insights from yeast vacuole inheritance. *Nat. Rev. Mol. Cell Biol.* 7:243-252.
- Weisman, L. S., R. Bacallao, and W. Wickner. 1987. Multiple methods of visualizing the yeast vacuole permit evaluation of its morphology and inheritance during the cell cycle. *J. Cell Biol.* 105:1539-1547.

- Wierzbicki, A. S. 2007. Peroxisomal disorders affecting phytanic acid  $\alpha$ -oxidation: a review. *Biochem. Soc. Trans.* 35:881-886.
- Wu, X. S., K. Rao, H. Zhang, F. Wang, J. R. Sellers, L. E. Matesic, N. G. Copeland, N. A. Jenkins, and J. A. Hammer, III. 2002. Identification of an organelle receptor for myosin-Va. *Nat. Cell Biol.* 4:271-278.
- Xiang, X. and M. Plamann. 2003. Cytoskeleton and motor proteins in filamentous fungi. *Curr. Opin. Microbiol.* 6:628-633.
- Yamamoto, K. and H. D. Fahimi. 1987. Three-dimensional reconstruction of a peroxisomal reticulum in regenerating rat liver: evidence of interconnections between heterogeneous segments. *J. Cell Biol.* 105:713-722.
- Yan, M., N. Rayapuram, and S. Subramani. 2005. The control of peroxisome number and size during division and proliferation. *Curr. Opin. Cell Biol.* 17:376-383.
- Yang, H. C., A. Palazzo, T. C. Swayne, and L. A. Pon. 1999. A retention mechanism for distribution of mitochondria during cell division in budding yeast. *Curr. Biol.* 9:1111-1114.
- Yin, H., D. Pruyne, T. C. Huffaker, and A. Bretscher. 2000. Myosin V orientates the mitotic spindle in yeast. *Nature.* 406:1013-1015.